FAA-76-3

REPORT NO. FAA-RD-76-90

ATCRBS IMPROVEMENT PROGRAM REFLECTOR ANTENNA DEVELOPMENT

P.N. Richardson

TEXAS INSTRUMENTS INCORPORATED
Equipment Group
13500 North Central Expressway
Dallas TX 75222

JUNE 1976

FINAL REPORT

Prepared for

U.S. DEPARTMENT OF TRANSPORTATION
FEDERAL AVIATION ADMINISTRATION
Systems Research and Development Service
Washington DC 20591

Technical Report Documentation Page

1. Report No.	2. Government Accession No.	3. Recipient's Catalog No.
FAA-RD-76-90		

4. Title and Subtitle	5. Report Date
ATCRBS IMPROVEMENT PROGRAM REFLECTOR ANTENNA DEVELOPMENT	June 1976
	6. Performing Organization Code
7. Author(s)	8. Performing Organization Report No.
P.N. Richardson	DOT-TSC-FAA-76-3
9. Performing Organization Name and Address	10. Work Unit No. (TRAIS)
Texas Instruments Incorporated * Equipment Group 13500 North Central Expressway Dallas TX 75222	FA619/R6112
	11. Contract or Grant No. DOT-TSC-602
12. Sponsoring Agency Name and Address	13. Type of Report and Period Covered
U.S. Department of Transportation Federal Aviation Administration Systems Research and Development Service Washington DC 20591	Final Report April 1973-March 1974
	14. Sponsoring Agency Code

15. Supplementary Notes

*Under contract to: U.S. Department of Transportation
Transportation Systems Center
Kendall Square
Cambridge MA 02142

16. Abstract

This report describes the results of a program undertaken by Texas Instruments Incorporated, under contract to the Transportation Systems Center (TSC), to investigate improved antennas for the Air Traffic Control Radar Beacon System (ATCRBS).

Under this program, an engineering model of a new ATCRBS reflector antenna system was developed and tested. The antenna system was designed primarily for use in terminal area air traffic control, collocated with an Airport Surveillance Radar (ASR).

Also developed during this program was an integral beacon feed for the ARSR-2 radar, to give improved beacon coverage for en-route sites.

17. Key Words	18. Distribution Statement
ATCRBS Reflector Antenna Radar Beacon System ATCRBS Improvement Program Antenna, Reflector, for ATCRBS/ MARK X IFF	DOCUMENT IS AVAILABLE TO THE PUBLIC THROUGH THE NATIONAL TECHNICAL INFORMATION SERVICE, SPRINGFIELD, VIRGINIA 22161

19. Security Classif. (of this report)	20. Security Classif. (of this page)	21. No. of Pages	22. Price
Unclassified	Unclassified	148	

Form DOT F 1700.7 (8-72) Reproduction of completed page authorized

PREFACE

The major part of the work described in this report was performed between April 1973 and March 1974, and was funded under contract DOT-TSC-602. Two other contracts also contributed hardware and data to the program: the ATCRBS Reliability Demonstration (DOT-TSC-932), and the Improved Omnidirectional Antenna and Rotary Joint (DOT-TSC-993). Some pertinent data from these programs are included in this report.

Dr. Rudolph M. Kalafus and Mr. Frank LaRussa were TSC technical monitors for this program. Mr. James E. Kuhn, also with TSC, has been instrumental in arranging for field test of the antennas, and served as technical monitor for the reliability demonstration. The technical assistance of these men and that of numerous other DOT personnel are gratefully acknowledged.

METRIC CONVERSION FACTORS

Approximate Conversions to Metric Measures

Symbol	When You Know	Multiply by	To Find	Symbol
	LENGTH			
in	inches	2.5	centimeters	cm
ft	feet	30	centimeters	cm
yd	yards	0.9	meters	m
mi	miles	1.6	kilometers	km
	AREA			
in^2	square inches	6.5	square centimeters	cm^2
ft^2	square feet	0.09	square meters	m^2
yd^2	square yards	0.8	square meters	m^2
mi^2	square miles	2.6	square kilometers	km^2
	acres	0.4	hectares	ha
	MASS (weight)			
oz	ounces	28	grams	g
lb	pounds	0.45	kilograms	kg
	short tons (2000 lb)	0.9	tonnes	t
	VOLUME			
tsp	teaspoons	5	milliliters	ml
Tbsp	tablespoons	15	milliliters	ml
fl oz	fluid ounces	30	milliliters	ml
c	cups	0.24	liters	l
pt	pints	0.47	liters	l
qt	quarts	0.96	liters	l
gal	gallons	3.8	liters	l
ft^3	cubic feet	0.03	cubic meters	m^3
yd^3	cubic yards	0.76	cubic meters	m^3
	TEMPERATURE (exact)			
°F	Fahrenheit temperature	5/9 (after subtracting 32)	Celsius temperature	°C

Approximate Conversions from Metric Measures

Symbol	When You Know	Multiply by	To Find	Symbol
	LENGTH			
mm	millimeters	0.04	inches	in
cm	centimeters	0.4	inches	in
m	meters	3.3	feet	ft
m	meters	1.1	yards	yd
km	kilometers	0.6	miles	mi
	AREA			
cm^2	square centimeters	0.16	square inches	in^2
m^2	square meters	1.2	square yards	yd^2
km^2	square kilometers	0.4	square miles	mi^2
ha	hectares (10,000 m^2)	2.5	acres	
	MASS (weight)			
g	grams	0.035	ounces	oz
kg	kilograms	2.2	pounds	lb
t	tonnes (1000 kg)	1.1	short tons	
	VOLUME			
ml	milliliters	0.03	fluid ounces	fl oz
l	liters	2.1	pints	pt
l	liters	1.06	quarts	qt
l	liters	0.26	gallons	gal
m^3	cubic meters	35	cubic feet	ft^3
m^3	cubic meters	1.3	cubic yards	yd^3
	TEMPERATURE (exact)			
°C	Celsius temperature	9/5 (then add 32)	Fahrenheit temperature	°F

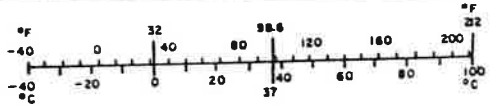

TABLE OF CONTENTS

LIST OF ILLUSTRATIONS

LIST OF TABLES

SECTION I

INTRODUCTION AND SUMMARY

General Remarks

This report describes the results of a program undertaken by Transportation Systems Center (TSC) and Texas Instruments Incorporated to investigate improved antennas for the Air Traffic Control Radar Beacon System (ATCRBS). Under this program, an engineering model of a new ATCRBS reflector antenna system was developed and tested. The antenna system was designed primarily for use in terminal area air traffic control, collocated with an Airport Surveillance Radar (ASR). Also developed during this program was an integral beacon feed for the ARSR-2 radar, to give improved beacon coverage for en-route sites. This integral feed is similar in concept to the NADIF array now in use at some ARSR sites; however, it also has azimuth monopulse, and is compatible with a passive horn modification of ARSR.

New ATCRBS Reflector

The new ATCRBS reflector antenna system described herein consists of a directional antenna, an omnidirectional antenna, a rotary joint, and a pedestal/drive system. As a group, these components replace the present 28-foot linear array ("hogtrough") and SLS dipole, to provide improved beacon coverage. Figure 1-1 shows this antenna installed at the NAFEC beacon test site.

Pattern Requirements

The significant performance difference between the "improved ATCRBS" reflector and the presently used beacon antenna is in elevation pattern shape. The present beacon antenna has a broad elevation pattern, giving coverage from the horizon to about 30 degrees elevation. The broad pattern also strongly illuminates the terrain surrounding the antenna, resulting in ground reflections. These reflections cause deep nulls in the elevation pattern, giving lost beacon coverage at some elevation angles. Figure 1-2 shows typical coverage for the present system. Other problems also result from excessive ground illumination. Nulls in the SLS antenna pattern cause lost SLS or ISLS coverage at some elevations. At other elevations, peaks of the SLS pattern are aligned with nulls of the directional pattern, which can cause "main-beam kill," a phenomenon in which the SLS system blanks valid interrogations. Another problem occurs when the directional antenna operates over smooth, non-horizontal terrain: energy is reflected to other azimuths, giving false targets at these azimuth angles.

The new antennas discussed in this report minimize the problems just mentioned by greatly reducing illumination of the surrounding terrain. This is realized using the sector-beam elevation pattern shown in Figure 1-3. Uniform gain is provided from the horizon to +30 degrees, but the pattern cuts off very quickly (at least of 3 dB per degree) below the horizon. Nulls in the elevation pattern are greatly reduced (Figure 1-4), and the possibility of false targets is similarly reduced. The SLS antenna has a matching rolloff of energy at the horizon, giving reduced nulls for better SLS coverage.

Reflector Antenna

The ATCRBS reflector is 30 feet wide and 10 feet tall, and has three feed horns. The multiple feed horns are used to give maximum horizon cutoff and good high-angle coverage, with minimum antenna height. The three-feed configuration gives a measured horizon cutoff of 3.2 dB per degree, which approaches the maximum theoretical cutoff realizable for this height (consistent with low elevation sidelobes).

In azimuth, the antenna has a pencil beam shape with a 2.3 degree beamwidth, and also has a low-sidelobe monopulse difference pattern. Multiple waveguide modes in the feed horn ensure optimum feed patterns for both sum and difference. The reflector surface is 1/2-inch expanded aluminum mesh supported by contoured vertical tubes. The back structure is welded aluminum tubing. The antenna is designed for outdoor operation in extremes

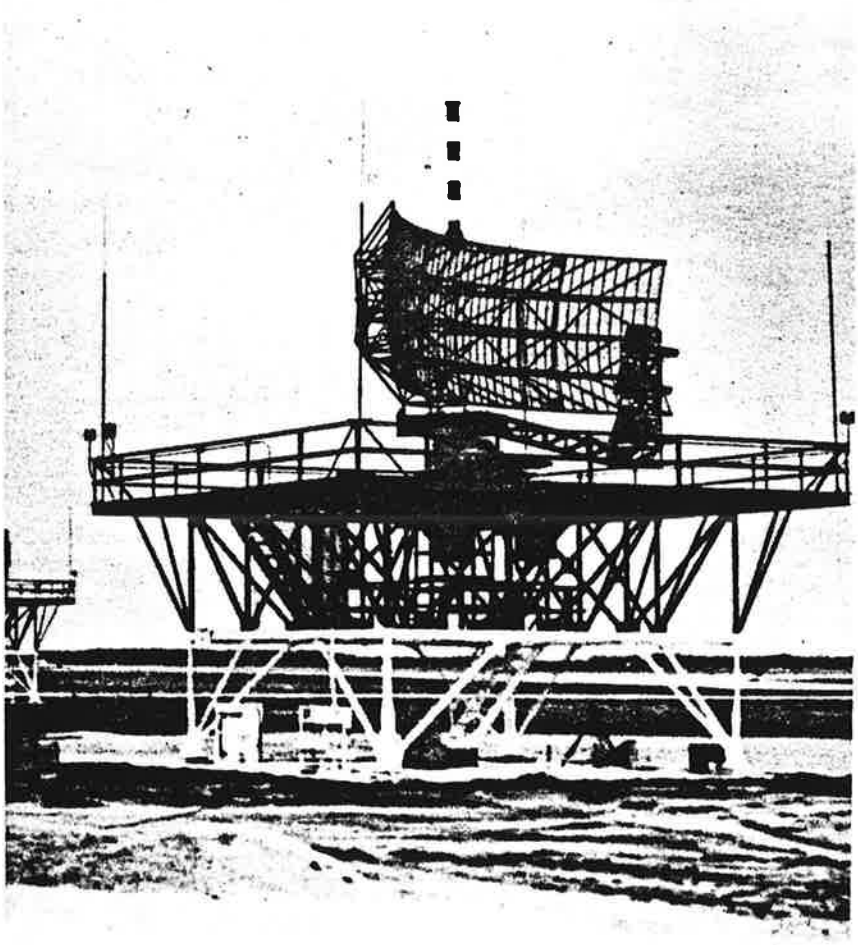

Figure 1-1. New ATCRBS Reflector

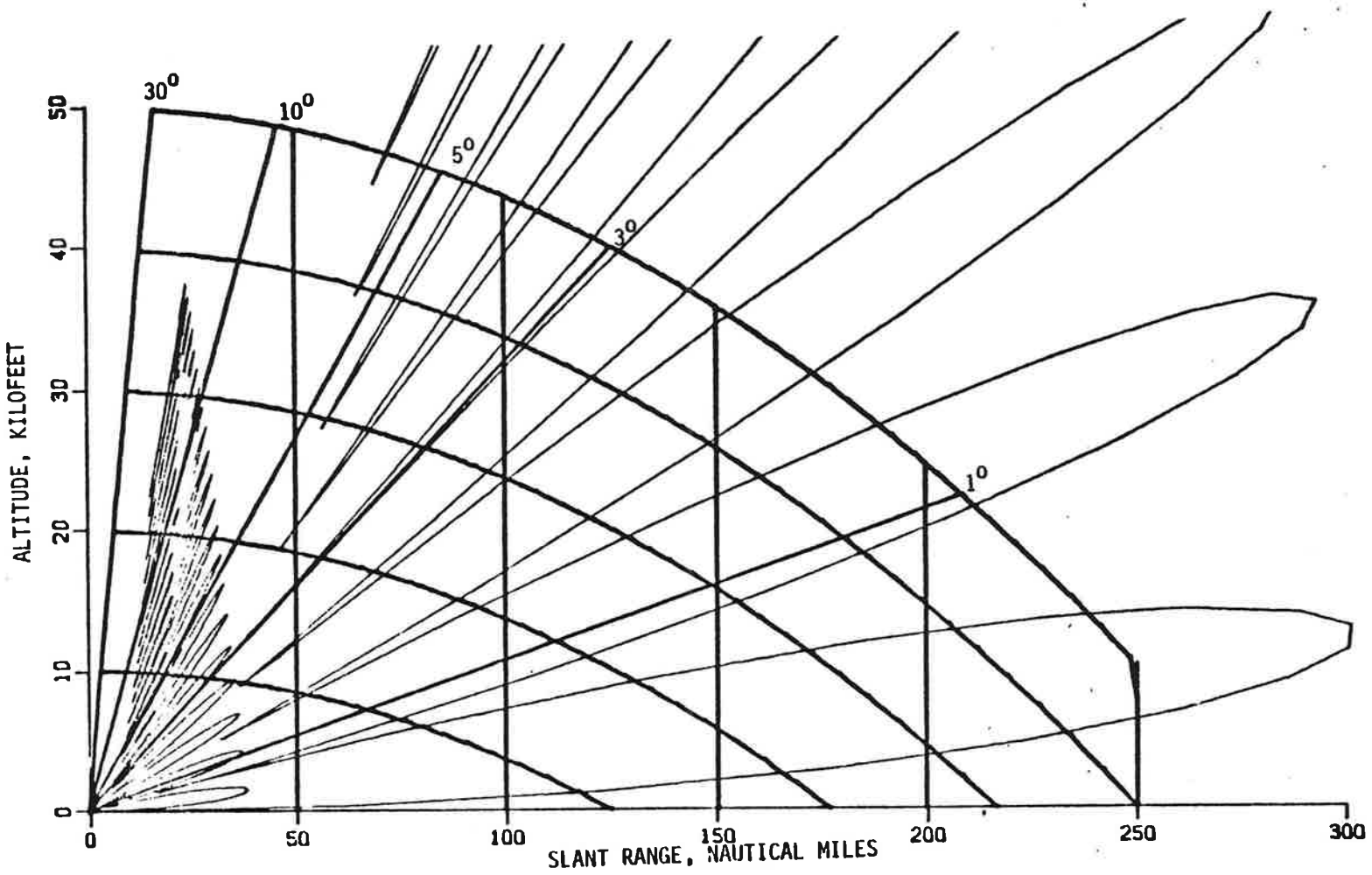

Figure 1-2. Coverage for 28-Foot Linear Array

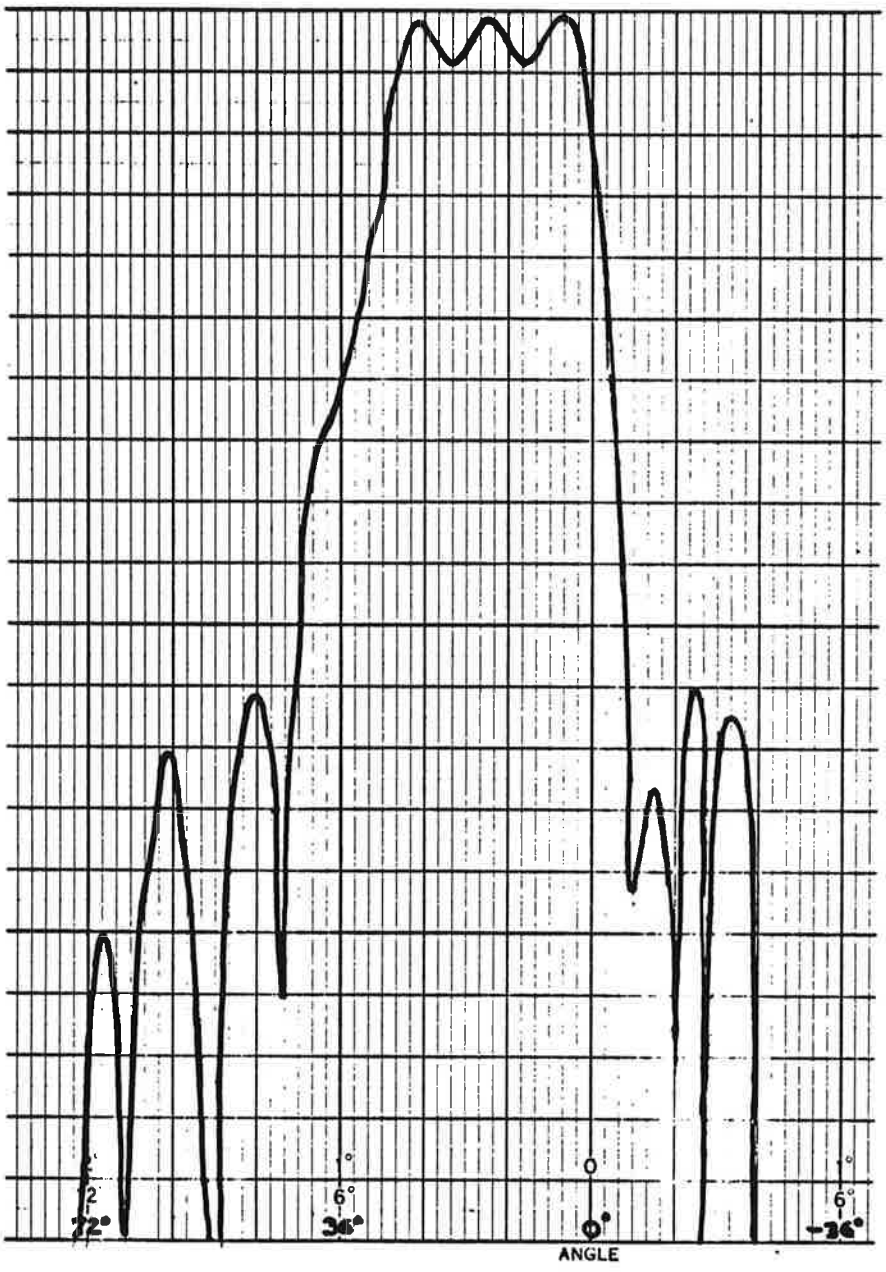

Figure 1-3. Elevation Pattern For New ATCRBS Reflector

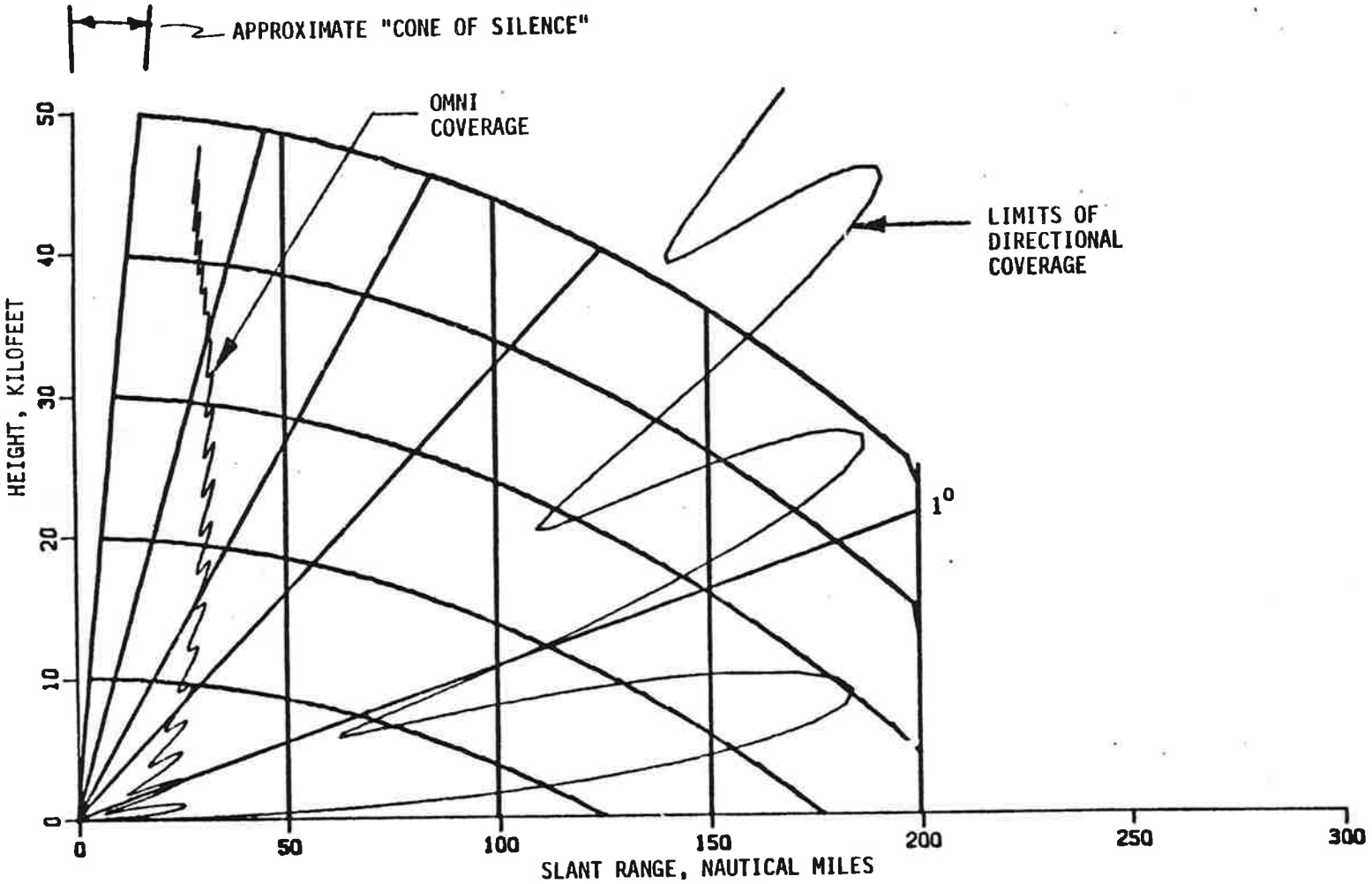

Figure 1-4. Coverage With New ATCRBS Reflector

of wind and ice. The feed horns are of welded aluminum construction and are sealed against moisture. The feed horns are interconnected using aluminum-jacketed coaxial cables and stripline power dividers. The straight-forward design and rugged construction of the antenna assure years of reliable operation with minimum maintenance.

Drive System

To be compatible with existing PPI displays, the reflector must rotate synchronously with a primary radar antenna such as the ASR-7, ASR-8, or ARSR-2; that is, the directional beams of the beacon and radar antennas must be aligned in azimuth at all times. Synchronous operation is achieved using dual drive motors coupled through a planetary gearbox. A 30-horsepower induction motor provides the power to turn the antenna at the required speed, and a smaller, 2-horsepower, DC motor makes corrections in the antenna pointing direction, as required, through the planetary gearbox. An antenna control cabinet senses errors in the antenna position and commands the DC motor to make the necessary corrections. Synchronization within ±0.25 degrees is achieved in moderate winds.

The antenna pedestal is an ASR-7 design modified to add the planetary drive system and larger drive motors. The pedestal will support the antenna in winds up to 130 knots when there is no ice on the reflector or to 105 knots with a fully iced reflector. Drive motors are sized to maintain synchronized rotation in 85-knot winds with an iced reflector.

Omnidirectional Antenna

For sidelobe blanking, two omnidirectional antenna arrays were developed. One array used a 13-element array of vertical dipoles fed to give an elevation pattern which matched the reflector elevation pattern. A second, improved design uses a unique "bent-slot" element which has excellent azimuth omnidirectionality. The improved design has additional elevation coverage above +30 degrees to blank high-angle sidelobes and back-lobes of the reflector. The omnidirectional antenna mounts on top of the reflector. Both designs are housed in cylindrical fiberglass radomes for environmental protection. For field tests, use of the improved omni with its additional high angle coverage is recommended.

Rotary Joint

Two rotary joints were provided with the ATCRBS antenna. Each has three RF channels (sum, difference, and omni) and a direct drive shaft for the APG (azimuth pulse generator). One unit, purchased from Diamond Antenna Company (DICO), employs rubbing contacts at each RF junction. This unit failed several times during early system tests, apparently due to seizure at the rubbing contacts. The unit was subsequently repaired by the manufacturer, but because its reliability was questionable, a second, non-contacting, rotary joint was designed. This design uses the same L-band rotary couplers as Texas Instruments ASR-8 rotary joint; it is entirely non-contacting and has been shown to be quite reliable over a wide range of environmental

extremes. For the reliability demonstration, and in field tests to date, the non-contacting rotary joint has been used exclusively.

Tower Modification

A modification for a standard ASR-7 tower was designed and built; this modification extends the tower upper deck and re-arranges the guard rails to accomodate the larger "ATCRBS Improvement" antennas. With the modifications, the tower deck is 32 feet square. Two identical modification kits were provided, and are now installed at the NAFEC beacon test facility. The tower extensions are installed on the two standard 17-foot ASR towers shown in Figure 1-1.

ARSR Integral Beacon Feed

The ARSR-2 antenna is a 45-foot wide, 23-foot tall, spoiled-parabola reflector. Properly illuminated, this reflector can give a beacon pattern having a 2.35 degree azimuth beamwidth and excellent horizon cutoff. The elevation pattern has a modified cosecant shape rather than the desired uniform gain sector beam, but this appears to be acceptable for the ATCRBS system. To allow simultaneous use of the ARSR-2 reflector for both the ARSR and ATCRBS functions, an integral beacon feed was developed for the ARSR radar.

Design of the integral feed was complicated by the requirement to locate the beacon feed around the ARSR-2 primary and passive feed horns which already occupied the focal region of the reflector. Ideally, the reflector illumination should emminate from a phase center at the reflector focus (or slightly below it), and only the center 30 feet of the reflector should be illuminated to give a 2.35 degree beamwidth.

The feed design which evolved is shown in Figure 1-5. In consists of a pair of dipoles beside the ARSR horn and a narrow slot element between the primary and passive horns. The slot is the principal feed element, but the dipoles are required to narrow the feed pattern (to illuminate only 30 feet of the reflector) and to move the phase center of the feed array to slightly below the focus. The integral feed was tested with an ARSR-2 reflector at a Raytheon antenna range; it gave approximately the desired patterns, but the beam was tilted approximately 1.5 degrees higher in elevation than desired. Attempts to change this elevation tilt by varying the relative power to the slots and dipoles (somewhat as is done with the NADIF array) had an adverse effect on azimuth patterns.

An omnidirectional antenna was provided for use with the integral feed. This antenna uses a "bent-slot" element for good azimuth omnidirectionality, and has a modified cosecant elevation pattern. It is housed in a fiberglass radome and mounted on a tower beside the ARSR reflector.

Related Reports

A number of other reports have been prepared as a part of this program

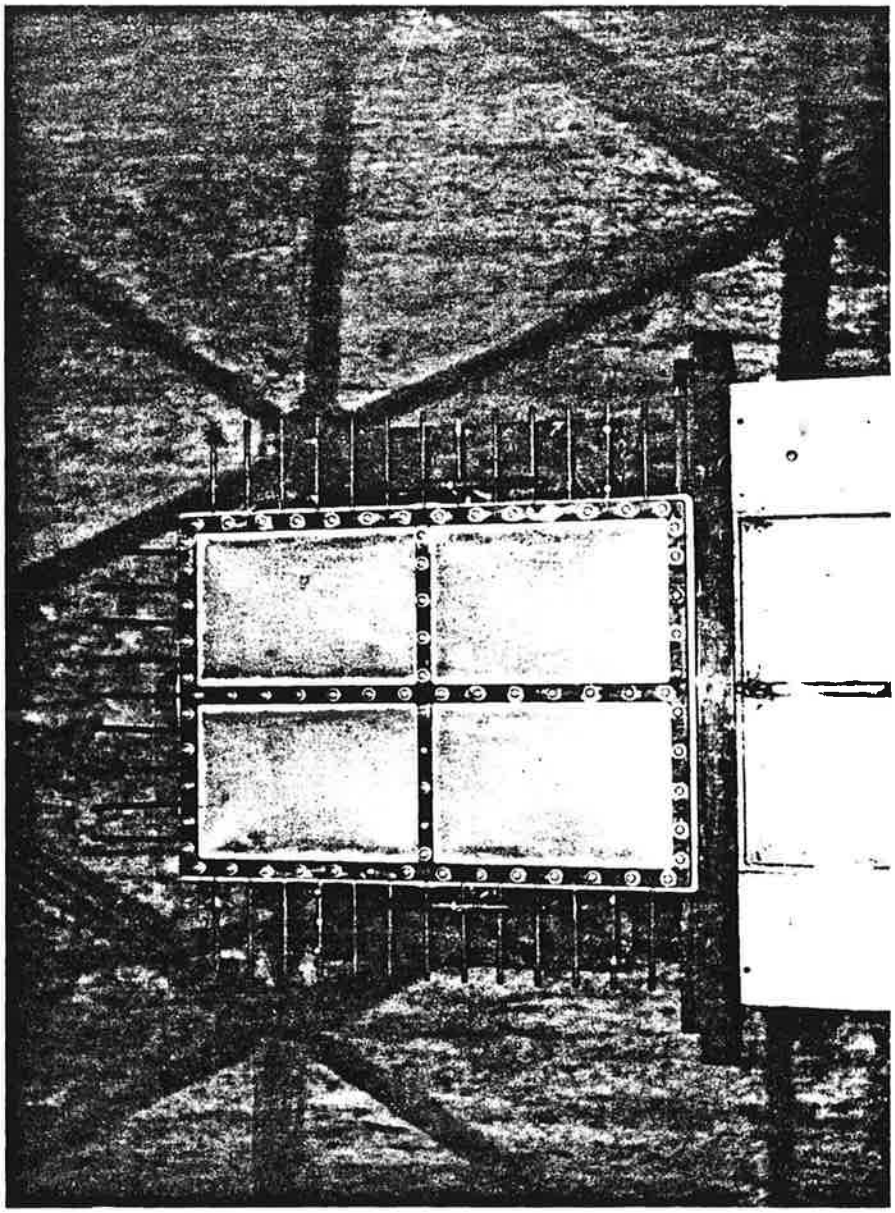

Figure 1-5. ARSR-2 Beacon Integrated Feed

to document the detailed results of various activities. This final report, to a large extent, summarizes and unifies the information from these reports. For complete details on specific points, the reader is referred to the related reports listed in Table 1-1.

Table 1-1. Related Reports.

Report Name	Date
ATCRBS Improvement Program, Phase I Final Report	Oct. 1973
Factory Test Data, ATCRBS Reflector	Apr. 1974
Factory Test Data, ARSR Integral Feed	Apr. 1974
Factory Test Data, Omni Antenna for ATCRBS Reflector	May 1974
Factory Test Data, Omni Antenna for ARSR Integral Feed	Apr. 1974
Instruction Manual, ATCRBS Reflector	May 1974
Instruction Manual ARSR Integral Feed	June 1974
ATCRBS Reliability Demonstration Test Results	Dec. 1975
Proposal to Supply an Improved Omnidirectional Antenna and Rotary Joint	Oct. 1974
Test Data for Improved Omnidirectional Antenna and Rotary Joint	Mar. 1975
Synchronization Instruction Manual	June 1975

(All reports prepared by Texas Instruments Incorporated)

SECTION II

NEW ATCRBS REFLECTOR

Specifications

The electrical specifications for the new reflector are summarized in Table 2-1. The reflector was designed to meet these specifications, and the design calculations met or exceeded all goals. Measured performance of the hardware met almost all specifications. A few sidelobe and gain values at about 30 degrees elevation were slightly outside of specification limits.

Field experience with this and other ATCRBS antennas has shown that these specifications quite well define the ATCRBS performance for both terminal and en-route applications. The backlobe specification is probably too high; it appears that backlobe suppression needs to be about -25 dB. Also, at some sites it appears desirable to extend elevation coverage to +40 degrees instead of the specified 30 degrees.

Mechanically, the antenna generally conforms to the requirements of FAA-G-2100-1 It is designed for outdoor operation in 85-knot winds with 1/2 inch of radial ice on the reflector. Survival wind loads are 105-knots with 1/2-inch radial ice, or 130-knots uniced. The synchronization servo system is designed to maintain ±1/4-degree alignment between the ASR and ATCRBS reflectors.

Possible Approaches

During initial design of the ATCRBS reflector, several different antenna types were considered for forming the desired pattern shape. These candidate antenna types included:

- Planar array antenna
- Single-feed, doubly curved reflector
- Multiple-feed, doubly curved reflector
- Singly-curved reflector, shaped in elevation, with horizontal line-source array feed to give elevation pattern shape
- Modification to existing ASR-7 reflector.

The tradeoffs among these various antenna types are discussed in detail in the Phase I engineering report. A doubly-curved reflector was selected as the best design, because it offered good electrical performance, and promised to be simple, reliable, and reasonably low cost.

Table 2-1. Summary of Performance for New Reflector

Physical Quantity	Specification
Directional pattern gain on nose	>18 dB
Azimuth beamwidth at 1,030 MHz	
Horizon (3 dB)	2.25 to 2.45 degrees
Horizon (10 dB)	<4.5 degrees
Up to 35 degrees (3 dB)	2.25 to 3.5 degrees
Up to 35 degrees (10 dB)	<6 degrees
From -2 degrees to +25 degrees	Horizon ±15%
Azimuth sidelobes at 1,030 MHz, 0-to5-degree elevation	21 dB
Azimuth sidelobes at 1,030 MHz, +5 degrees to +30 degrees	18 dB
Azimuth sidelobes at 1,030 MHz -2 degrees to 0 degrees	15 dB
Azimuth sidelobes at 1,030 MHz, +30 degrees to +35 degrees	15 dB
Azimuth backlobes	21 dB
Elevation pattern peak at 1,030 MHz (beam nose)	<5-degree elevation
Minimum power from 1-to+5-degree elevation	nose -3 dB
Maximum power -1 degree and below	nose -7 dB
Maximum power -5 degrees and below	nose -21 dB
Maximum power at +50 degrees	nose -15 dB
Maximum power +60 degrees and above	nose -21 dB
Ripple, +5 degrees to +30 degrees	<3 dB
Elevation pattern at 1,090 MHz	
Coverage +5 to +35 degrees	(1,030) ±3 dB
Coverage -5 to +5 degrees	(1,030) ±1 dB
Directional beam skew, elevation from lower 3-dB point to +30 degrees	±0.20 degree
Directional beam squint, 1,030/1,090 from lower 3-dB point to +30 degrees	±0.10 degree
Cross-polarized radiation (1,030 MHz) from -2 to +25-degree elevation	>15 dB down
Cross-polarized response (1,090 MHz)	>18 dB down

Initial Design

A three-month design period was undertaken before fabricating hardware for the reflector. The electrical characteristics of this initial design are summarized in the following paragraphs.

Synthesis

1. General Technique

The ATCRBS reflector was synthesized by first determining a central section vertical contour and feed configuration which gave the desired elevation pattern, and then extending each central rib point along focused contour to give the desired azimuth beamwidth. This technique of separating the elevation synthesis from the azimuth synthesis is commonly used in reflector design because it gives a great simplification in numerical computation. This simplification was particularly important for the ATCRBS synthesis because of the added complication of multiple feed horns. Assumption of separability, while not strictly true mathematically, has been shown to be quite accurate for most reflector antennas.

2. Central Rib Synthesis

The central chord of the reflector was synthesized using a computer program based on the theory of generalized LaGrange multipliers. In order to form the specified elevation pattern this program can simultaneously vary the following parameters of a multiple-feed reflector:

Feed horn positions

Feed horn tilt angles

Feed horn apertures

Feed horn amplitudes and phases

Reflector contour.

The synthesized elevation pattern is shown in Figure 2-1. The component elevation beams of three feed horns were combined in the correct amplitude and phase to give the composite elevation pattern shown. Figure 2-2 describes the central section contour. (Reflector coordinates are in wavelengths at 1060 MHz.) The contour deviates from a true parabola, particularly at the top where it is curled back slightly away from the feed. This modifies the aperture phase, causing each component beam to roll off more sharply on the side near the side near the horizon. Feed horn parameters for the central rib synthesis are shown in Table 2-2. (Dimensions in wavelengths at 1060 MHz.) The feeds are offset below the reflector to minimize aperture blockage. To simplify azimuth focusing of the reflector, the upper feed horn was constrained to point at the upper portion of the reflector, the central horn was aimed at the center of the reflector, and the lower horn was aimed near the bottom of the reflector.

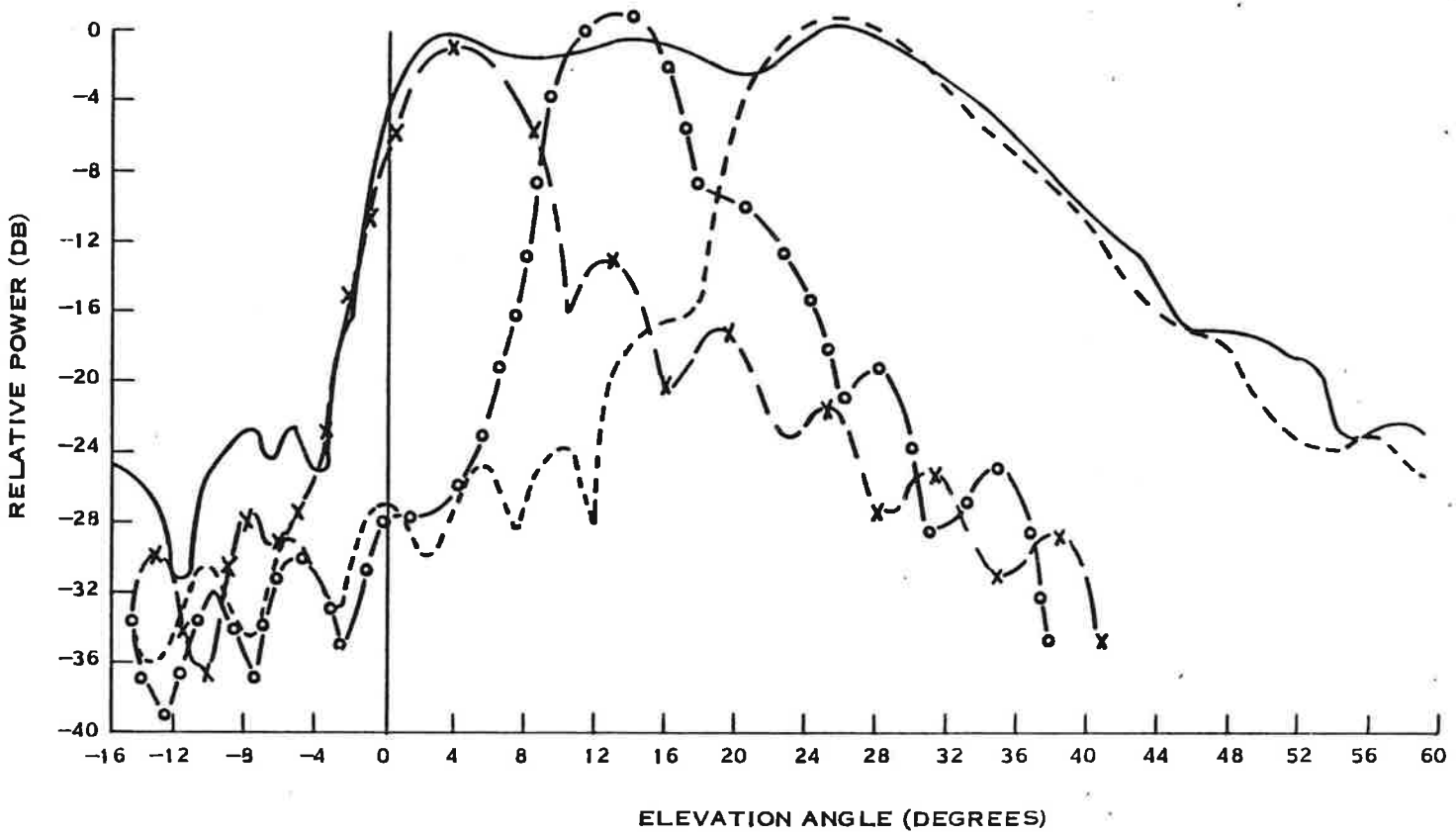

Figure 2-1. Component Beams of Two-Dimensional Problem

REFL. PT.	REFLECTOR COORDINATES PX(I)	PY(I)
27	-12.2808	8.50999
26	-12.3371	8.09367
25	-12.4007	7.67734
24	-12.4686	7.26102
23	-12.5382	6.84470
22	-12.6073	6.42837
21	-12.6746	6.01205
20	-12.7385	5.59572
19	-12.7982	5.17940
18	-12.8529	4.76308
17	-12.9020	4.34675
16	-12.9450	3.93043
15	-12.9815	3.51411
14	-13.0113	3.09778
13	-13.0341	2.68146
12	-13.0497	2.26513
11	-13.0579	1.84881
10	-13.0584	1.43249
9	-13.0512	1.01616
8	-13.0361	0.599840
7	-13.0128	0.183517
6	-12.9814	-0.232807
5	-12.9415	-0.649131
4	-12.8931	-1.06545
3	-12.8361	-1.48178
2	-12.7702	-1.89810
1	-12.6954	-2.31443

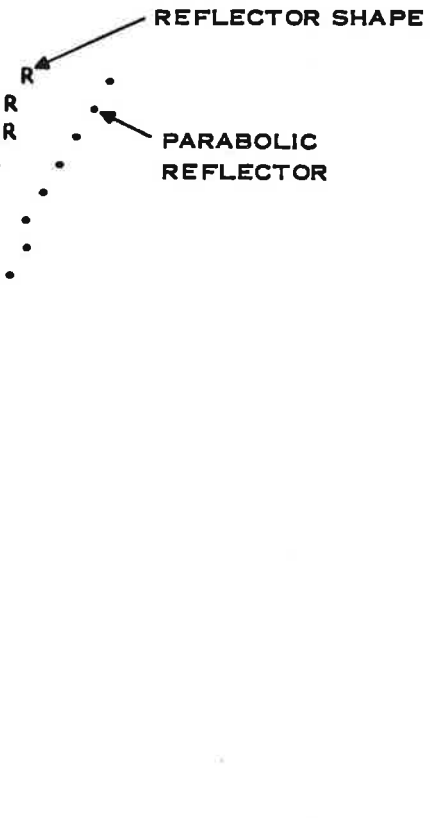

Figure 2-2. Central Section Contour

Table 2-2. Feed Parameters for Central Rib Synthesis

Parameter	1	2	3
Horn Mouth X-coordinate	0.908	+1.349	-4.217
Horn Mouth Y-coordinate	-0.33	-0.66	-1.14
Phase Center X-coordinate	0.802	-1.519	-4.624
Phase Center Y-coordinate	0.015	-0.024	-0.064
Tilt Angle, degrees	18.5	14.9	20.7
Flare Angle, degrees	20.0	20.0	20.0
Aperture Length	1.6	2.0	2.4
Relative Power, dB	0.0	+1.46	+4.20
Relative Phase, degrees	0.0	89.1	-47.6

3. Azimuth Focusing

The next step in synthesis was extending the central chord into focused azimuth contours. The width of the reflector is determined primarily by two specifications: the azimuth beamwidth and azimuth sidelobe level. It was found that a 30-foot reflector width would give the required 2.35 degrees beamwidth, with enough edge illumination taper to give typically 24-dB sidelobes. This is slightly wider than the 28-foot linear array now used, for two reasons: it is not possible to realize high efficiency aperture excitations (such as the Taylor distributions) with a reflector, and some compromises in azimuth focusing were necessary to "distribute" the focus among the three feeds, which caused a slight beam broadening.

The basic problem of extending a central vertical chord into a full reflector is that of focusing, or requiring energy along some azimuth contour to be co-phasal at some elevation angle. The elevation angle at which this co-phasal condition is imposed is generally taken as the departing ray angle (as predicted by ray optics) for the particular central-chord point being extended. The azimuth contour along which to extend the central chord point can be chosen arbitrarily, but in most reflectors has been chosen to lie in the plane of the departing ray, because for this special case every contour becomes a parabola.

The ATCRBS central chord is quite close to a parabola over most of its length, so most departing rays are horizontal; however, because of the phase correction at the top of the reflector, optics predicts that some rays are spoiled to higher angles. Applying the classic technique of azimuth extension along contours lying in the plane of the departing ray, it was

therefore found that most of the strips were horizontal, except for some strips near the top of the reflector. These top strips curved outward and upward because the optically-predicted ray was upward; this resulted in a reflector that was taller than 10 feet at the outer edges.

Since the departing-ray-plane azimuth extension gave an undesirable reflector shape, and since the spoiled top of the reflector is too small in wavelengths to apply ray optics anyway, it was decided instead to extend all central rib points along horizontal contours. This technique caused no degradation in azimuth focusing, and yielded an easily-illuminated constant-height reflector.

In generating azimuth-section strips, the multiplicity of feed points presents a problem which does not occur in the usual single-feed case. For each azimuth strip, a "virtual focus" must be specified, and regardless of where this focus is placed, some of the feed points are de-focused. Hence, some degree of azimuth pattern degradation is experienced for some or all of the feeds. For this reflector, different parts of the reflector were focused for different horns, For example, the upper part of the reflector was focused for the top horn, because most of the illumination at the top comes from the top horn.

The ATCRBS reflector was designed with the top 3.5 feet of the reflector focused at the top horn. The focus for the middle three feet was linearly distributed along a line joining the upper and lower horns. The lower most 3.5 feet was focused for the bottom horn.

Calculated Performance

As expected, the calculated elevation pattern for the three-dimensional reflector showed some slight differences from the originally synthesized two-dimensional approximation. It was necessary to slightly readjust the feed parameters to achieve best elevation patterns. Table 2-3 gives the readjusted feed parameters. Only the position of the first horn and the relative excitations had to be changed.

The calculated elevation pattern is shown in Figure 2-3, and pertinent characteristics are given in Table 2-4. Pattern cutoff at the horizon was calculated to be 3.3 dB per degree.

Calculated azimuth sum and difference patterns are shown in Figure 2-4. Beamwidths and sidelobe levels are summarized in Figure 2-5. The 3 dB beamwidth tends to become too broad near 30 degrees elevation; this was corrected by designing the lowermost feed horn to have a slightly wider azimuth pattern, to illuminate more of the reflector. This beamwidth condition could not be modeled on the computer, because the reflector analysis program assumed the same azimuth beamwidth for all feed horns.

Monopulse performance is shown in Figures 2-6, 2-7, and 2-8. The voltage ratios shown in Figure 2-6 are defined by:

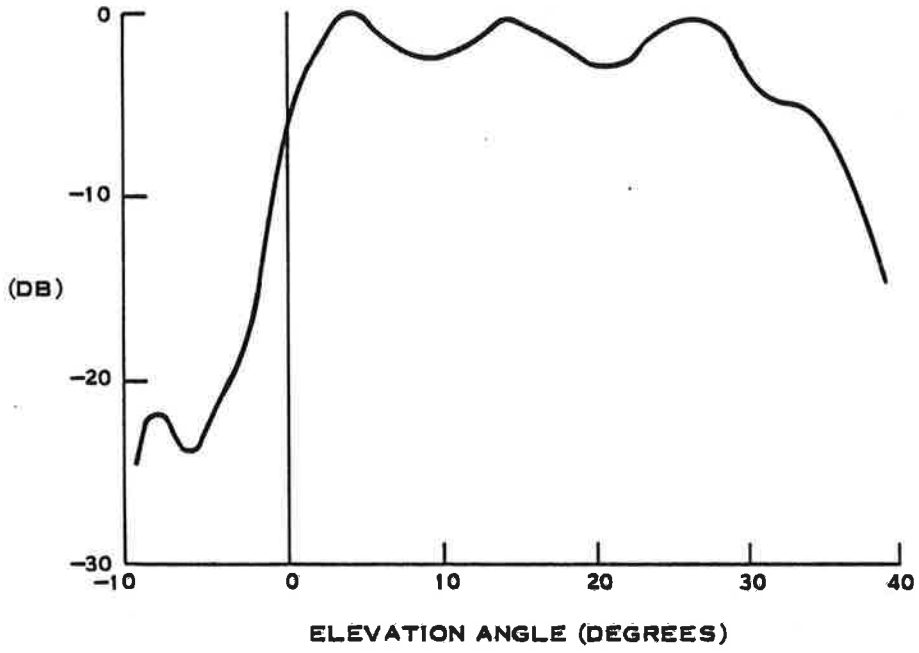

Figure 2-3. Calculated Elevation Pattern for New Reflector

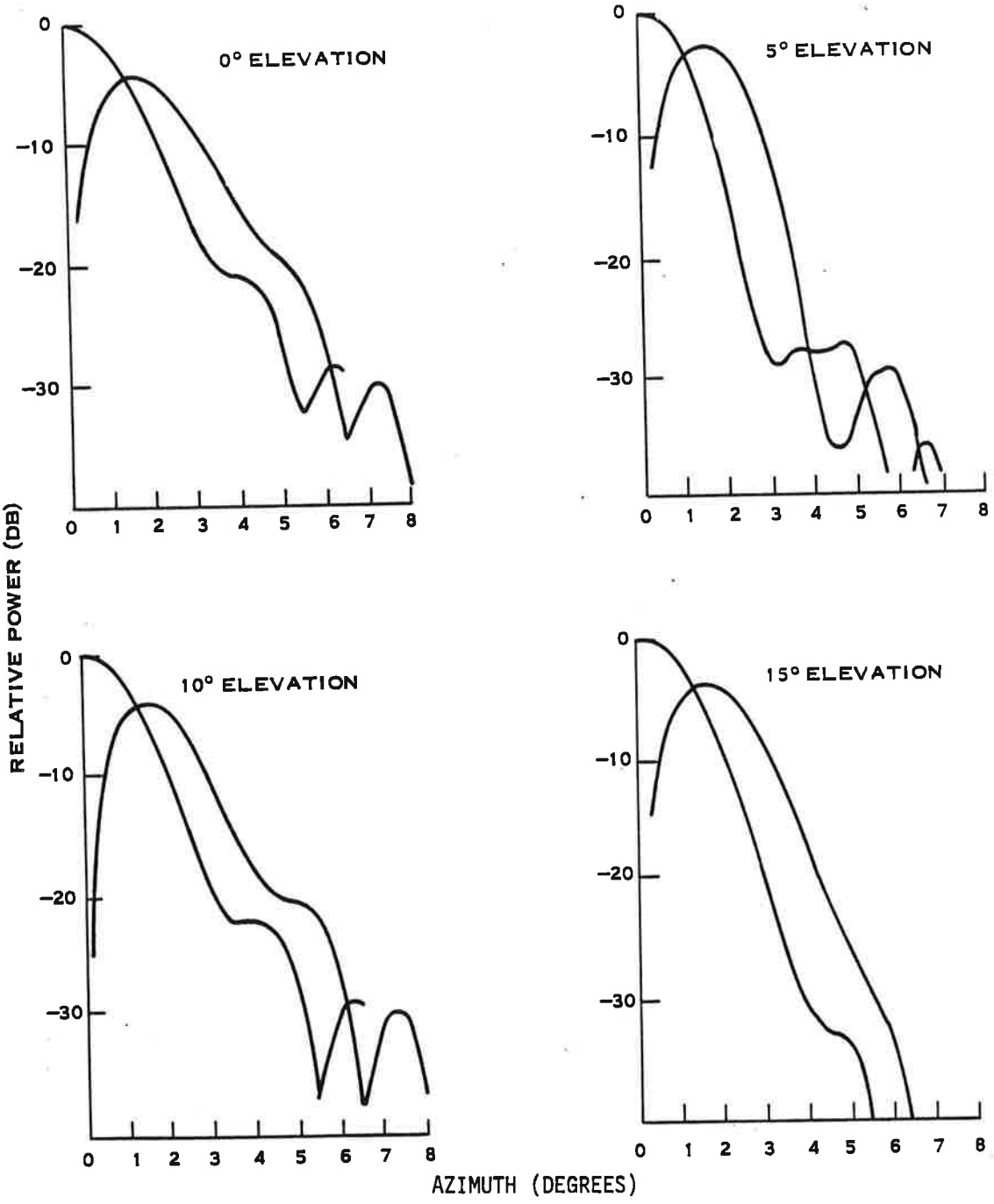

Figure 2-4. Calculated Azimuth Patterns for New Reflector (Sheet 1 of 2)

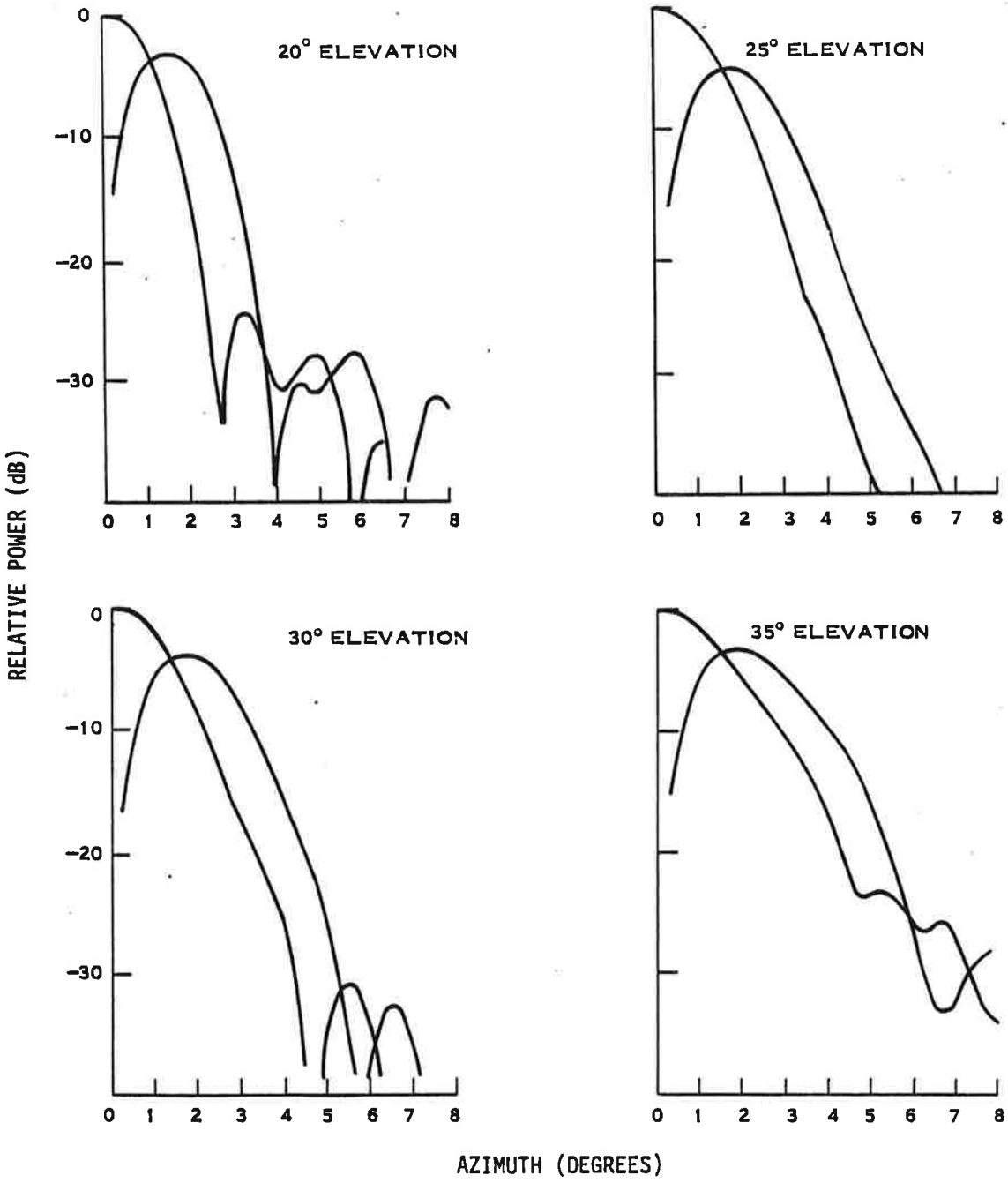

Figure 2-4. Calculated Azimuth Patterns for New Reflector (Sheet 2 of 2)

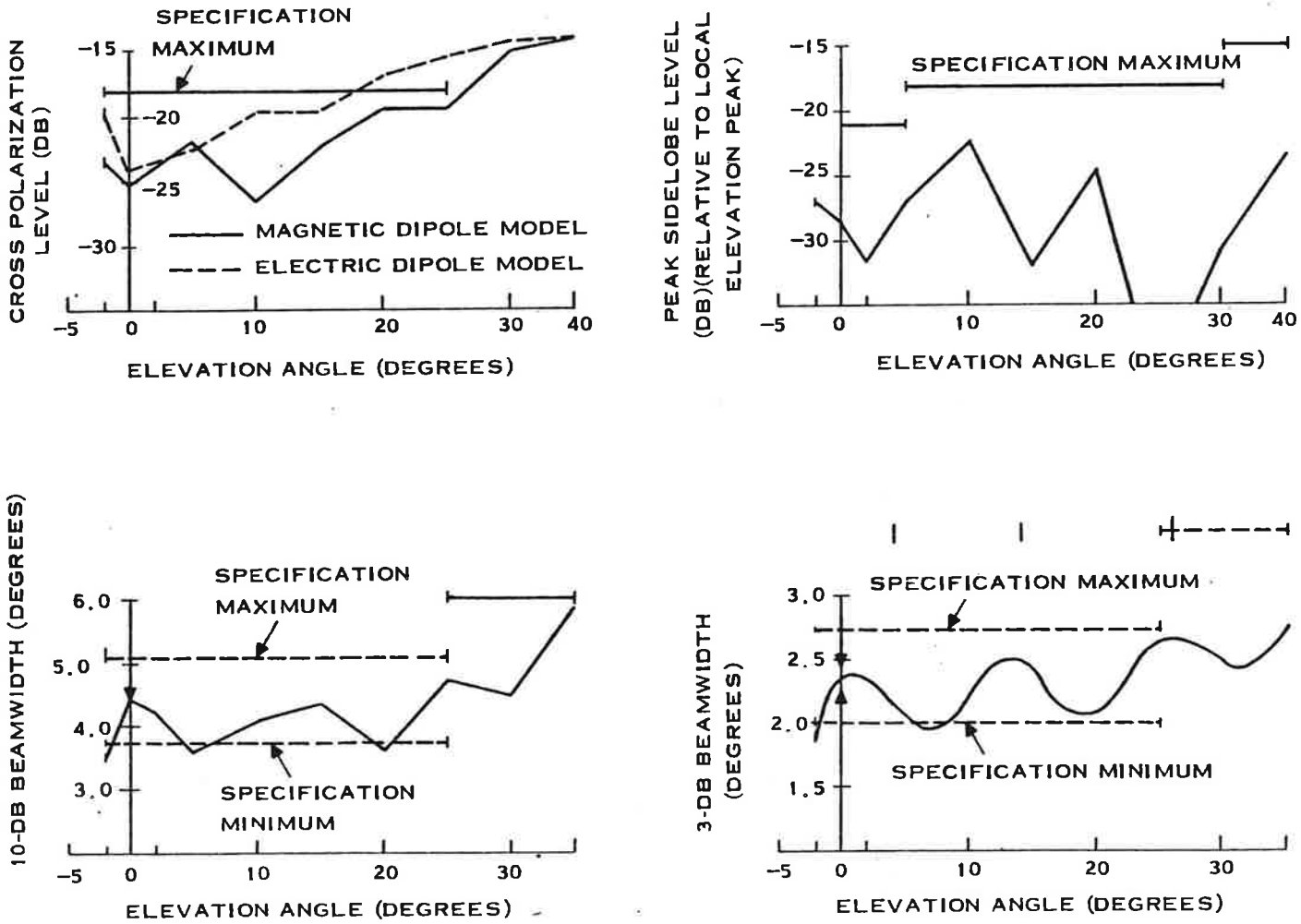

Figure 2-5. Calculated Azimuth Performance Data for New Reflector

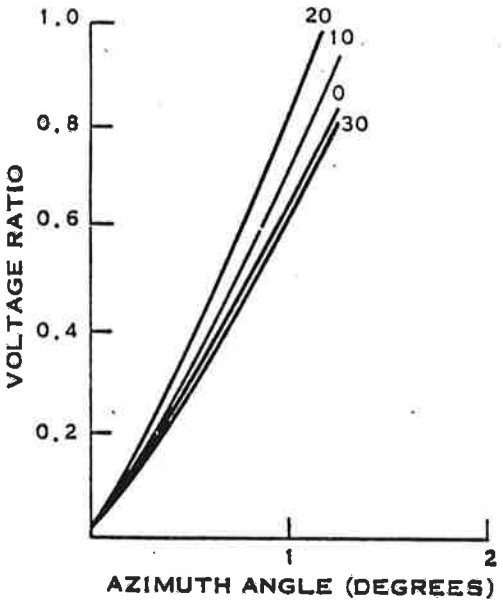

Figure 2-6. Δ/Σ Linearity

Figure 2-7. Normalized Monopulse Slope K_M

$R(\phi) = \Delta(\phi)/\Sigma(\phi)$, ϕ = azimuth angle.

The slope of these curves is of interest for off-boresight processing. At the horizon, the slope varies from 0.62/degree at boresight to 0.74/ degree at 1.25 degrees off boresight. At 20 degrees elevation, the slope varies from 0.74 to 1.16 over the same range.

Table 2-3. Readjusted Feed Parameters

Parameter Dimension	1	2	3
y-position (inches)	10.0	-17.0	-51.6
z-position (inches)	0.2	0.3	0.7
Tilt angle (degrees)	18.5	14.9	20.7
Aperture width (inches)	21.2	21.2	20.1
Aperture height (inches)	17.9	22.3	26.8
Power (dB)	0.0	3.3	4.8
Phase (degrees)	0.0	222.0	222.0

Table 2-4. Elevation Characteristics (Computed)

Characteristic	Achieved	Specified
Horizon slope	3.3 dB/degree	>2.2 dB/degree
Beam peak	3.9 degrees	<5 degrees
Power from 1 to 5 degrees	-2.8 dB	>-3 dB
Power below -1 degree	-9.1 dB	<-7 dB
Power below -5 degrees	-21.6 dB	<-21 dB
Power at 50 degrees	-23.5 dB	<-15 dB
Power at 60 degrees	-30.2 dB	<-21 dB
Ripple	2.7 dB	<3 dB
Power at 30 degrees	-3.1 dB	>3 dB

Figure 2-7 is a plot of a standard parameter of monopulse direction-finding sensitivity in which the slope is found by

$$k_m = \frac{\theta_3}{\sqrt{G_o}} \qquad \frac{\partial F_d}{\partial \phi}\Big|_{\phi = 0}$$

where

θ_3 = 3 dB beamwidth

G_o = maximum power gain

F_d = azimuth difference pattern (volts).

It is desirable for the difference pattern phase to be ±90 degrees from the sum pattern phase. Figure 2-8 shows the Σ-Δ phase difference as a function of azimuth, calculated at several elevation angles.

Feed Horn Design

It is well known that sum and difference secondary patterns for a reflector cannot be optimized using two side-by-side horns fed in and out of phase. If the horns are properly sized for a good sum beamwidth, edge illumination is too high and the difference mode, and high sidelobes result. Conversely, if the horns are made large enough for good difference patterns, feed horn sidelobes will illuminate the reflector in the sum patterns.

This problem can be overcome using multimode waveguide horns. By exciting various combinations of TE_{10}, TE_{20}, and TE_{30} modes in a horn of proper width, independent control of feed illumination for the sum and difference patterns can be realized.

These optimum monopulse horns have been used for the ATCRBS reflector. The upper two horns are designed for approximately a -16 dB edge taper for both the sum and difference modes. The lower-most horn is designed for -12.5 dB edge illumination for both modes, to prevent azimuth beam broadening at high elevation angles.

Mechanical Design

The reflector back structure and feedhorn support frame of the ATCRBS new-rotator design were optimized to minimize deflections caused by static and dynamic loading and to prevent structural failure or degradation in environmental extremes. Reflector contour deflections and feedhorn displacement can result in increased sidelobe levels, loss of gain, and beam skewing if they are of sufficient magnitude. To minimize degradation of electrical performance results, a detailed structural analysis was made to determine the deflections associated with various loading conditions and to learn their impact on system performance.

A structural analysis of the new-rotator antenna involved stress and deflection calculations for frame structures which cannot be simplified to a level which is amenable to elementary frame analysis techniques. Therefore, a finite element structural computer antenna model was formulated.

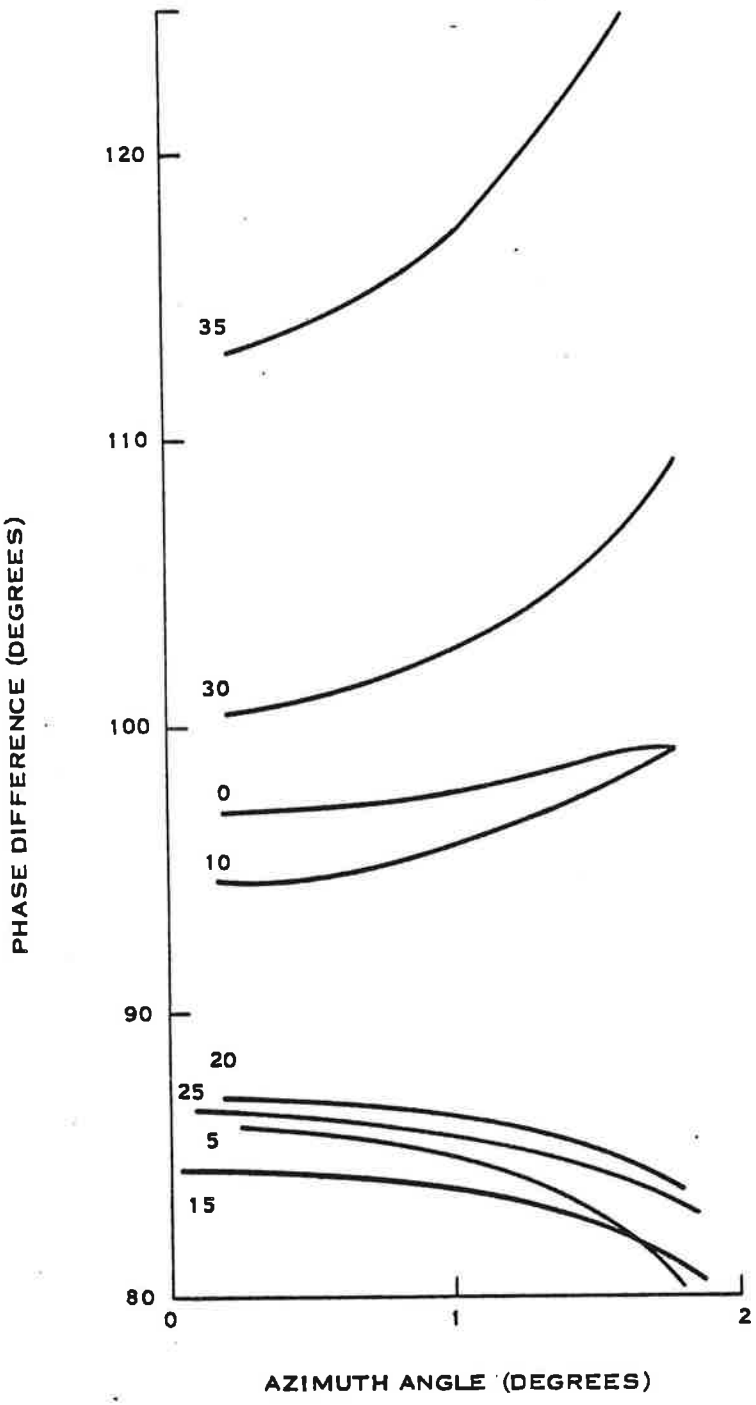

Figure 2-8. Σ-Δ Phase Difference

The technique employed for the reflector and feed structure was the stiffness method of analysis. The total structure is considered an assembly of finite structural elements connected at a number of discrete points (nodes). Since the stiffness (force deflection) characteristics for each member are known, the stiffness relationships for the assembly can be determined using standard matrix manipulations.

The initial reflector design was a synthesis of numerous basic N and K truss forms. Figures 2-9 and 2-10 are isometric projections of the finite element models for the reflector and the feedhorn support. The finite element analysis produced all the nodal point deflections and the tensile, compressive, shear, and bending stresses in all members. Structural stiffness was then optimized to yield deflections which would not degrade performance under the specified range of loading conditions. Effects of the top-mounted omni-directional antenna were included in the analysis. The new-rotator deflections under worst case operating conditions were calculated to be 0.4-inch maximum reflector contour deflection and 0.6-inch maximum top feedhorn deflection. After optimizing for maximum stiffness consistent with minimum weight and inertia, the stress levels of each member due to survival-condition loading were examined using classical theories of failure to ensure structural integrity.

Reflector Fabrication

The 30-foot wide, 10-foot high ATCRBS reflector was fabricated as follows. The contour of the reflector, as defined by the synthesis procedure, was transferred to numerous sheet-metal templates, with each template representing a particular vertical or horizontal chord on the reflector. Forty-five vertical templates and five horizontal templates were used; the templates were formed on a numerical-control sheet metal punch, using contour points taken directly from the computer synthesis routine. Horizontal and vertical contour ribs of aluminum tubing were then hand-formed to the templates. The contour ribs and other tubular members were then welded together on a large weld-fixture which accurately positions all contour tubes in the correct relationship. Finally, expanded aluminum screen is carefully tack-welded to the contour tubes to form an accurate, smooth reflector surface (Figure 2-11). The finished reflector than was painted using an electrostatically charged sprayer, ensuring a uniform, wrinkle-free and lasting paint surface which provides excellent corrosion protection.

The 30-by 10-foot reflector was built in three sections: a center section 18 feet wide and 10 feet tall, and two "wings", each 6 feet wide and 10 feet tall. The three piece construction technique was used because a weld fixture large enough to accomodate the entire reflector was not available. The reflector was built using the ASR-7 weld fixture, which will accomodate a maximum reflector width of 18 feet. This fixture is shown in Figure 2-12. The reflector center section and the two wings were aligned using contour templates, and bolted together.

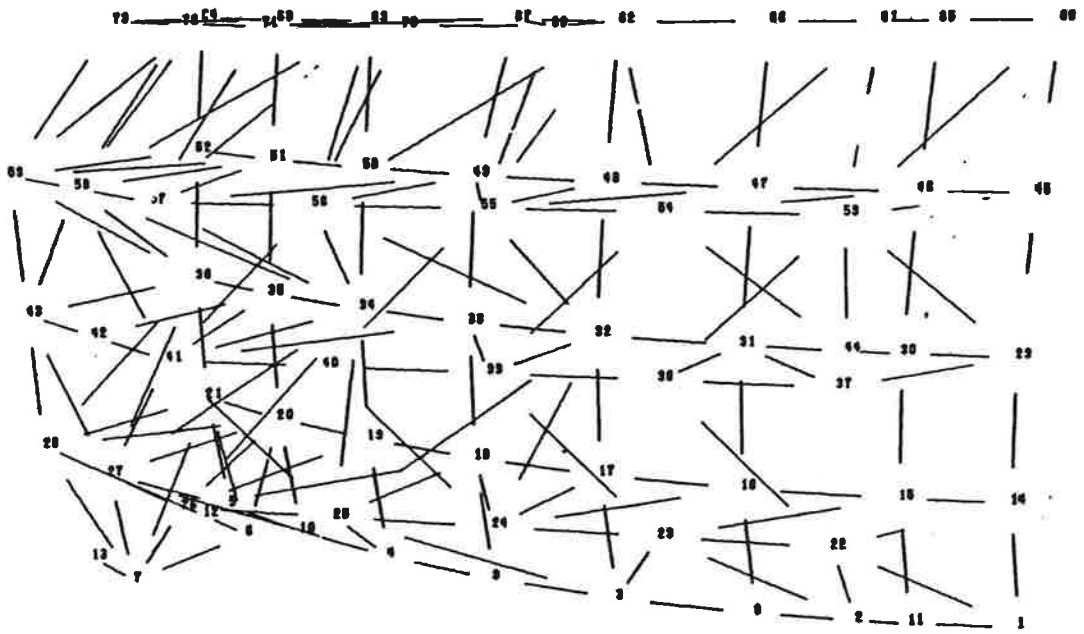

Figure 2-9. Finite Element Model for Analysis of ATCRBS Reflector Back Structure

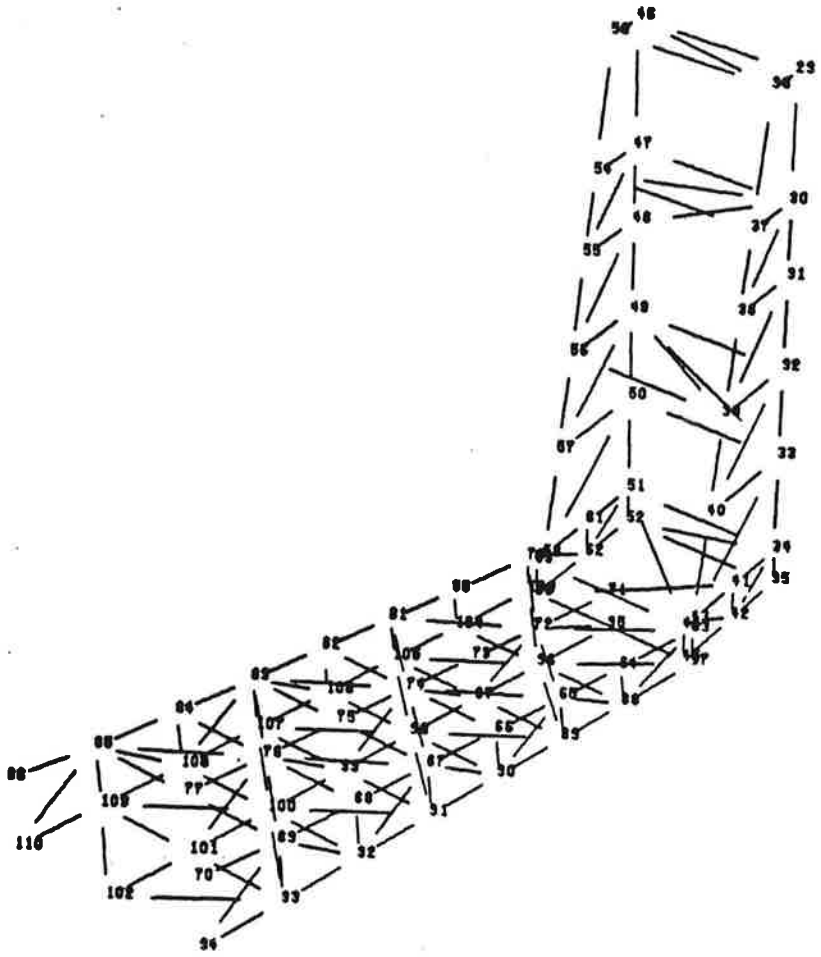

Figure 2-10. Finite Element Model for Analysis of ATCRBS Feed Support

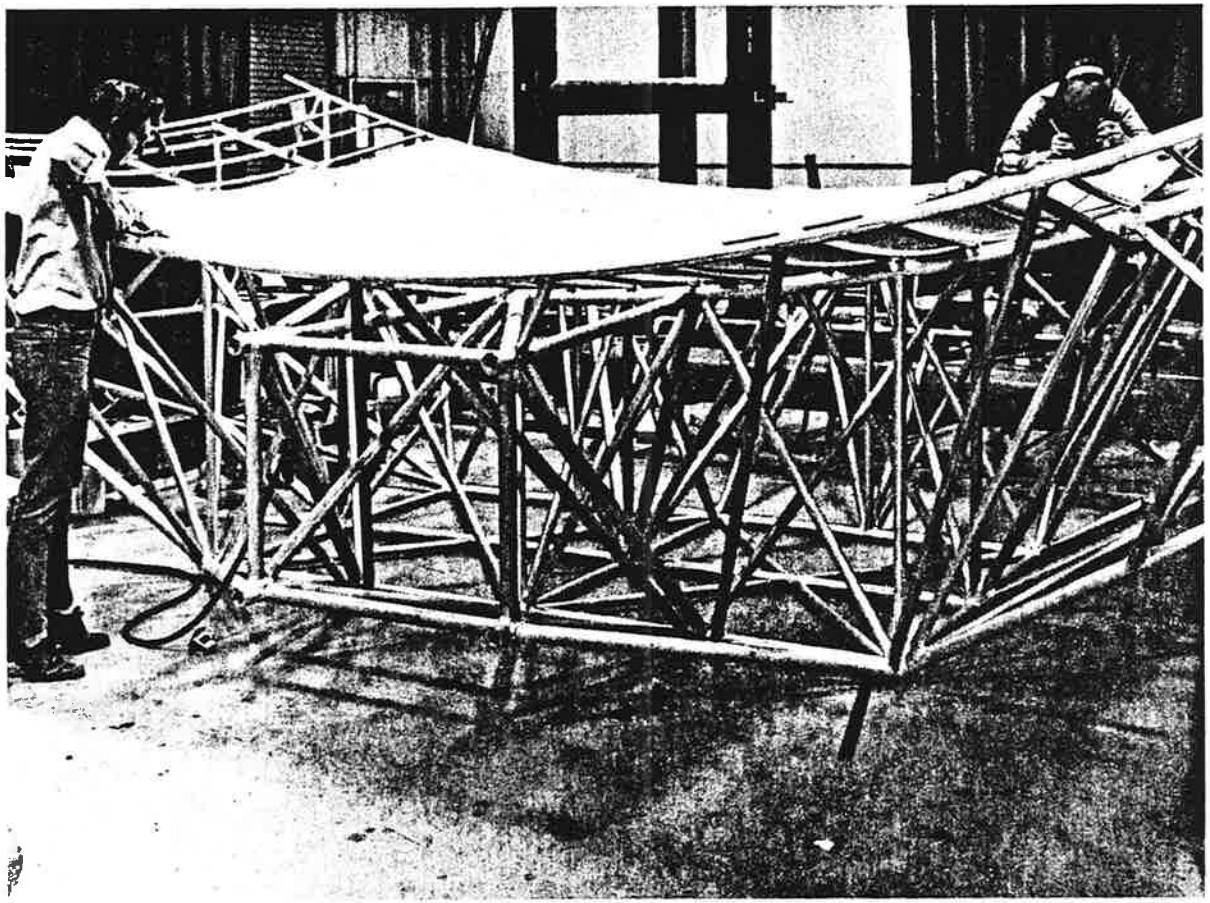

Figure 2-11. View of Screen Being Welded to Reflector

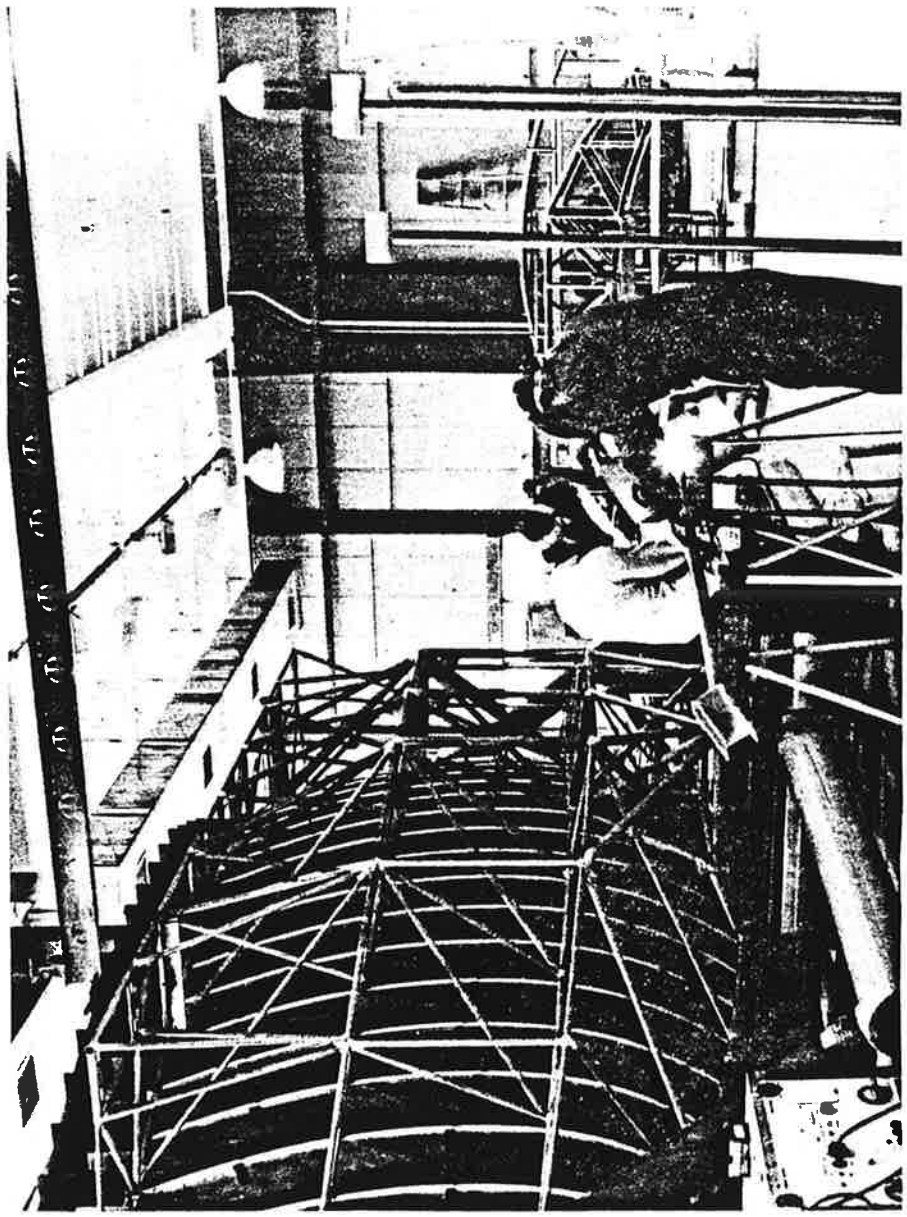

Figure 2-12. Reflector Welding Fixture

The three feedhorns were constructed of welded sheet metal. Before assembling, the welded horns were treated with a system of finishes for corrosion protection. The horn assembly includes the electrical probes and associated connectors installed onto the horn body. A 0.060-inch-thick fiberglass and epoxy laminate covers each horn aperture to protect the horns from adverse environmental conditions. The completed feed horns are installed in adjustable slides in the feed support of the reflector.

Measured Performance

Pattern Range

The ATCRBS reflector was tested on Texas Instruments 1700-foot antenna range shown in Figures 2-13 and 2-14. The source antenna for this range is located near the top of the 75-foot transmit tower. The receiving tower is equipped with an azimuth-over-elevation-over-azimuth positioner which is located 92 feet above the ground. The ATCRBS antenna was mounted with the back of the reflector attached to the upper azimuth table, and azimuth pattern cuts were recorded by rotating the lower azimuth table. Patterns were therefore great-circle cuts rather than conical cuts. The range is equipped with three rows of diffraction fences to suppress ground reflections.

The 1700-foot range is slightly too short to fulfill the usual far field criterion.

$$L = 2\frac{d^2}{\lambda} \approx 1900 \text{ feet.}$$

Typically, errors from a too short range appear as a small gain reduction and small changes in sidelobe level and null depths. Sidelobe changes will be on the order of 0.5 dB at the 20 dB level; therefore, the 1700-foot range does not grossly degrade the accuracy of the measured data.

Pattern Data

Measured principal plane patterns for the ATCRBS reflector are shown in Figures 2-15 and 2-16. Elevation azimuth sum and difference patterns, measured at +4 degrees elevation, are shown in Figure 2-17. Elevation patterns for 1030 MHz and 1090 MHz are compared in Figure 2-18. A complete tabulation of azimuth pattern data for all elevation angles is shown in Table 2-4, and plotted in Figures 2-19 through 2-23.

Most of the data is within specification limits. The high sidelobes and broad beamwidths near 30 degrees elevation are believed to be due to interaction between the lower feed horn and the feed boom (Figure 2-24); the boom probably distorts the lower horn feed pattern. The horn and boom are quite near because of mechanical constraints; the feed boom could not be lowered because it would strike the drive motor, and it would make the horn stack taller and more susceptible to deflection (causing beam skew) in high winds. However, these constraints need apply only to the engineering

Figure 2-13. Antenna Test Tower

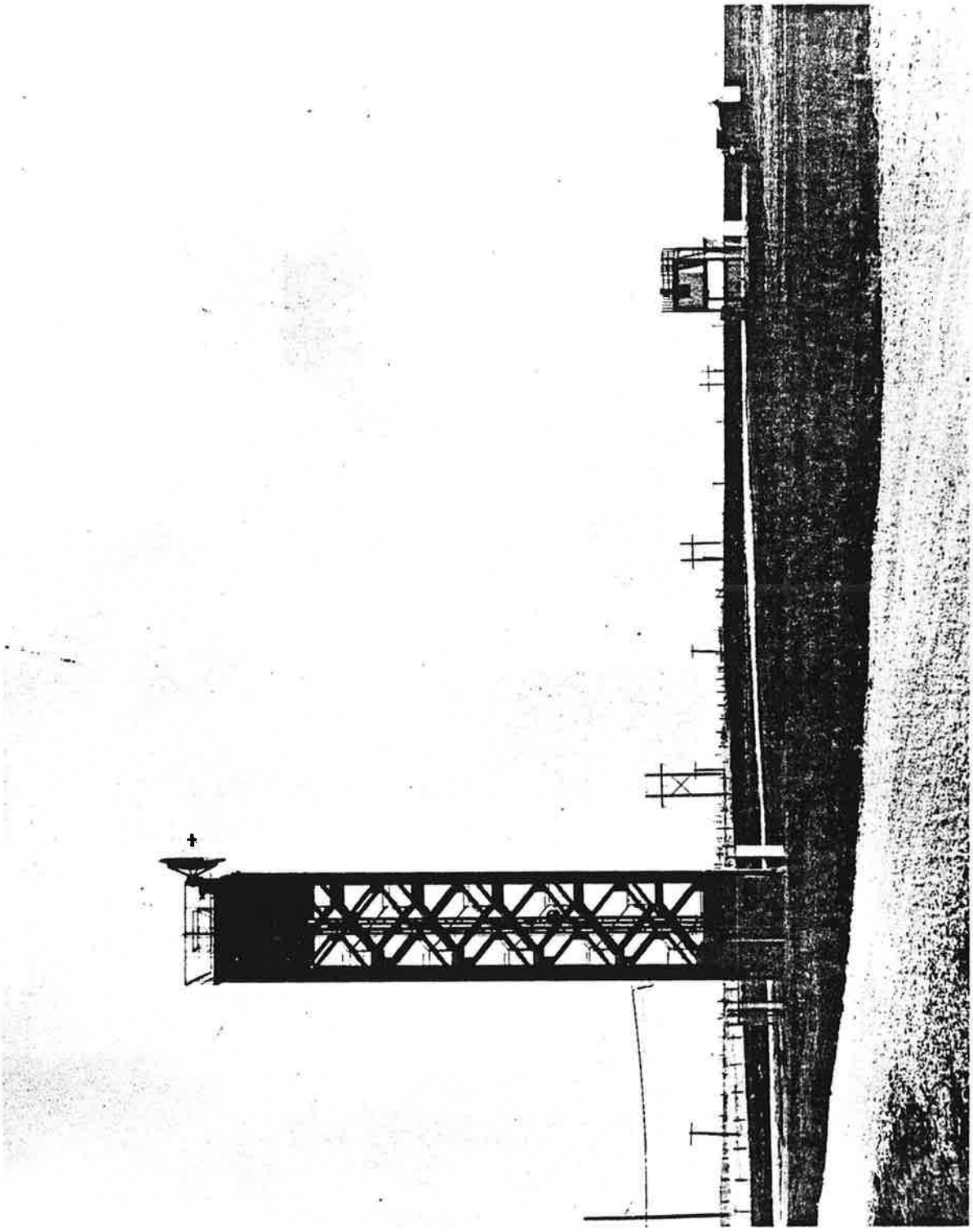

Figure 2-14. Transmit Tower

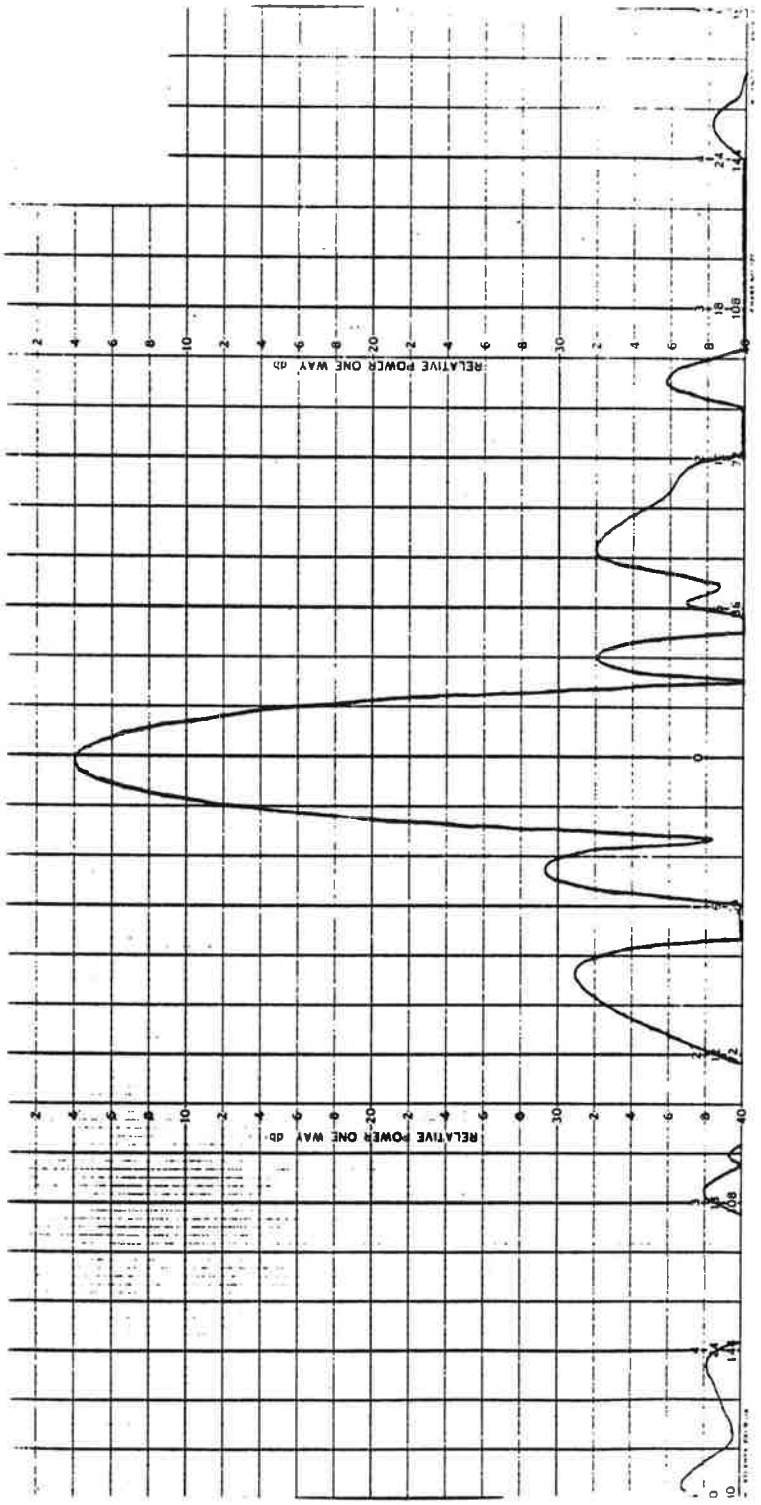

Figure 2-15. Measured Azimuth Patterns (Sheet 1 of 2)

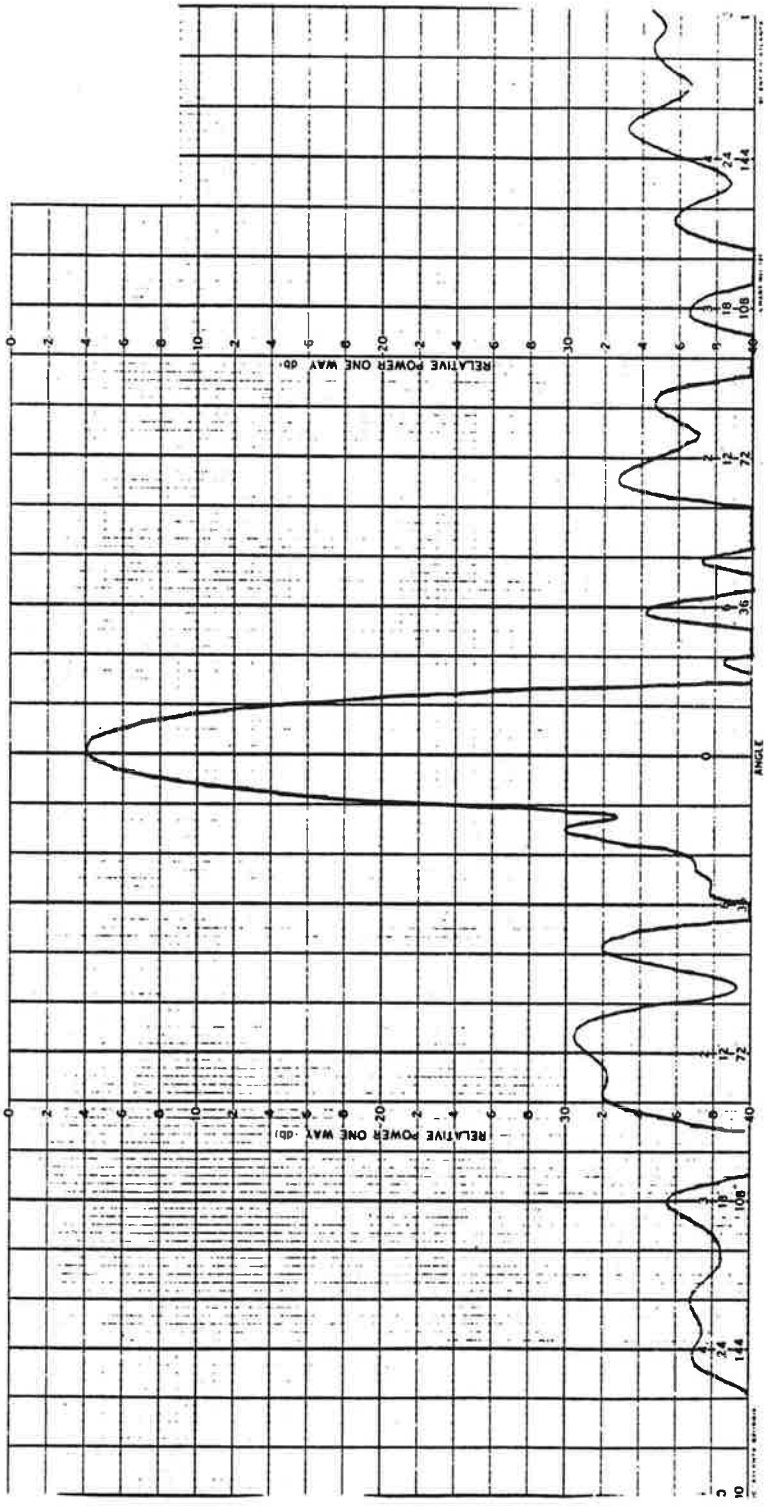

Figure 2-15. Measured Azimuth Patterns (Sheet 2 of 2)

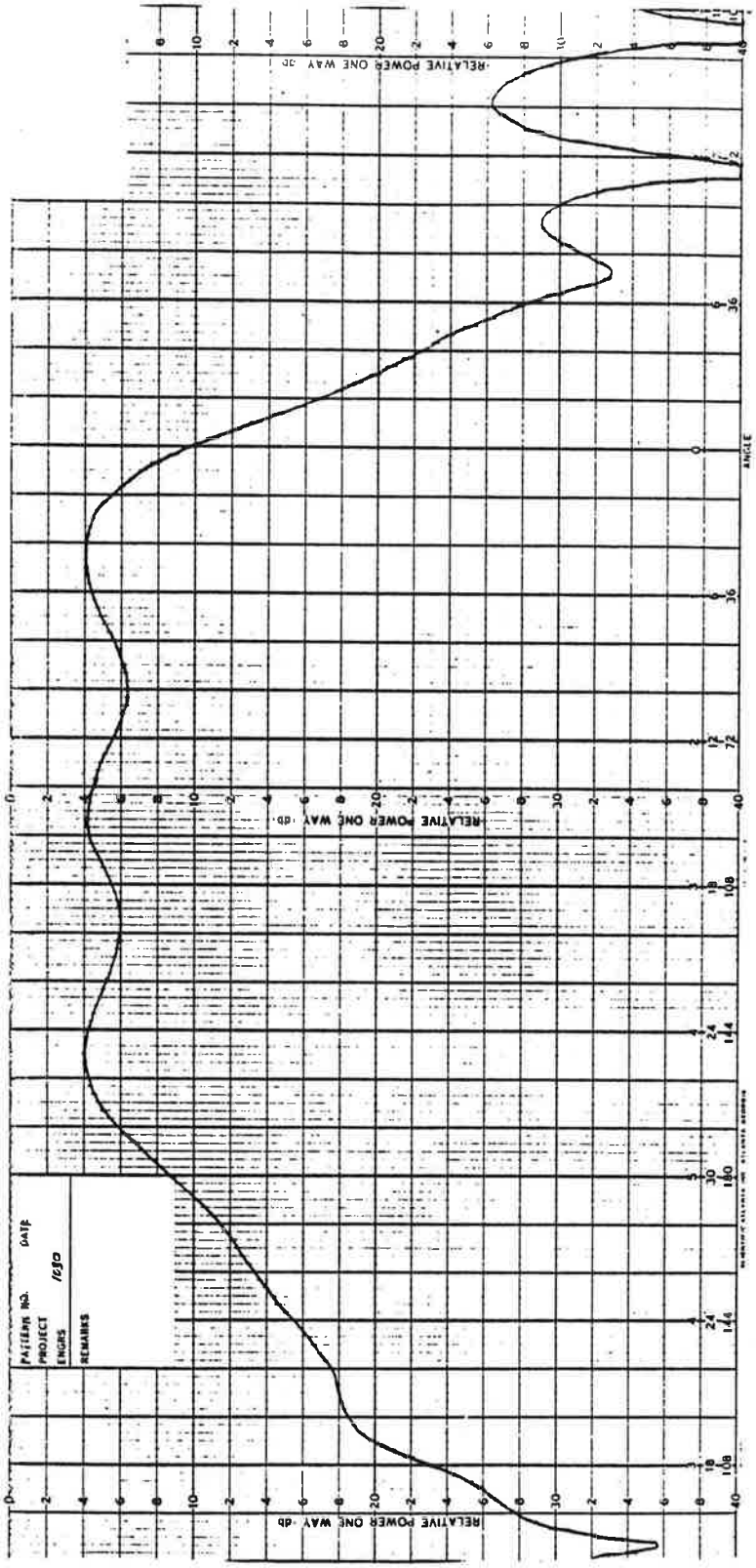

Figure 2-16. Measured Elevation Patterns (Sheet 1 of 2)

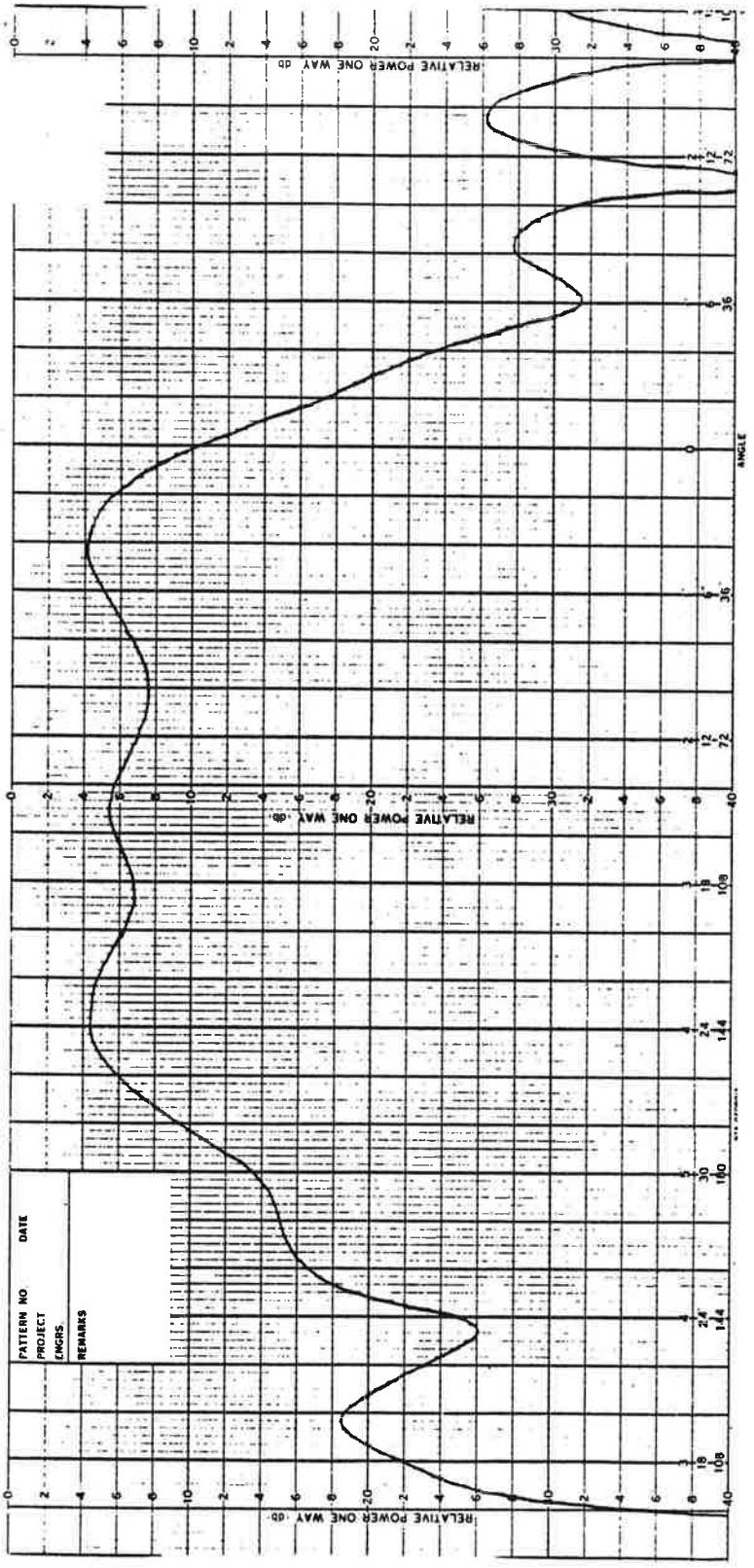

Figure 2-16. Measured Elevation Patterns (Sheet 2 of 2)

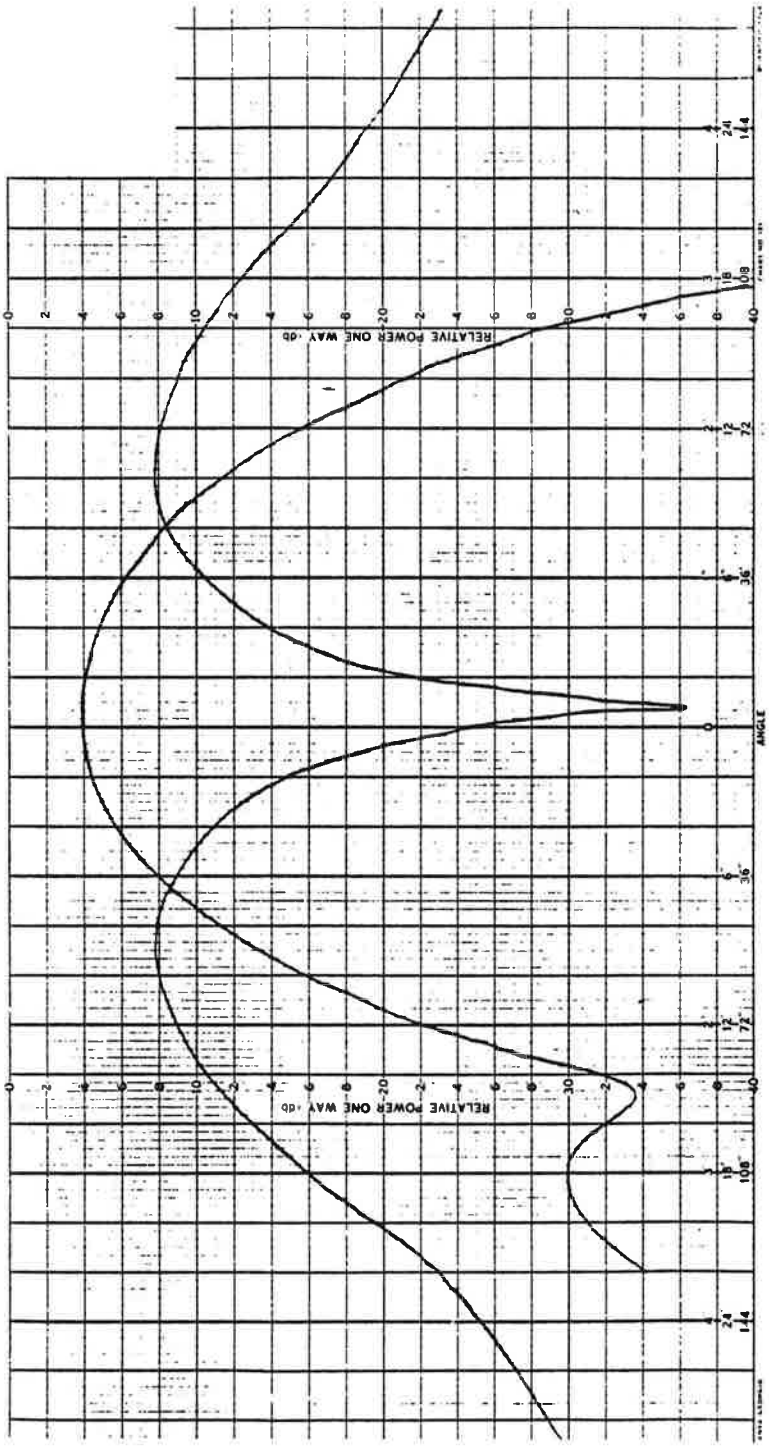

Figure 2-17. Expanded Azimuth Pattern at 1090 MHz

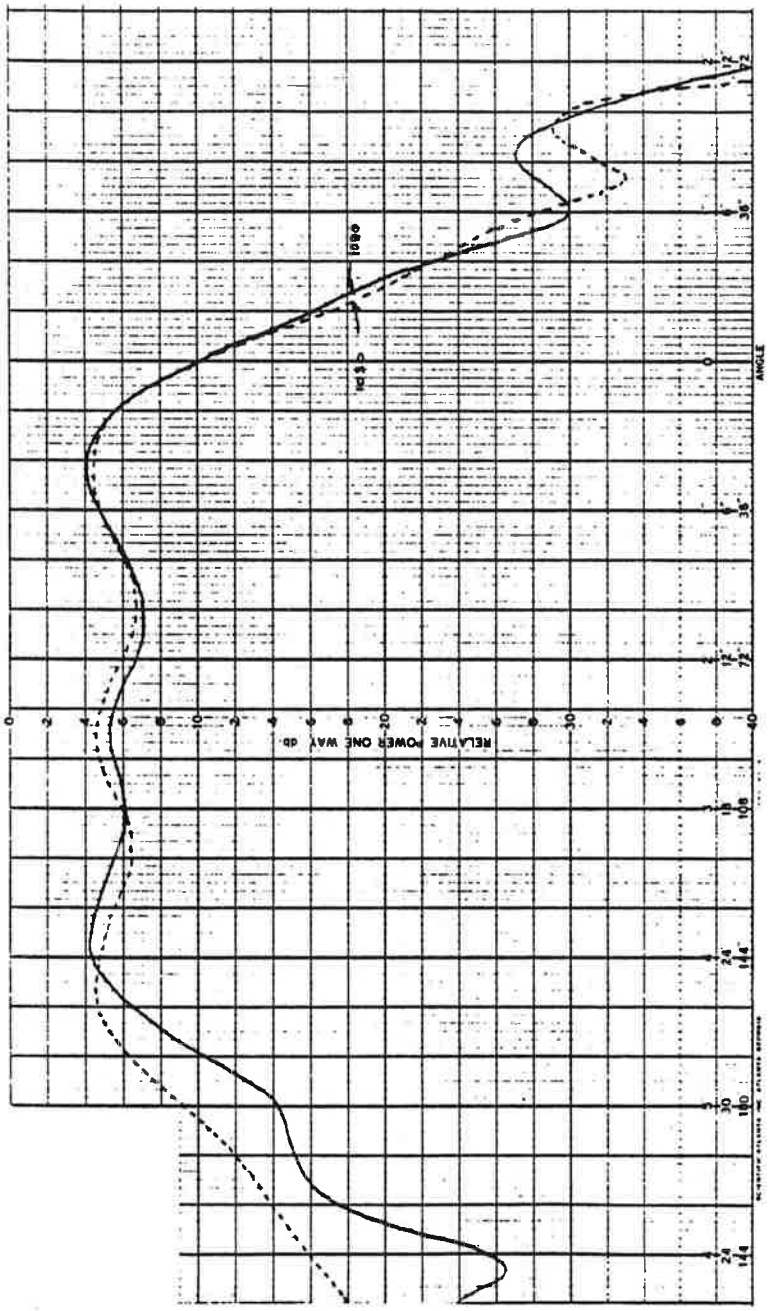

Figure 2-18. Transmit/Receive Pattern Match

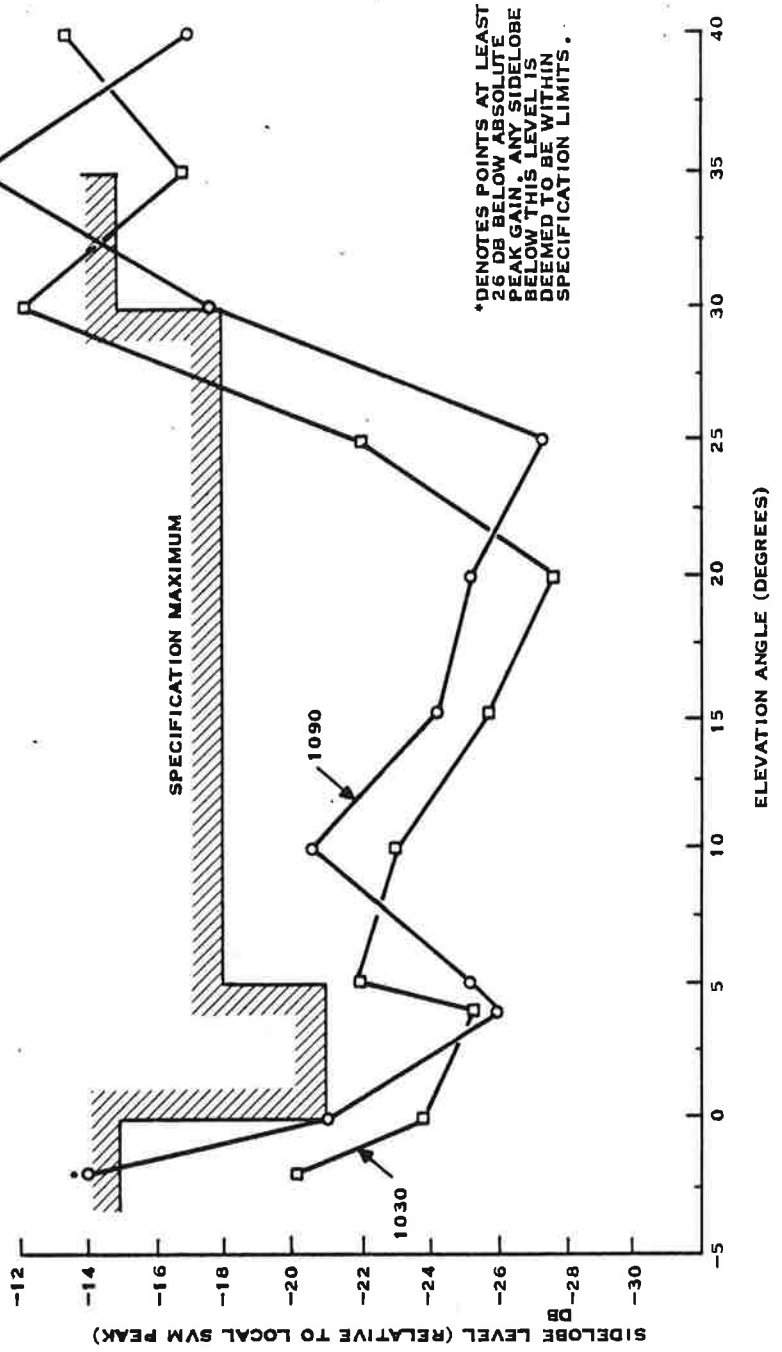

Figure 2-19. Measured Azimuth Sidelobe Levels, Sum Pattern

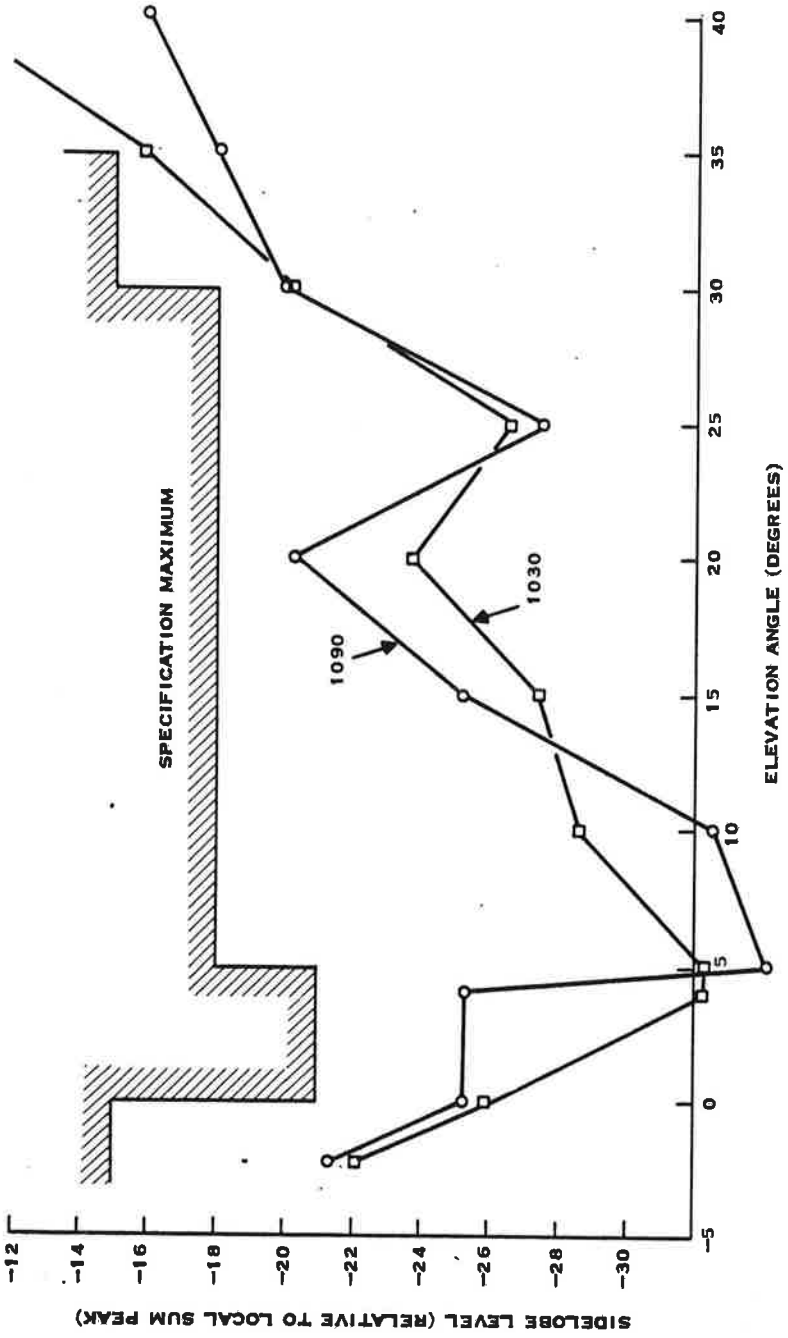

Figure 2-20. Measured Azimuth Sidelobe Levels, Difference Pattern

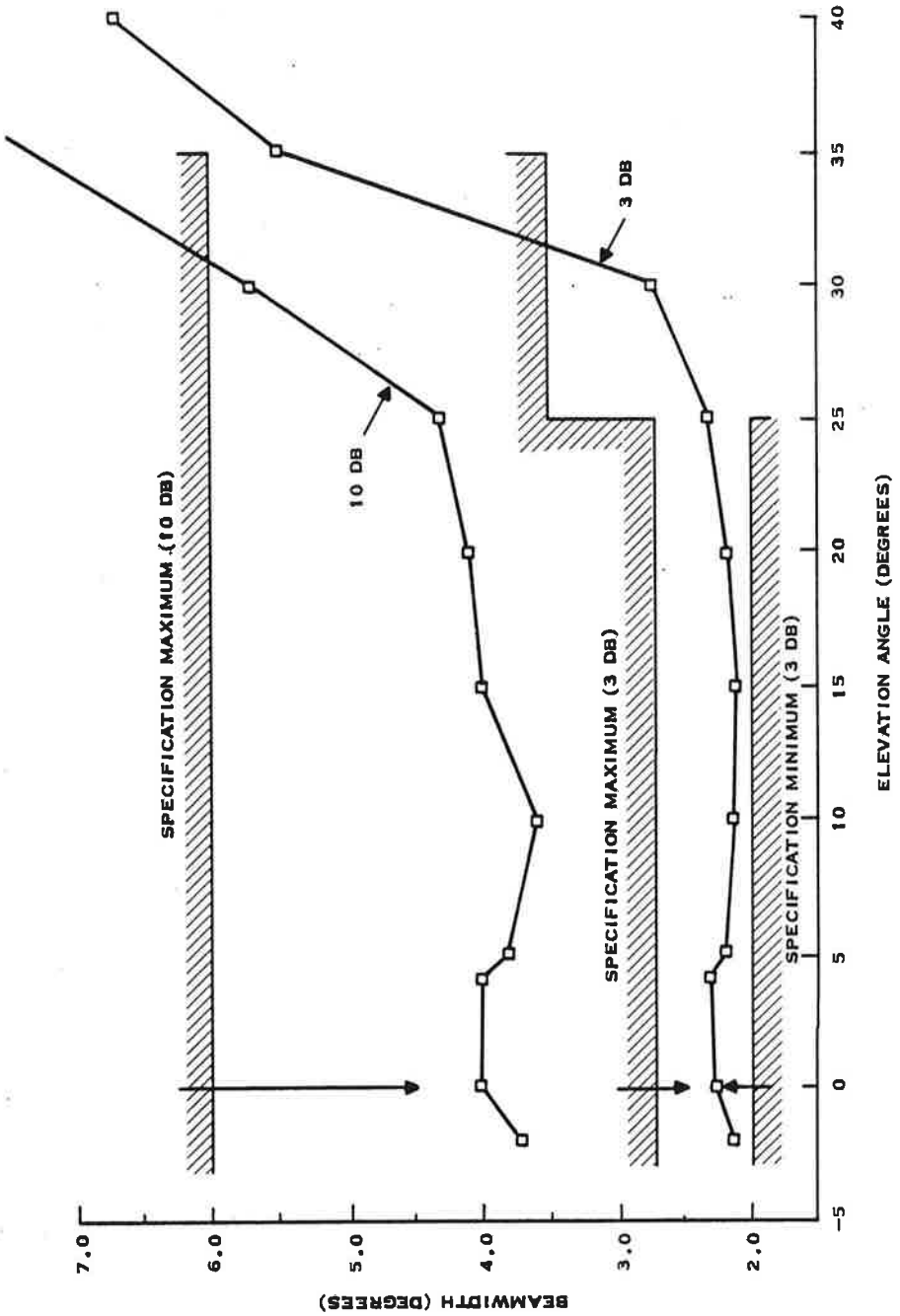

Figure 2-21. Azimuth Beamwidths at 1030 MHz

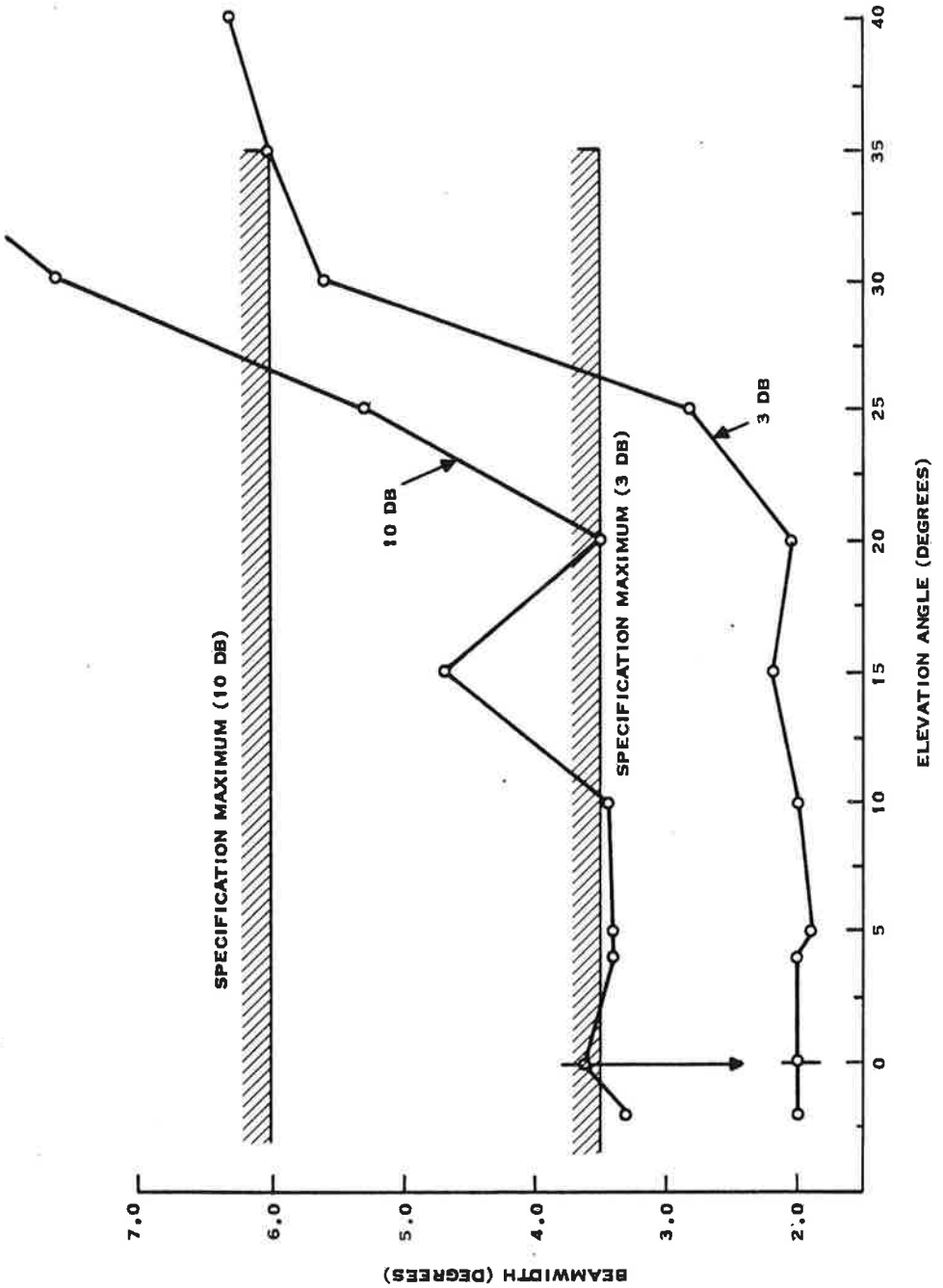

Figure 2-22. Azimuth Beamwidths at 1090 MHz

model which uses a modified ASR-7 pedestal. Production antennas can have a new pedestal design with the drive motors located below the pedestal. This will allow redesign of the feed support to give more clearance for the lower horn.

Beam skew and squint were measured by defining beam center as the mid-point of the half power points in azimuth. The zero shown in Figure 2-21 is an arbitrary antenna range zero, and has no particular relationship to mechanical boresight of the antenna. Squint is an azimuth shift in the beam peak as frequency is varied, and skew is a shift in the azimuth peak from 0 to 30 degrees elevation.

Beam squint between 1030 and 1090 MHz is probably caused by amplitude variations in the 180-degree hybrids feed each horn. An amplitude plot for a typical hybrid is shown in Figure 2-23. At 1030 MHz, one side of the feed horn is about 0.3 dB hotter than the other side, causing a slight squint of the secondary beam. At 1090 MHz, the other side is "hotter," causing squint to the opposite side.

Beam skew probably came from the same source. A small impedance mismatch in one of the number 2 horn input ports, or a variation in its 180-degree hybrid, could have caused the skew at 10-degrees elevation. Skew could also have been caused by errors in the reflector contour, or by a lateral position error for horn number 2, but an electrical imbalance is believed to be a more probable cause.

Skew and squint are within specification, but tighter specifications are probably desirable for an accurate monopulse system. It should be possible to reduce skew and squint to less than 0.05 degrees by redesiging the hybrids for lower gain variation, and by using greater care in fabricating and tuning the feed horns and hybrids.

Gain

Antenna directivity was calculated to be approximately 27 dB, neglecting feed losses and spillover losses. Actual gain, measured by comparison with a standard gain horn, is 25.7 dB at 1030 MHz, and 25.4 dB at 1090 MHz. It is pleasing to note that losses were held to a minimum, but for proper SLS operation, the antenna actually has 3 to 6 dB too much gain (at least on transmit, and probably also on receive). In a typical system application gain can be reduced as required with an external attenuator.

Input Impedance

Input VSWR, measured in a 50 ohm system, is shown in Table 2-4. All values are within the specified maximum of 1.5.

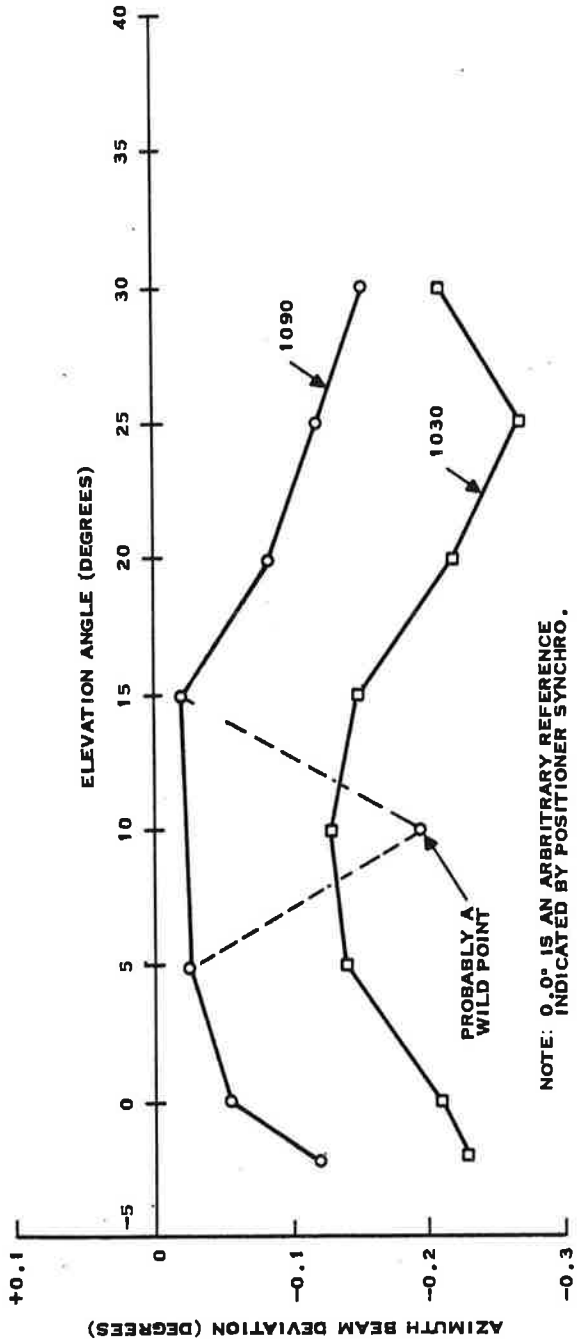

Figure 2-23. Beam Skew and Squint

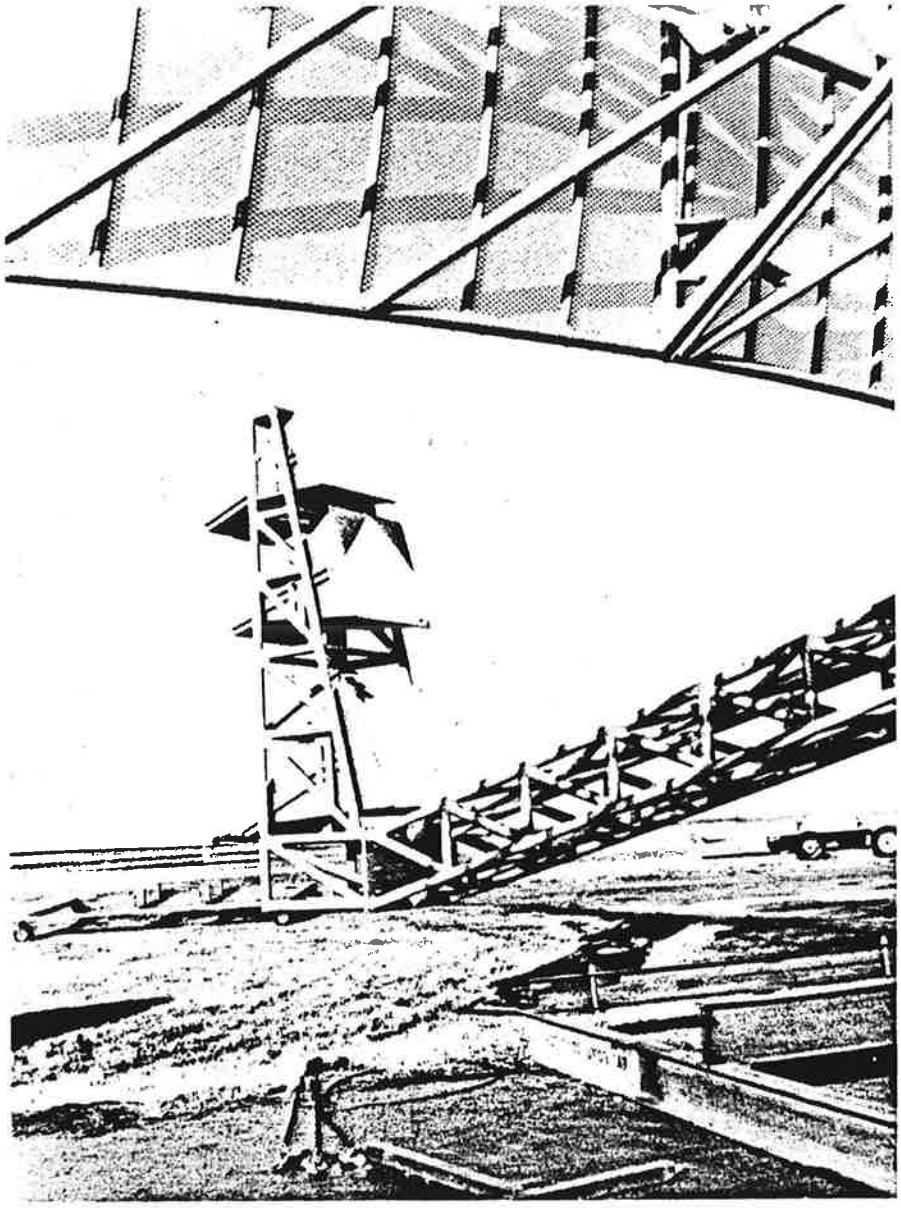

Figure 2-24. Feed Horns

Cross Polarization

A doubly-curved reflector will always generate a small cross-polarized component. Cross polarization increases as the feed horn(s) are increasingly offset, and is also greater for short-focus (small f/d) reflectors.

In the ATCRBS reflector, offset feeds are necessary to minimize aperture blockage, and even with a reasonably long focal length, a considerable cross-polarized component was generated. The upper feed horn, which provides coverage nearest the horizon, is least offset and produces little cross polarization. At higher elevation angles, however, cross polarization becomes significant.

Cross polarization is undesirable because it can introduce errors in monopulse direction finding. Severe cross polarization, in combination with a badly de-polarized airborne target, could also cause beam skewing on a PPI display. It is fortunate that cross polarization is lowest near the horizon, so that angular accuracy is not degraded for long-range targets.

Initial pattern range tests for the ATCRBS reflector showed that cross-polarization exceeded specification limits. The calculated data, Figure 2-6, predicted that cross-polarization was a potential problem, and measured levels were several dB worse than calculated.

To reduce cross-polarization, a polarization-sensitive screen of horizontal conductors was installed over the outer wings of the reflector. Only the outer area of the reflector was covered because that is where most of the de-polarization occurs; the center 16 feet of the reflector was not covered. The grid consisted of approximately 90 horizontal 0.060-inch diameter wires spaced at 1.25-inch intervals over each wing of the reflector.

A planar grid of this spacing would give 12 dB of attenuation to a horizontally polarized TEM Wave. An improvement of less than 12 dB actually resulted, for the following reasons:

- the grid was not planar, but followed the reflector elevation contour,
- only part of the reflector was covered,
- horizontal currents in the grid radiated some cross-polarized energy.

Nevertheless, the grid did reduce cross-polarization to specified values. Figures 2-25 and 2-26 show measured cross-polarization levels with the grid installed.

The horizontal wires which make up the grid are actually 0.060-inch diameter stainless steel cables. These cables are quite strong, and are

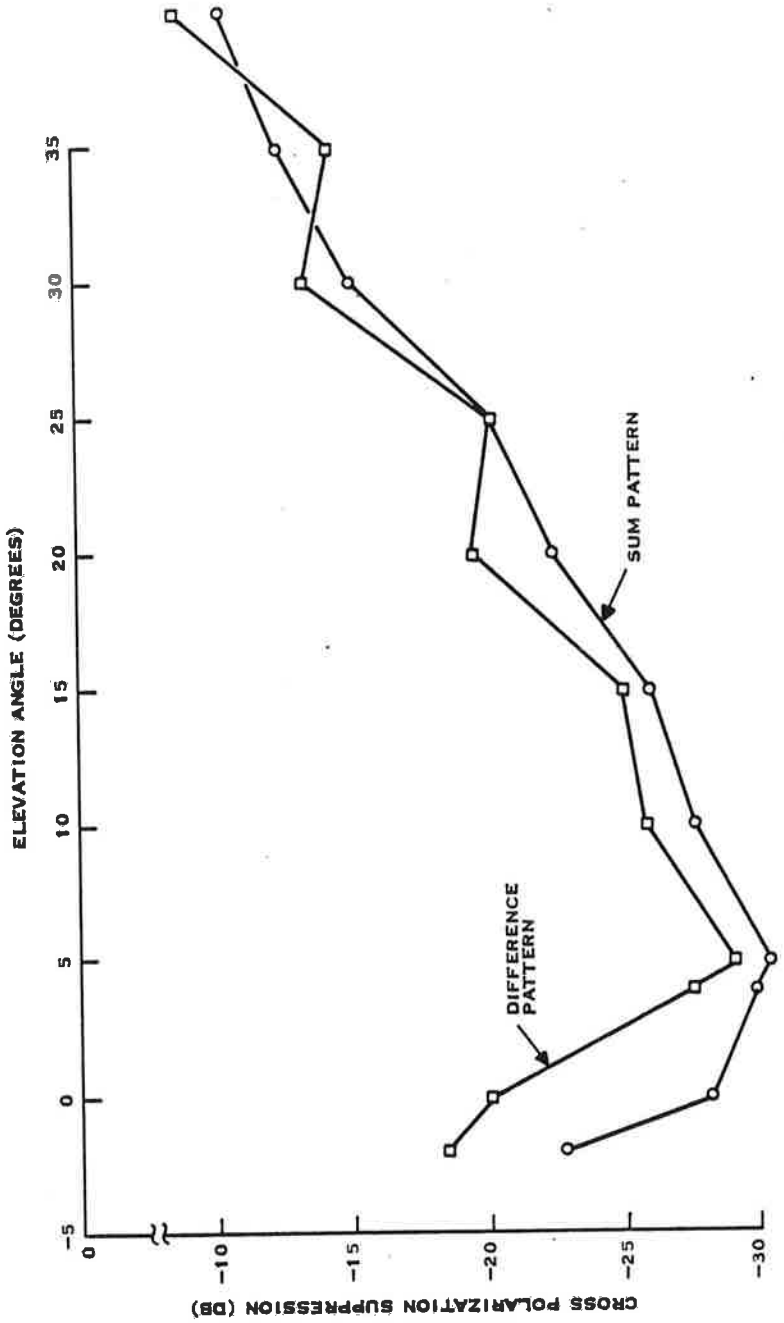

Figure 2-25. Cross Polarization at 1030 MHz

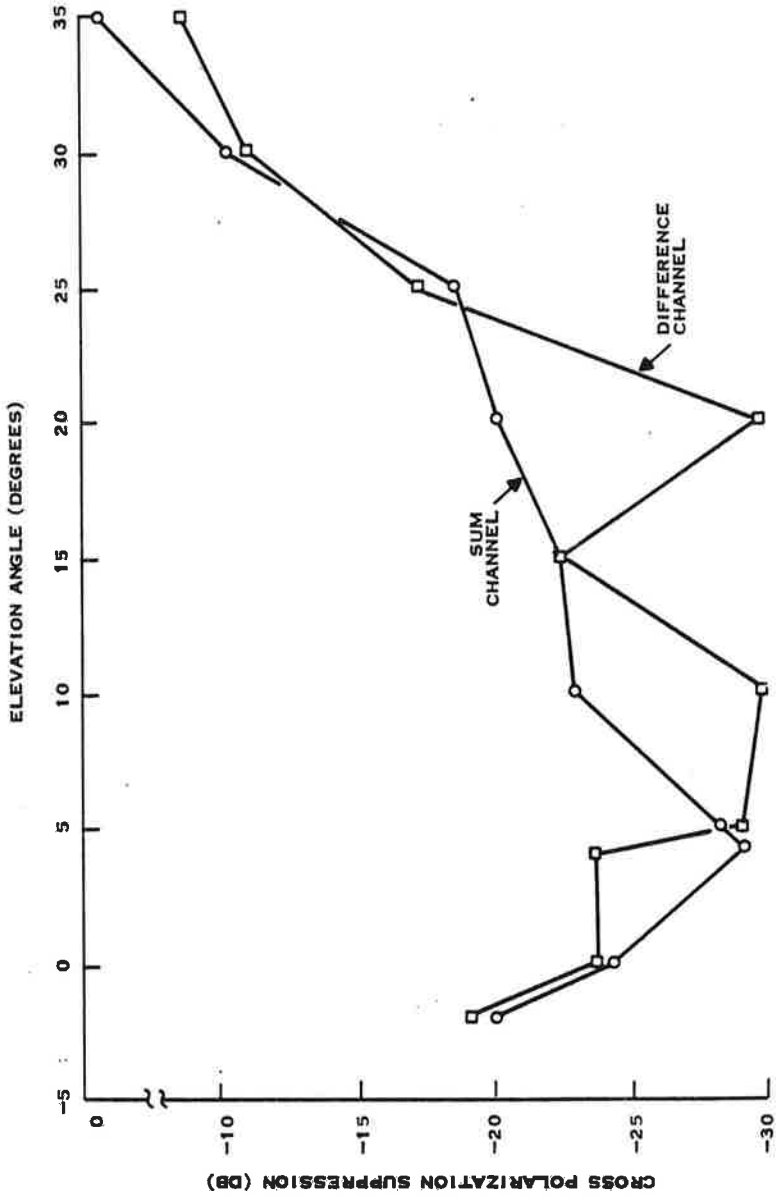

Figure 2-26. Cross Polarization at 1090 MHz

very resistant to fatigue failure. Each cable is attached directly to the reflector screen, seven feet in from the edge of the reflector, using a screw, nut and washer installed through a crimped loop in the cable. At the outer edge, the cable is attached to the reflector using a small tensioning spring which is hooked through the reflector screen. This spring keeps the cable straight and tight, while allowing freedom of movement if it is inadvertently snagged.

Any damaged grid wire can be easily replaced by un-hooking the tensioning spring and removing the screw at the inboard end. One damaged grid wire, or even several damaged wires will not significantly change cross polarization, so if a grid wire should be damaged, it is recommended that it simply be removed. In approximately one and one-half years of use, there has been no evidence of damage to, or foreign objects caught in, the grid.

Backlobes

Backlobes on a reflector antenna result from feed energy which is "spilled over" the edges of the reflector. Relative backlobe level is dependent on edge illumination, reflector size, and reflector gain. The ATCRBS reflector has an edge illumination of -8 dB (composite for all three horns). This edge taper will ensure about -30 dB backlobes for a normal pencil beam reflector. The ATCRBS reflector, however, because of its highly spoiled elevation beam, has about 7 dB less gain than an equivalent pencil-beam reflector, so relative to beam peak, a higher backlobe level (about -23 dB) is indicated for ATCRBS.

Measured backlobe level is plotted in Figure 2-27. Typical backlobe structure is shown in the 360-degree pattern plot of Figure 2-28. All values are within the 21 dB specification limits. As pointed out, these backlobe levels were measured in great-circle cuts rather than in conical cuts, so they do not represent exactly the backlobes as seen by a target aircraft, except at 0 degrees elevation. Airborne recorded data from field test, which represents true conical-cut data, confirms that backlobes are approximately -23 dB.

Studies of SLS operation, considering the effects of differential lobing, have shown that the -21 dB backlobe specification is probably too high; backlobes should be -25 dB or greater to prevent backlobe punch-through for all targets. Backlobes for the ATCRBS reflector can be improved by designing for greater edge illumination taper, particularly at the top and bottom of the reflector. Edge illumination can be increased by narrowing the feed horn patterns or by increasing the height of the reflector. A combination of these two approaches is believed to be the optimum path for backlobe reduction on the ATCRBS reflector.

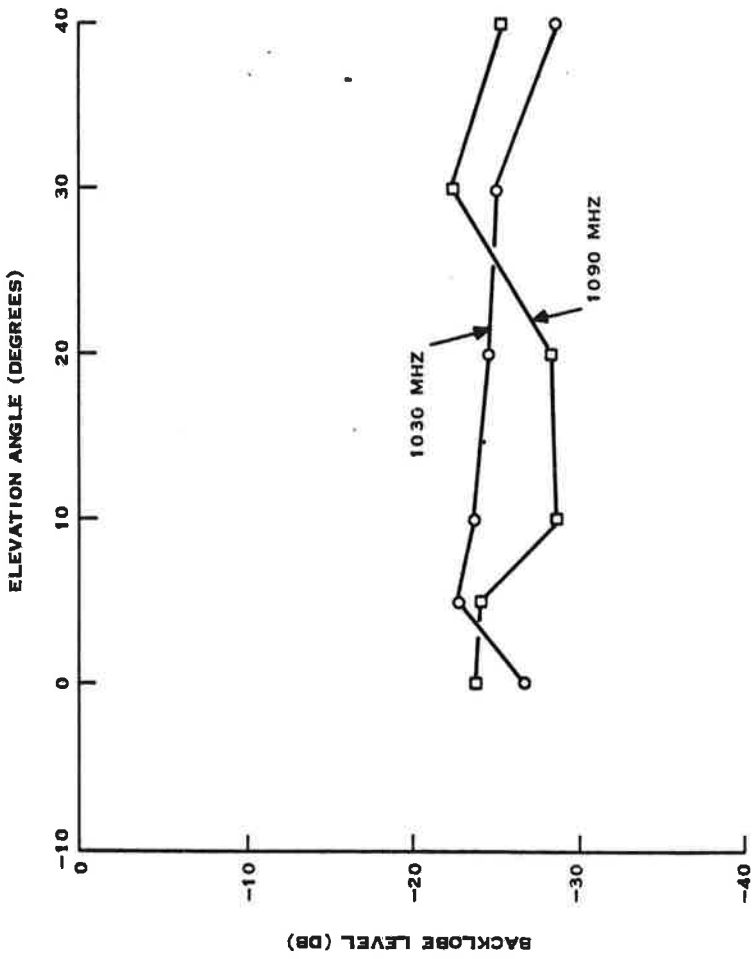

Figure 2-27. Measured Backlobe Level

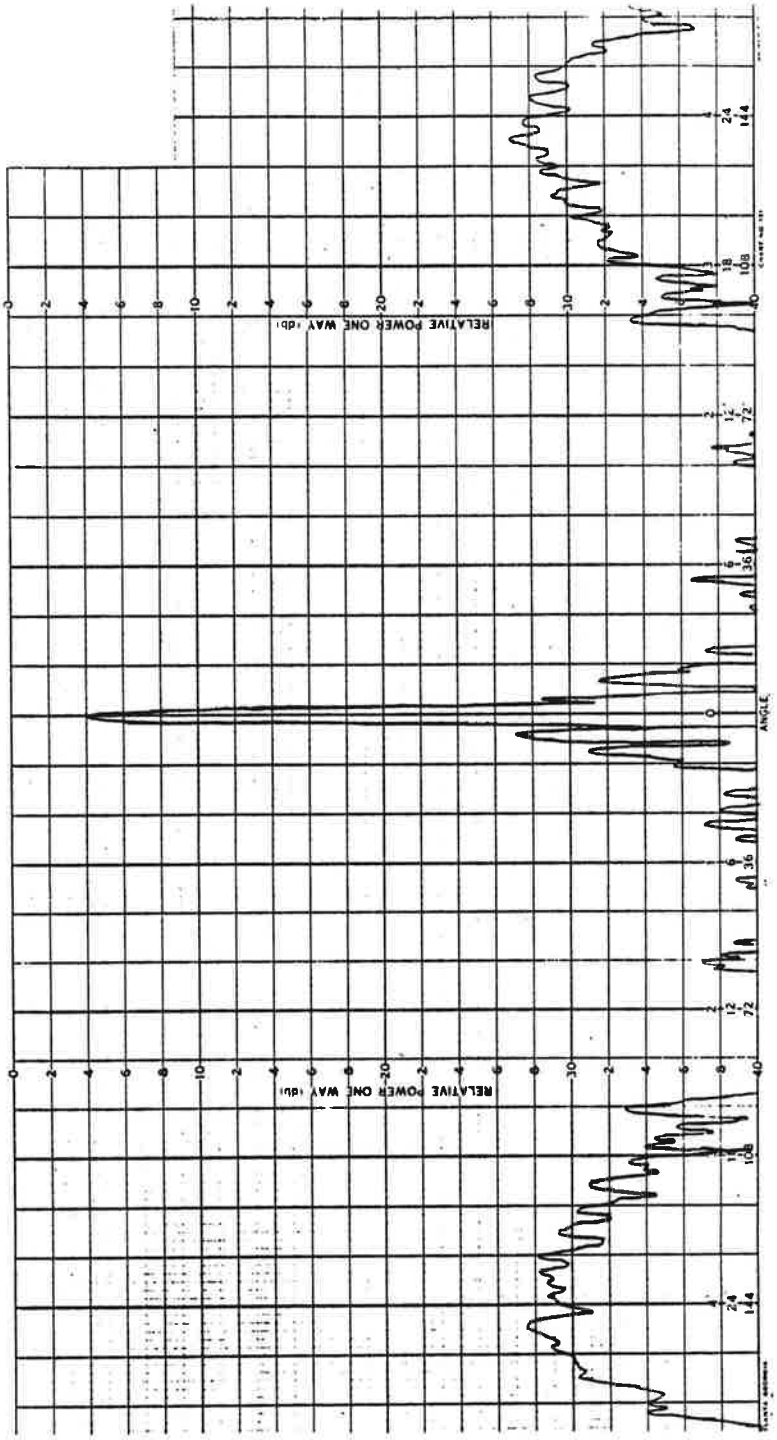

Figure 2-28. 360-Degree Azimuth Pattern at Nose of Beam (1030 MHz)

SECTION III

PEDESTAL, DRIVE SYSTEM, AND ROTARY JOINT

General

A pedestal and drive system were designed and fabricated for use with the ATCRBS system. The drive system has the capability to synchronize the rotation of the antenna to an associated primary radar, such as an ASR-7 or an ARSR-2. The drive assembly is designed for mounting on a standard ASR tower. An antenna control rack houses the electronic circuits required to maintain synchronization; this rack is designed for installation in the radar shelter. Figures 3-1 and 3-2 show photographs of the drive system and controller.

Pedestal

The ATCRBS pedestal is a standard ASR-7 design, modified by cutting away part of the drive motor support to accomodate the synchronized drive system. Because the ATCRBS antenna is larger than the ASR-7 antenna, dead weight loads and wind loads on the pedestal are increased. Analysis has shown that, even with the greater loads, the ASR-7 pedestal with the ATCRBS reflector will survive almost any wind and ice conditions.

Mechanical Design

Major pedestal components are shown in Figure 3-3. The reflector and feed are attached to the spider casting. The spider casting and base casting are held together by the main bearing. The ring and pinion gear set rotates the spider casting and antenna. Reduction ratio for the ring and pinion set is 5.38:1. All major pedestal parts are aluminum, except the gears and bearing which are steel. The pedestal includes 1X and 10X synchros for azimuth position pickoff. The synchros are 115V, 60 Hz units; they are not presently used in the ATCRBS system but are available for use if required later.

Loading

Wind creates the greatest loads on the pedestal. It is calculated that a 130-knot wind exerts a 138,000-foot-pound overturning moment on the ASR-7 reflector when the reflector screen is coated with ice. The ASR-7 pedestal is designed to survive this load, and has demonstrated the capability in actual tests. The larger ATCRBS reflector will, of course, see even higher wind loads. Figure 3-4 compares the overturning moment for the ASR and ATCRBS reflectors. Fully iced, the ATCRBS reflector reaches a 138,000-foot-pound over-turning moment at 105 knots wind velocity, and 214,000-foot-pounds at 130 knots. The pedestal has been tested to the 105-knot value and calculations predict that it will survive the 130-knot value, although with almost zero safety factor.

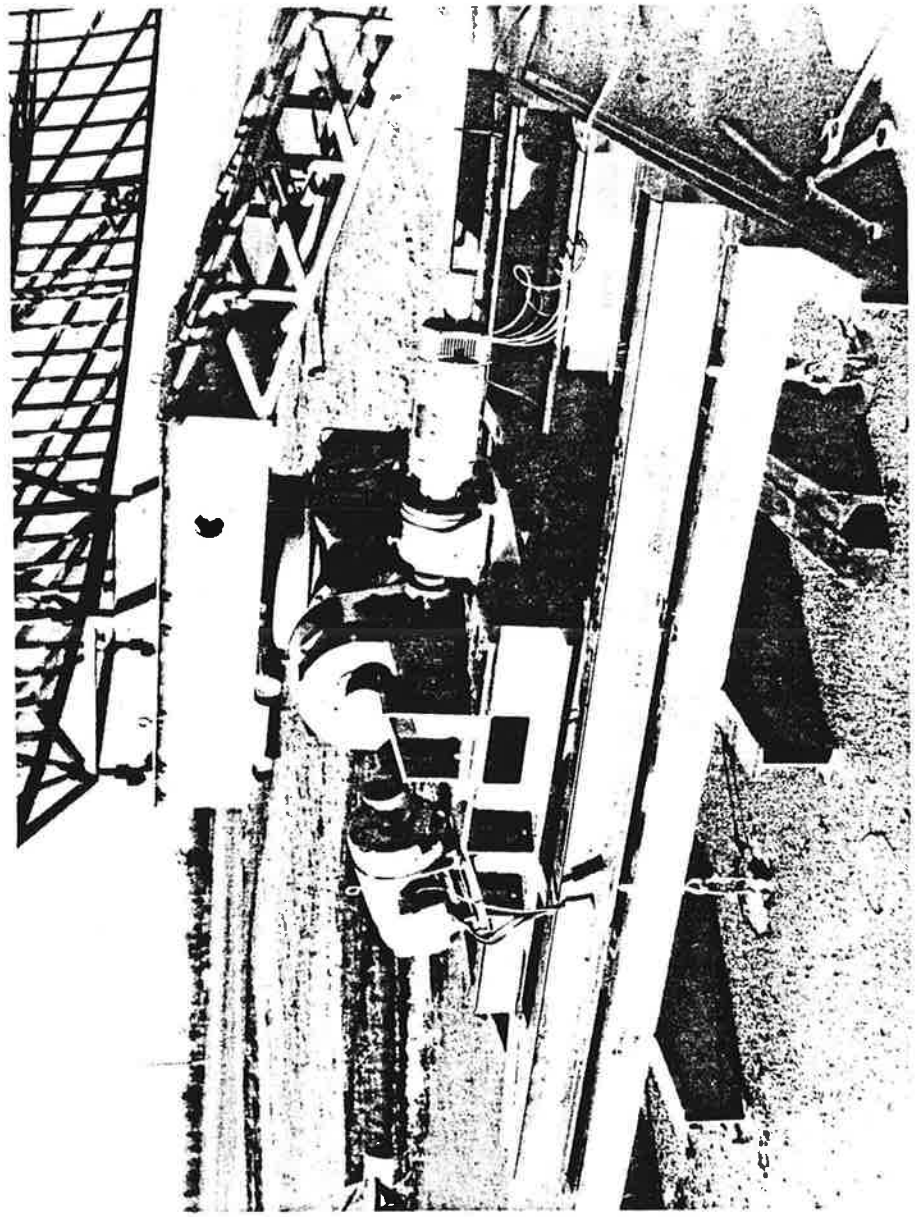

Figure 3-1. ATCRBS Drive System

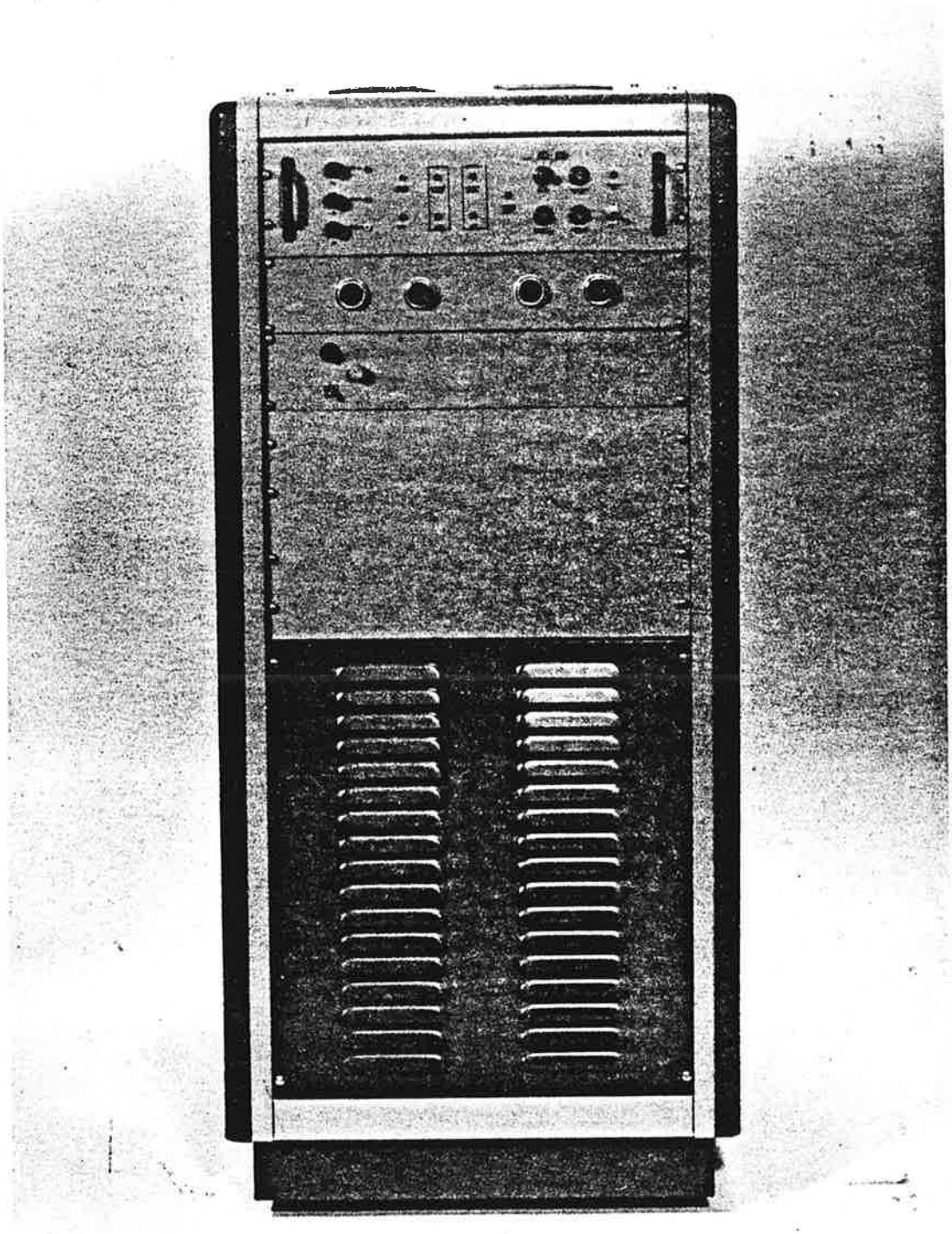

Figure 3-2. Antenna Controller

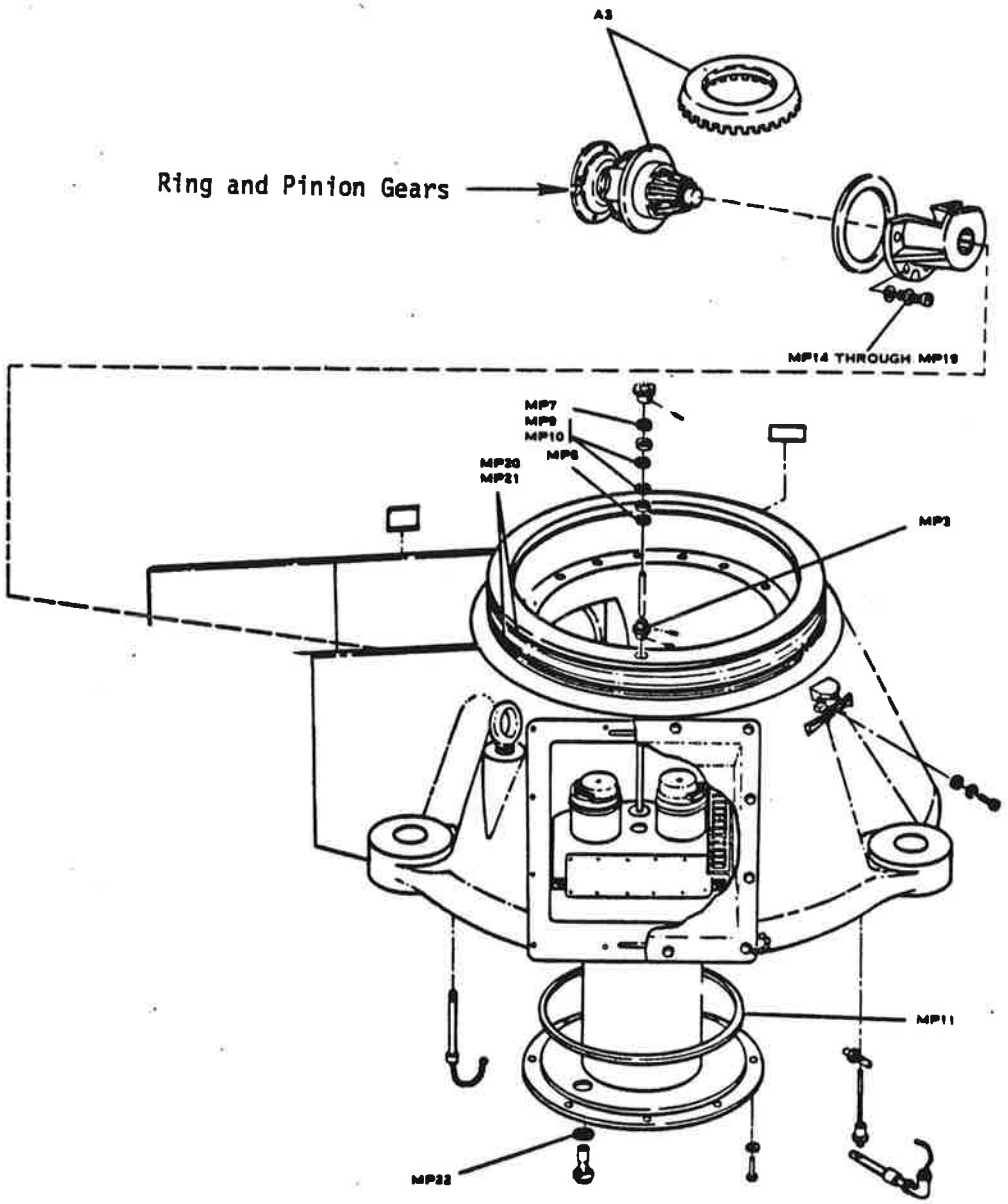

Pedestal Casting

Figure 3-3. Pedestal Components (Sheet 1 of 2)

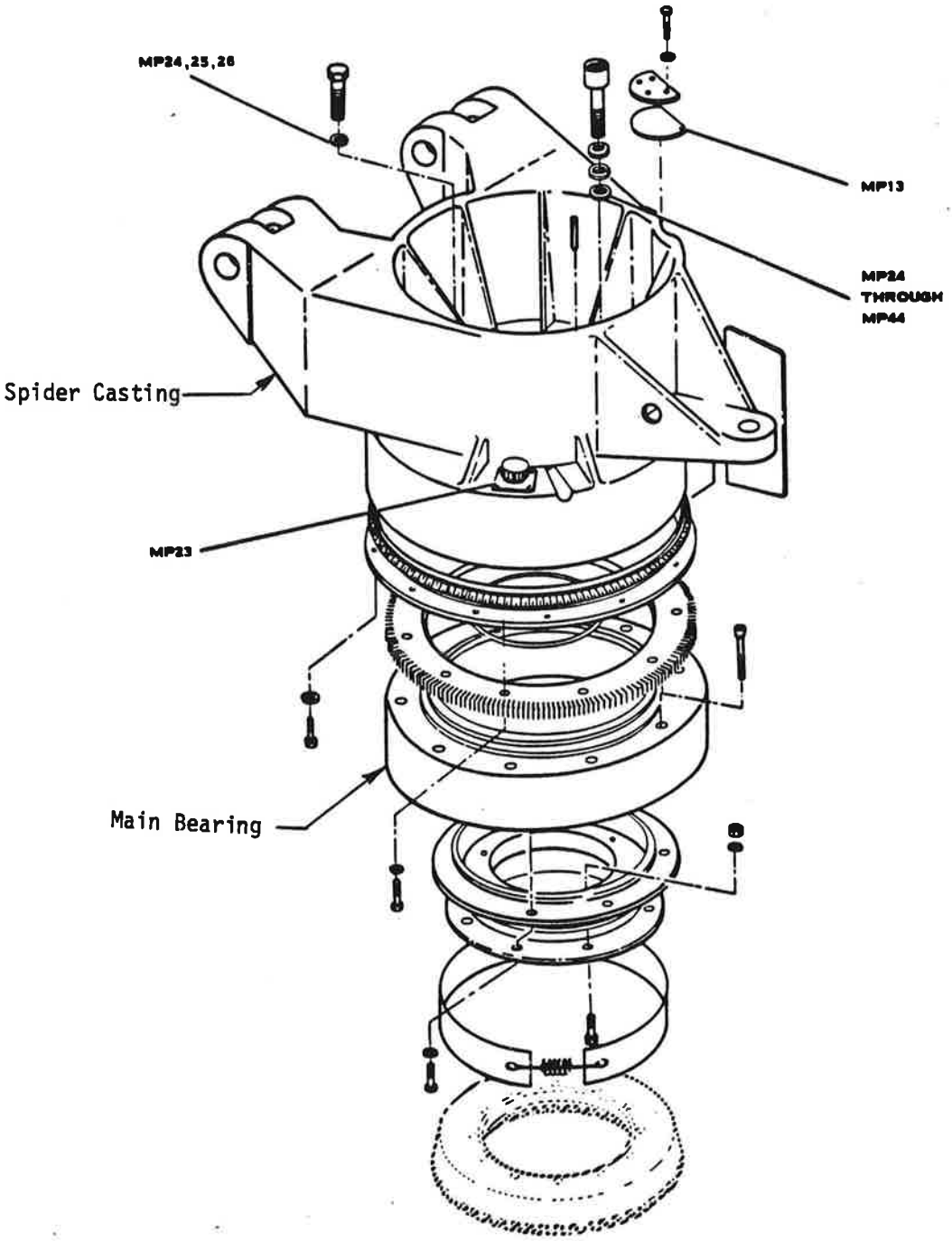

Spider Casting and Main Bearing

Figure 3-3. Pedestal Components (Sheet 2 of 2)

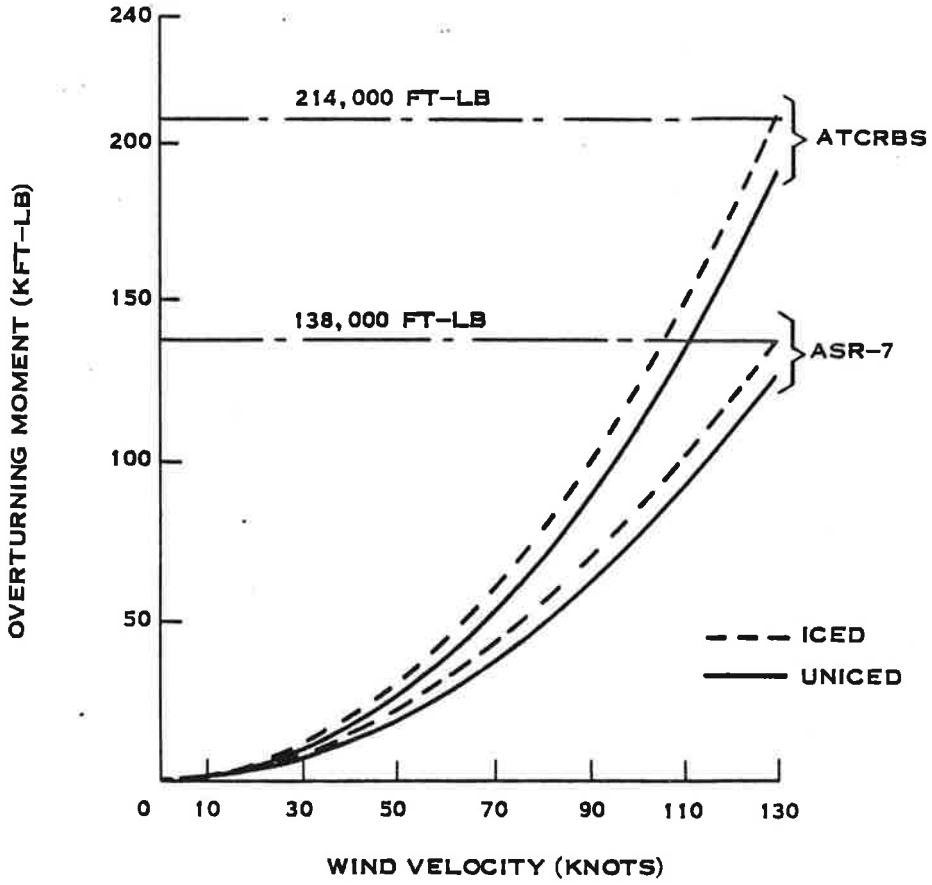

Figure 3-4. Calculated Overturning Moment Versus Wind Velocity

Wind also causes a torque on the pedestal which opposes the rotation (yaw torque). This yaw torque determines the drive horsepower for the antenna, and affects design of the pedestal gears. Figures 3-5 and 3-6 show the calculated yawing moment for a reflector rotating at 12.6 RPM in 85-knot and 30-knot winds. To maintain 12.6 RPM rotation of an iced reflector in an 85-knot wind, the motor is required to deliver an average of 35 horsepower. The ring and pinion gears are designed with a considerable margin for safety, and are entirely adequate for the torque encountered with the ATCRBS reflector.

Drive System

The drive system is shown in Figure 3-1. It consists of a planetary gearbox, servo motor, and main drive motor. (The main drive motor is coupled to the planetary gearbox through a small right-angle gearbox, not shown in the photograph). The main drive motor provides the torque necessary to rotate the antenna. The planetary gearbox serves two important purposes: it acts as a speed reducer for the main drive motor, to give the correct antenna speed, and it acts as a differential gearset through which the servo motor makes azimuth corrections to main synchronization. The servo motor is a reversible DC motor which corrects antenna speed and position errors; it is controlled by a closed-loop servo system.

Motors

The main drive motor is a 30-horsepower, design "B", induction motor. This is 15 percent less than the 35-horsepower maximum predicted by the yaw-torque analysis; however, discussions with motor manufacturers revealed that electric motors can be operated intermittently at above rated horsepower if adequate cooling is provided. The conditions that require maximum horsepower, high winds and/or subfreezing temperatures, will, of course, afford excellent motor cooling, so both motors are rated for continuous horsepower slightly below the absolute maximum required for an iced reflector in 85-knot winds. The drive motor is a dual speed unit; it can provide either 1725 RPM or 860 RPM outputs depending on how the motor windings are connected. This dual speed capability allows synchronization to a variety of ASR and ARSR radars. The motor requires 3-phase, 460 VAC, 60 Hz primary power.

Servo motor horsepower is fixed by a servo stability requirement which dictates that the main motor and servo motor must apply equal torques at the antenna axis. Since the servo motor gear reduction ratio is greater than the main motor reduction ratio by a factor of 18.5, servo motor horsepower should be:

$$\frac{30}{18.5} = 1.62 \text{ horsepower.}$$

A 2-horsepower, separately excited, DC motor was selected for the servo motor application. Maximum servo motor speed is 1800 RPM.

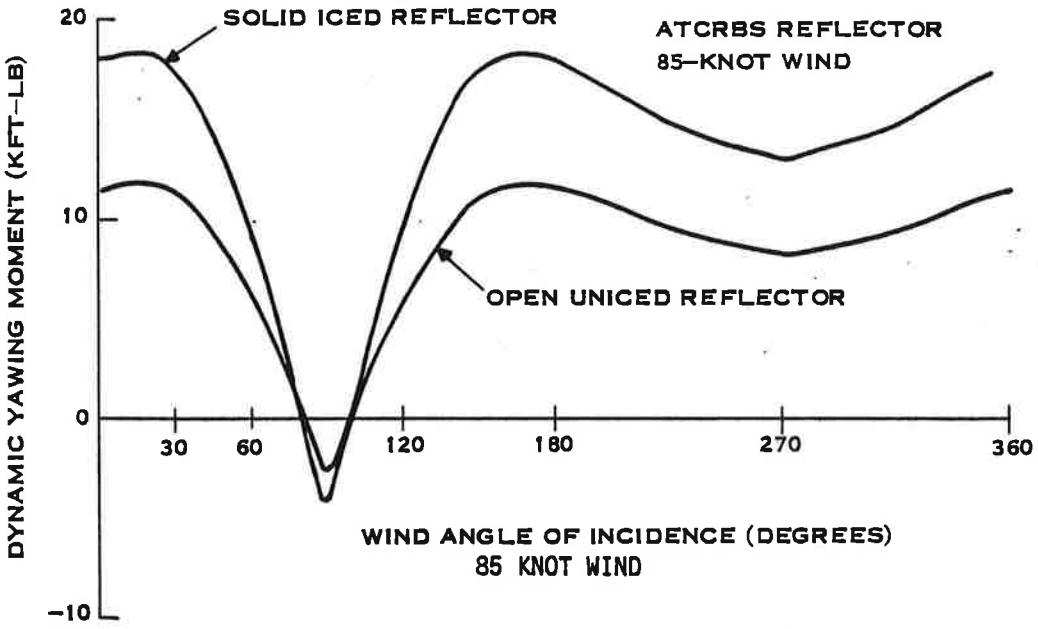

Figure 3-5. Calculated Dynamic Yawing Moment Versus Wind Angle of Incidence

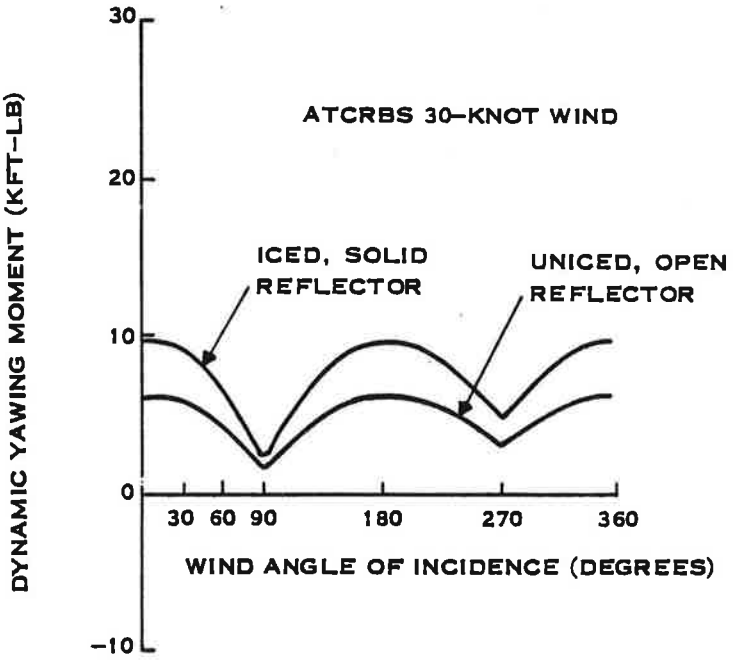

Figure 3-6. Calculated Dynamic Yawing Moment Versus Wind Angle of Incidence, 30-Knot Wind

Planetary Gearbox

A schematic drawing of a planetary gearset is shown in Figure 3-7. The main drive motor rotates the input sun gear. The ring gear is normally locked so that it does not rotate, so sun gear rotation causes the planet gears to rotate in an orbit around the sun. The output shaft, connected to the planet carrier, therefore rotates with the input. Speed reduction from input to output is fixed by the relative diameters of the sun, ring, and planets.

Rotation of the ring gear will also cause the planets (and hence the output shaft) to rotate. The servo motor can rotate the ring gear through the worm gear and worm wheel as shown in the diagram, to make small corrections in output shaft position. Use of a worm gear allows "free-run" operation with the servo-motor turned off, because friction in the worm prevents the ring gear from "back-driving" the servo motor.

The ATCRBS reflector uses multiple-stage planetary gearset, designed for 40-horsepower at 1800 RPM input. Reduction ratio from the main drive motor input to the gearbox output is 25.9:1. Reduction ratio from the worm gear input to the gearbox output is 53.5:1.

Servo Motor Gear Reducer

An integral gear reducer is bolted to the face of the servo motor. This reducer is a parallel-shaft, helical gear unit, with a reduction ratio of 9.5:1. This additional reduction gives the servo motor sufficient torque to meet the torque-balance requirement at the planetary gearset.

Right-Angle Gearboxes

The main drive motor is coupled to the planetary gearbox input through a right-angle gearbox. This gearbox is designed for 40 horsepower at 1800 RPM input. Two interchangeable gearboxes were supplied, one with a reduction ratio of 1:1 and another with a ratio of 1.29:1. For 12.6 or 6.3 RPM operation, the 1:1 gearbox is used. For 5 RPM operation, the 1.29:1 gearbox is used.

Reduction Ratios and Antenna Speeds

Overall gear reduction from the main drive motor to the antenna axis, including the right-angle gearbox, planetary gear reducer, and pedestal gears, is 139.3 with the 1:1 right-angle gears of 179.8 with the 1.29:1 right-angle gears. Using the full-load drive-motor speeds of 1725 RPM and 860 RPM, this gives antenna rotation rates of 12.4 RPM or 6.2 RPM with the 1:1 gearbox, and 9.6 RPM or 4.8 RPM with the 1.29:1 gearbox. The drive motor turns faster under lighter loads such as mild winds and no ice; it has been found that nominal rotation rates are 12.9 RPM or 6.4 RPM with the 1:1 gearbox, and 10.0 or 5.0 RPM with the 1.29:1 gearbox.

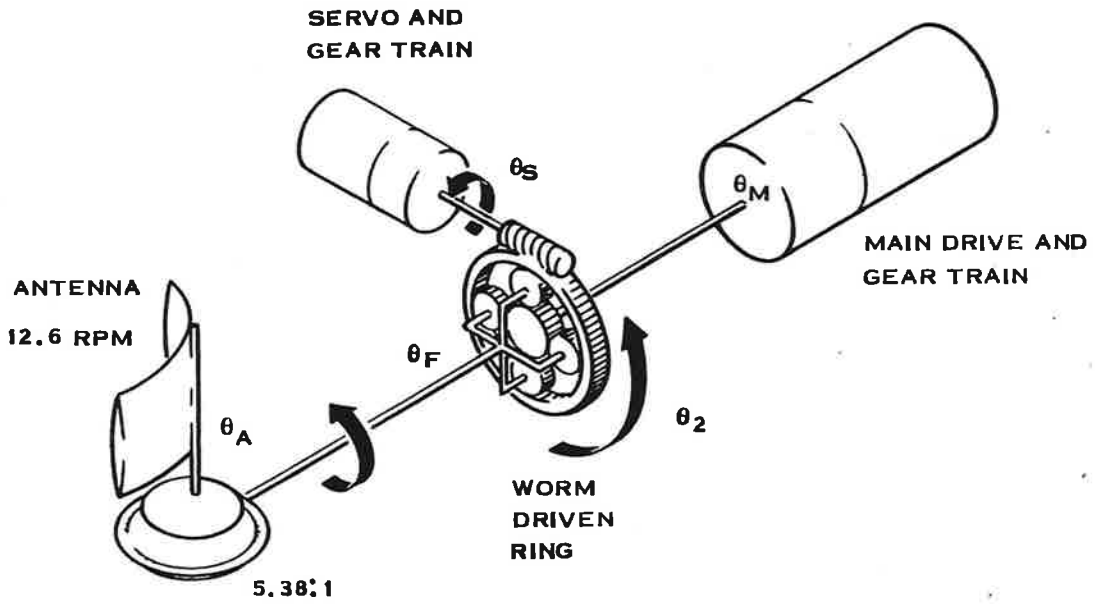

Figure 3-7. Planetary Gearset, Schematic Representation

Overall reduction ratio for the servo motor, including the integral speed reducer, worm gear, planetary gears, and pedestal, is 2734:1. Thus, the 1800 RPM servo motor can speed-up or slow-down the antenna rotation by 0.65 RPM.

Using the servo motor to vary the antenna speed, in combination with the various possibilities for main motor speed and right-angle gearbox ratios, a wide range of antenna speeds can be realized. These speed ranges are summarized in Figure 3-8. Additional speed possibilities could be realized by interchanging the gears in the 1.29:1 gearbox to give it a ratio of 0.78:1. Note, however, that drive motor torque would be inadequate for maximum wind conditions with this configuration.

Antenna Controller

Synchronization of the primary radar and ATCRBS antenna is accomplished by comparing ACP/ARP data from the ASR and ATCRBS antennas to derive an error voltage. The error voltage is amplified and used to drive the servo motor which corrects the position of the ATCRBS antenna relative to the ASR. Position correction is accomplished through the differential planetary transmission. A block diagram of the synchronization system is shown in Figure 3-9.

The electronic equipment required to detect and correct synchronization errors is housed in an equipment rack which is collectively called the antenna controller (Figure 3-2). The controller contains the error detection circuitry to sense synchronization errors, and the SCR circuitry to drive the servo motor. The error detection unit receives azimuth change pulses (ACP's) and azimuth reference pulses (ARP's) from both the primary radar and ATCRBS pedestals. Beginning at each ARP, the error detection unit counts ACP's from each antenna to derive a separate 12-bit binary number indicating the position of each antenna. These numbers are subtracted digitally to derive a digital error signal and then D/A converted to give an analog error signal for the motor controller.

The motor controller contains a full-wave, single-phase rectifier bridge for the motor field supply and a full-wave, single-phase thyrister bridge for armature control. Drive circuitry in the controller converts the input error voltage into properly timed pulses to trigger the thyristor gates.

Synchronization Accuracy

During the 30-day ATCRBS reliability demonstration, considerable data was recorded showing the tracking accuracy which could be achieved by the closed-loop synchronization system. The tracking accuracy achieved during light winds is shown in Figure 3-10; accuracy is consistently better than 1/4-degree, and is typically better than 1/8-degree.* For a PRF of

*It is believed that the accuracy is limited somewhat by the ACP sampling rate (about 1/12-degree) and by jitter in the ACP pulse train. To design a system for greater tracking accuracy, 13-bit or 14-bit encoders are recommenced for the ATCRBS and ASR antennas.

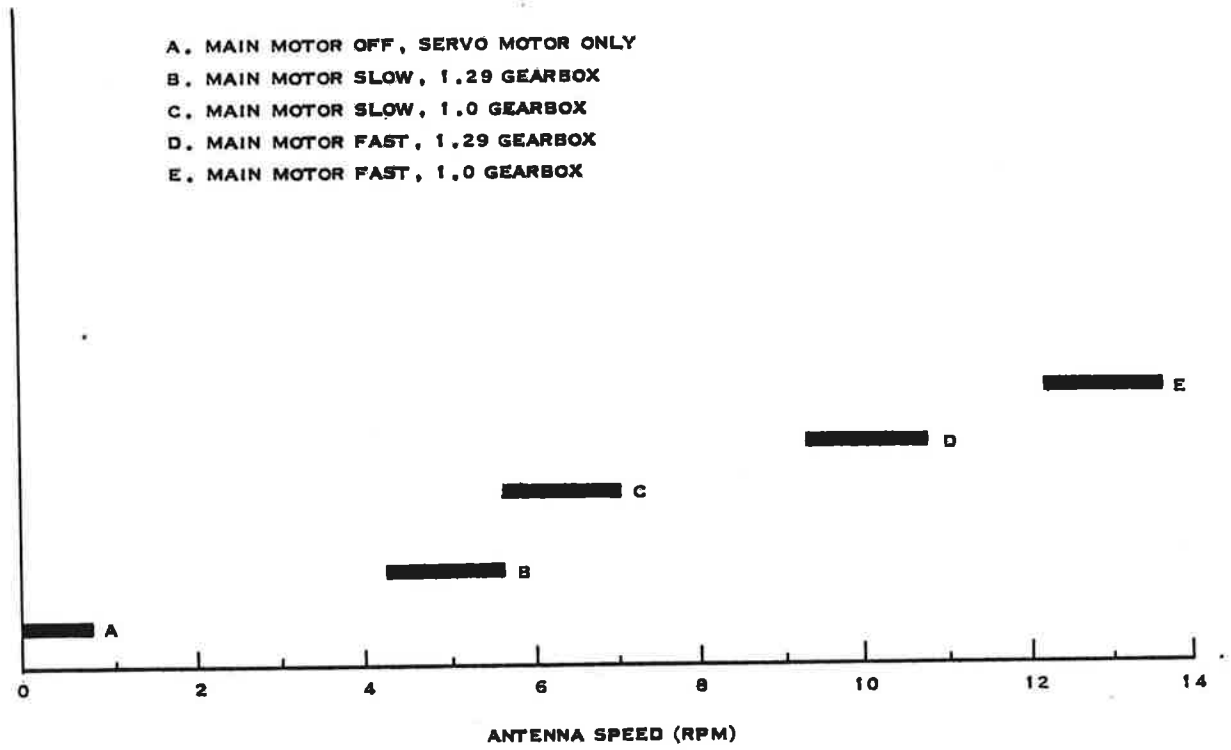

Figure 3-8. ATCRBS Reflector Rotation Rates

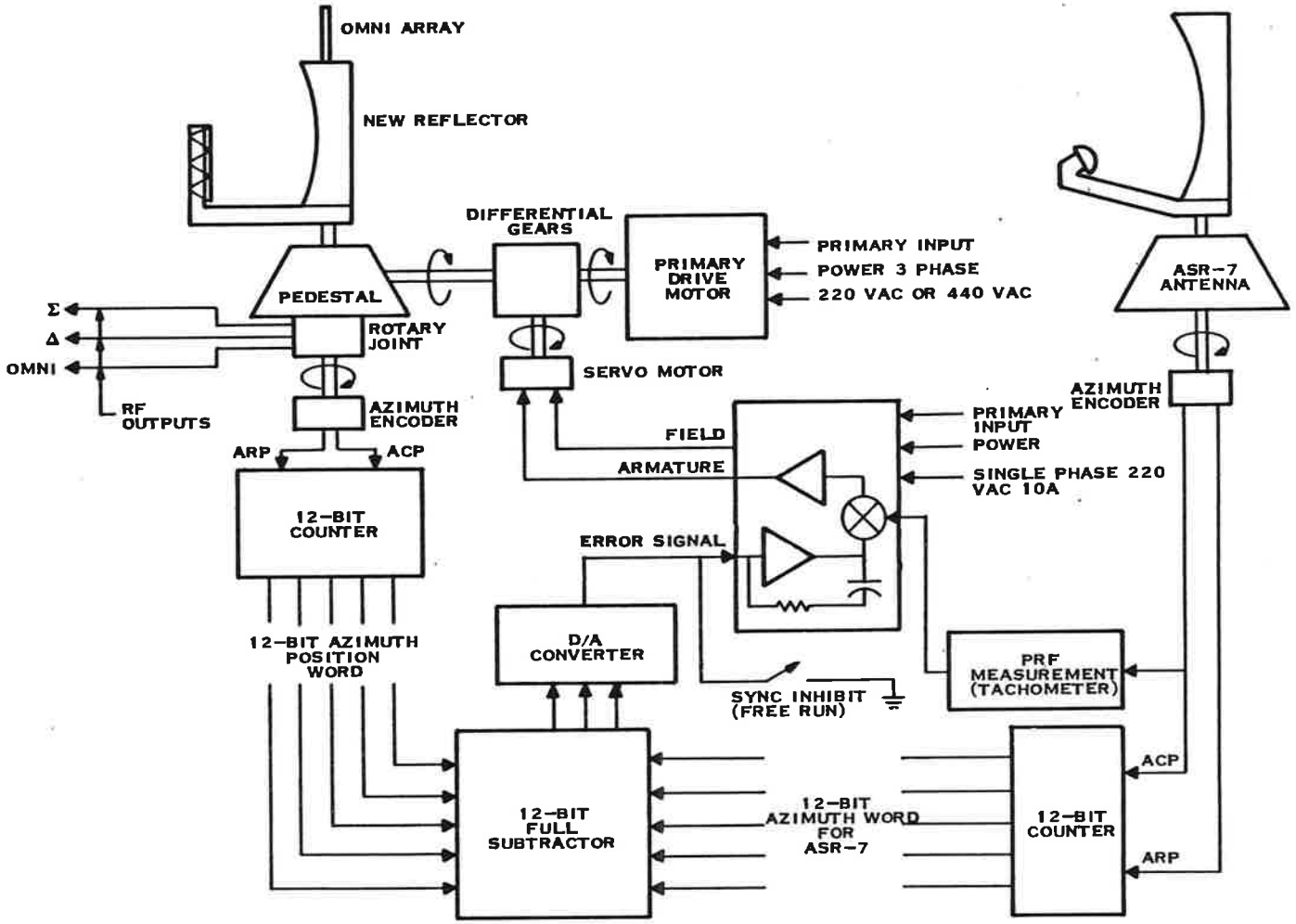

Figure 3-9. Antenna Controller, Block Diagram

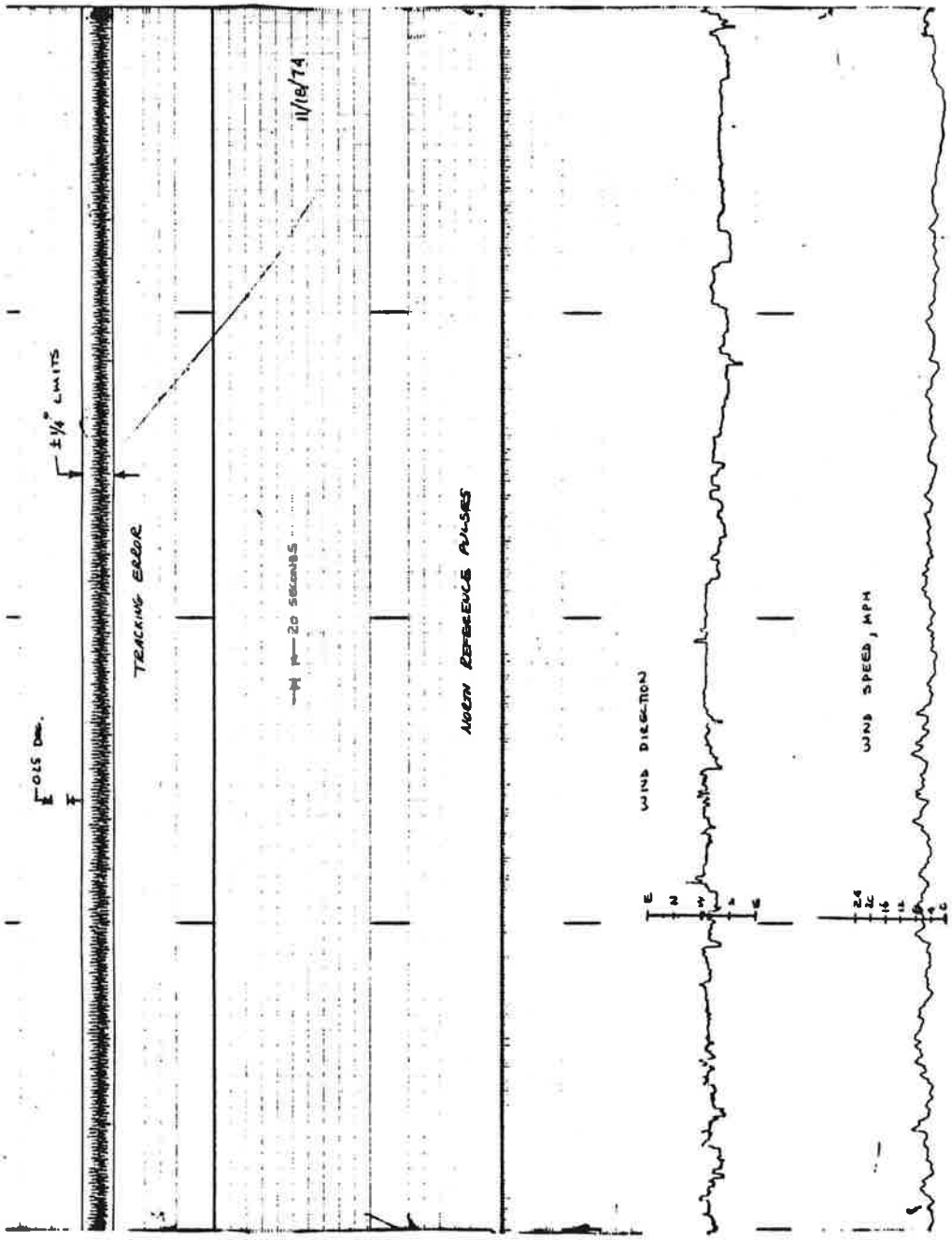

Figure 3-10. Tracking Error in Light Winds

315 Hz, the ATCRBS interrogator issues an interrogation about every 1/4-degree, so the tracking error is generally less than the width of one "hit" as seen on PPI display. In field tests, PPI observations and photos have shown no anamolies which have been attributed to synchronization errors; an observer is entirely unaware that he is viewing radar and beacon data from separate pedestals.

In higher winds, some errors up to 3/4 degree have been noted. These errors are apparently due to backlash in the pedestal gears when a gust of wind catches the feed horns. These errors are very short-lived, and are corrected by the synchronization system within a few tenths of a second.

In an automated system employing monopulse direction finding, where greater accuracy is desired, synchronization errors are of no particular consequence, because the APG data from the ATCRBS antenna can be used directly, for a very accurate indication of ATCRBS antenna position.

Rotary Joints

DICO Rotary Joint

During development of the ATCRBS reflector, a three-channel RF rotary joint was purchased from Diamond Antenna and Microwave Company (DICO). This rotary joint, shown in Figure 3-11, is a rubbing contact, RF slip ring design. The manufacturer's data sheet, shown in Figure 4-13, describes the principal electrical characteristics of the rotary joint. Phase measurements are not shown on the data sheet, but other measurements verified that phase wow is less than 3-degrees and phase tracking between channels is within 2-degrees.

During early system checkout, this rotary joint failed several times, apparently due to seizure of the rubbing contacts. The unit was subsequently repaired by the manufacturer; however, because reliability seemed questionable, this unit was reserved as a spare, and a new rotary joint, which employed an entirely non-contacting design, was developed.

Non-Contacting Rotary Joint

The new rotary joint, designed and built by Texas Instruments, is an entirely non-contracting unit with three identical, independent rotating sections. The design (See Figure 3-13) includes a mounting ring and drive shaft for the azimuth pulse generator (APG). Mounting interfaces are designed for direct installation in the ATCRBS pedestal. Input and output connectors are type "N" female.

Electrically, each rotary joint channel is basically a coaxial transmission line bent into an annular ring, as shown in Figure 3-14. The center conductor is fed with equal-amplitude in-phase signals at six places, resulting in a uniform amplitude, uniform phase TEM standing wave around the ring. The ring is split in half in the plane of the ring

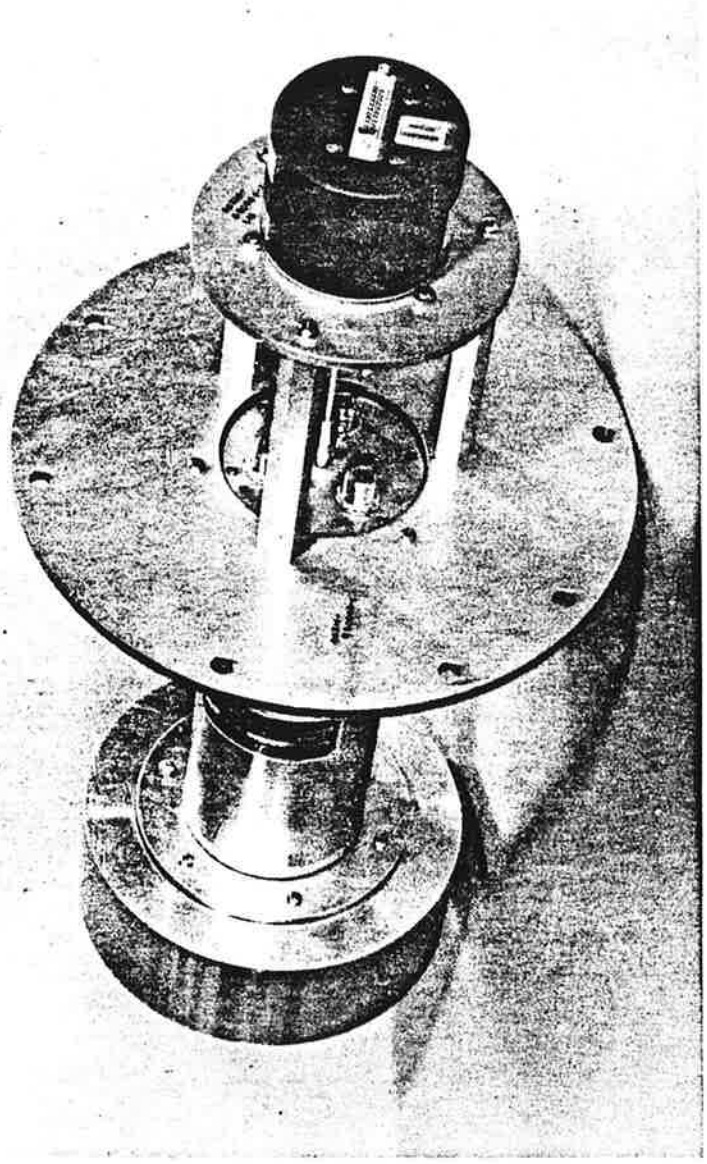

Figure 3-11. DICO Rotary Joint

DIAMOND ANTENNA & MICROWAVE CORP.
WINCHESTER, MASS.

TEST DATA SHEET

ITEM THREE-CHANNEL ROTARY JOINT

DIAMOND PART NO. 2313 SERIAL NO. 001

CUSTOMER Texas Instruments

P.C. NO. 52-743613 SPEC. NO. _____ TESTED BY HST

DIAMOND WORK ORDER NO. 21153RO DATE 4/19/74

CHANNEL I	Freq/GHz	VSWR	Ins. Loss/DB	WOW/db (less than)
	1010	1.17	.30	.05
	1050	1.18	.35	.05
	1090	1.17	.25	.05
CHANNEL II	1010	1.16	.35	.05
	1050	1.15	.30	.05
	1090	1.15	.30	.05
CHANNEL III	1010	1.19	.35	.05
	1050	1.17	.20	.05
	1090	1.11	.30	.05

DICO

ISOLATION:	Ch I-II	Ch II-III
1010	50+ db	50+ db
1050	50+ db	50+ dh
1090	50+ db	50+ db

Figure 3-12. DICO Rotary Joint Data Sheet

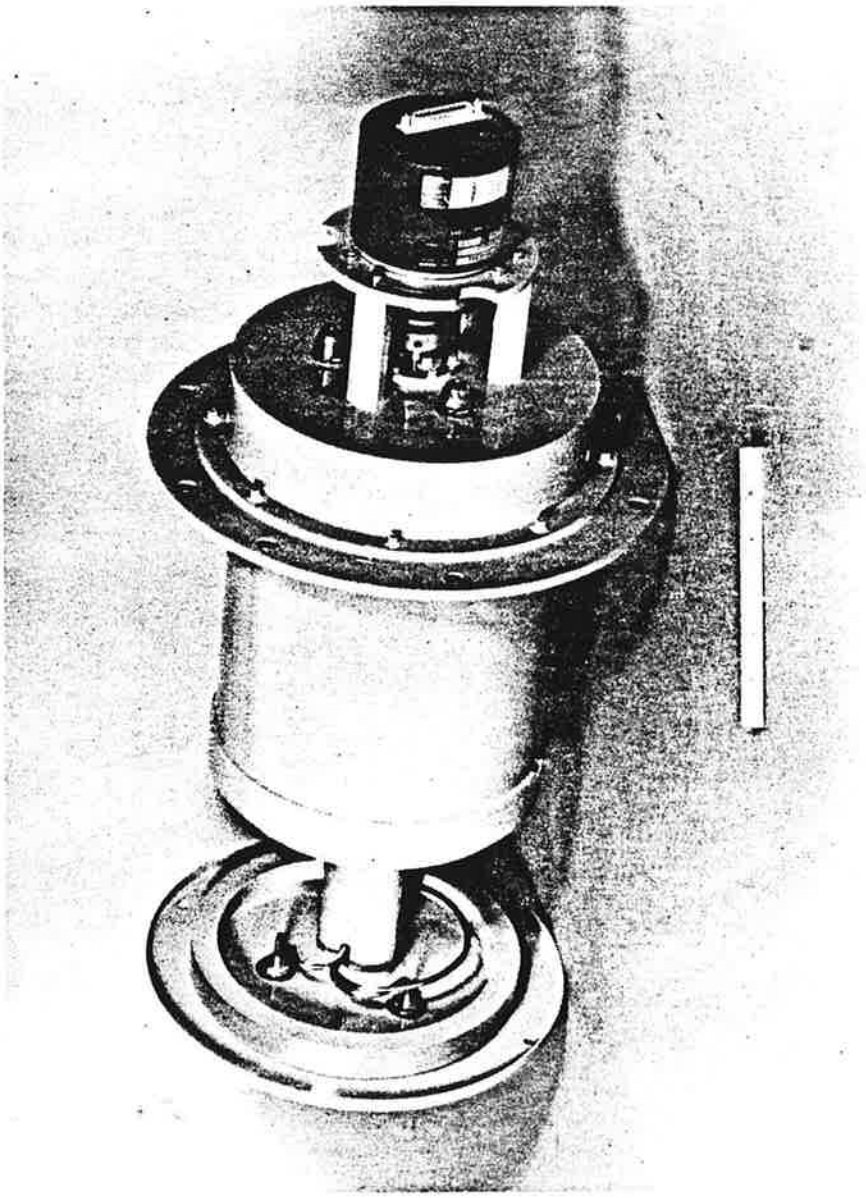

Figure 3-13. Three-Channel L-Band Rotary Joint

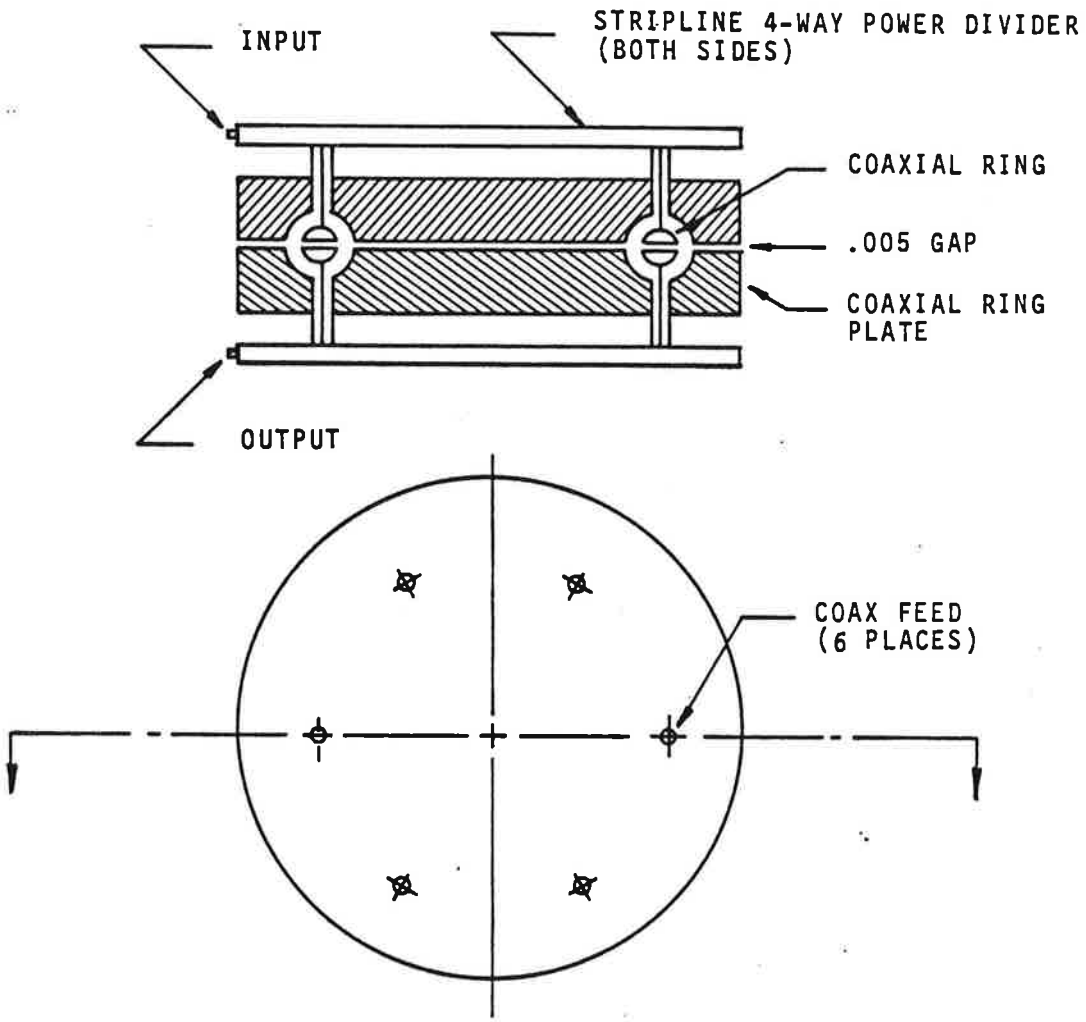

Figure 3-14. Coaxial Ring Rotary Joint

to permit rotation of the upper half relative to the lower half; the split does not disturb the TEM coaxial mode in the ring. By feeding both halves of the ring with stripline power dividers, a rotary joint design is realized which has very low phase and amplitude WOW. To make a three-channel rotary joint, three of these rings are stacked vertically. The large hole in the center of the ring provides room for the rotating RF cables and for the APG drive shaft. Each rotary joint is individually held in position by a precision ball bearing, and all three rings are sealed in an aluminum housing. Texas Instruments has a patent application pending on this design.

This rotary joint concept was originally developed for use in Texas Instruments ASR-8 radar. (In the ASR-8 configuration, three S-band rotary joint channels also pass through the center of the ring.) The ASR-8 configuration has successfully completed a series of severe environmental tests including temperature cycles in the presence of high humidity and salt spary. These tests provide assurance that the design is suitable for many years of service in a harsh environment.

Measured electrical performance for the new ATCRBS rotary joint is shown in Table 3-1.

Table 3-1. Electrical Performance of Texas Instruments Rotary Joint.

Frequency Band: 1.06 ± .03 GHz

	VSWR	INS. LOSS (dB)	WOW (dB)	Phase Tracking (Degrees)
Channel I	<1.15	0.64	0.05	±1.5
Channel II	<1.10	0.65	0.04	±1.5
Channel III	<1.15	0.66	0.05	±1.5
Isolation	I - II	I - III	II - III	
	> 60 dB	> 70 dB	> 60 dB	

SECTION IV

OMNIDIRECTIONAL ARRAYS

General

An SLS antenna having omnidirectional azimuth coverage is used in ATCRBS system to transmit the sidelobe blanking pulse P2. The omni antennas developed for use with the ATCRBS Improvement antennas are vertical collinear arrays having elevation patterns with characteristics matching the associated directional antennas; that is, fast rolloff of energy below the horizon, and uniform-gain or modified-cosecant coverage above the horizon. Three omni designs are discussed in the following sections; one for use with the ARSR-2 integral feed, and two different designs for use with the new ATCRBS reflector.

Omni for ARSR-2 Integral Feed

This omni was designed to have a vertical pattern shape approximating the modified-cosecant pattern of the ARSR-2 radar reflector. During the initial design phase, preliminary specifications were developed for this omni; a brief summary of these specifications is as follows:

Frequency of Operation	1030 ±2 MHz
Elevation Beamshape	Modified Cosecant, with field-selectable beam tilt
Horizon Cutoff (at -6 dB)	2.5 dB/degree
Azimuth Beamshape	
0 to +5° Elevation	Omnidirectional ±1 dB
+5° to +40° Elevation:	Omnidirectional ±1.5 dB
Gain, relative to linear isotropic:	+6 dB
Input VSWR	< 1.5
Power Handling	2.2 KW peak

General Description

The omni for the ASR-2 modification kit is a 16-element array fed with a stripline power divider network. The array element is a unique bent-slot design developed by Texas Instruments specifically for use in shaped-beam ATCRBS omni antennas. The stripline feed network provides the correct phase and amplitude at each element to yield a modified-cosecant pattern. A photograph of the array is shown in Figure 4-1. Figure 4-2 shows a picture of the NAFEC installation at Elwood, New Jersey, where this omni was field tested.

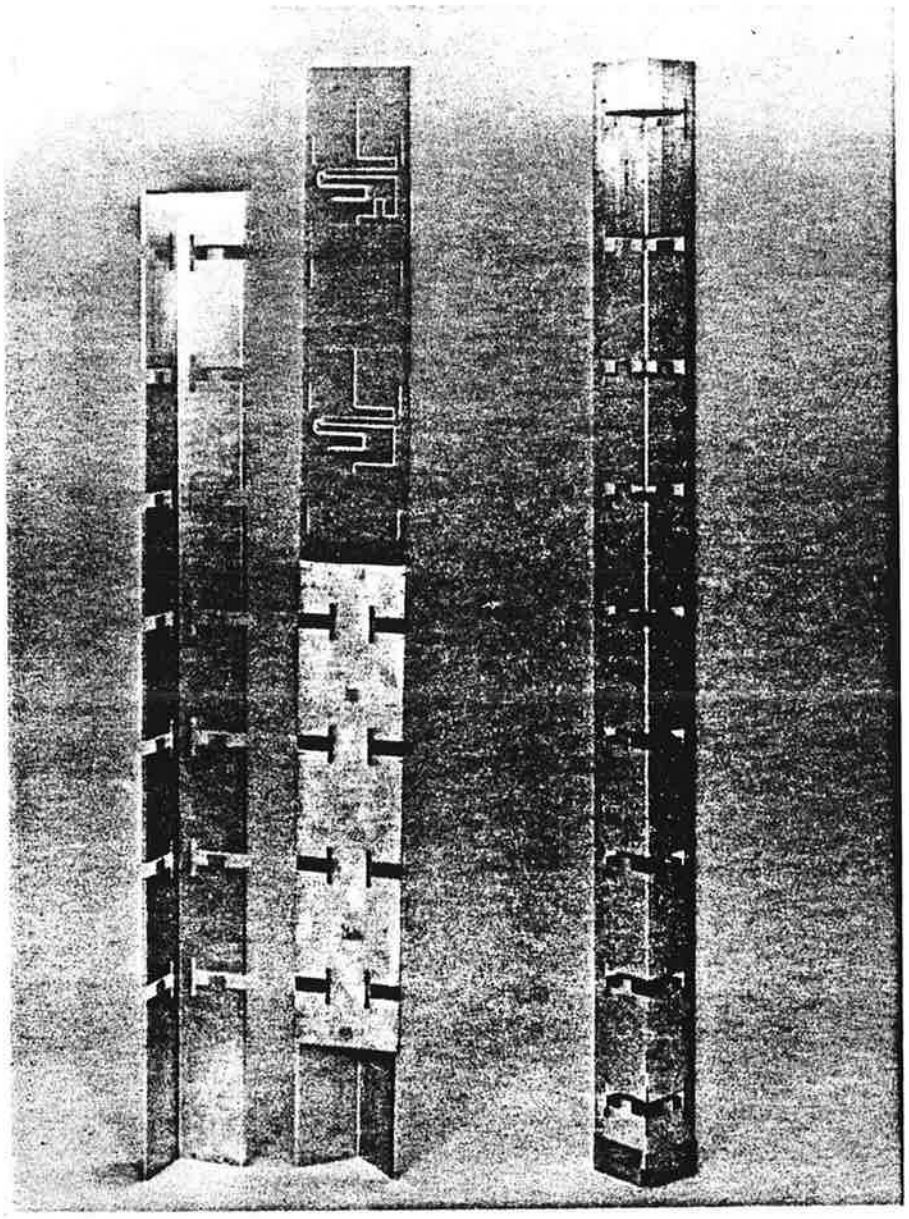

Figure 4-1. Omnidirectional Array Hardware

Figure 4-2. ARSR Omni Installation at Elwood, New Jersey

Radiation Patterns

A comparison of elevation patterns for the ARSR-2 modification kit and the associated omni are shown in Figure 4-3. Because the ARSR reflector is much taller (23-feet) than the omni (9-feet), horizon cutoff is not as sharp and the 3 dB beamwidth is greater. Computer simulation has shown that this mismatch does not drastically alter SLS operation.

The elevation pattern cuts off quickly above +30 degrees, much like the directional pattern. Field test results, however, showed a need for more high angle SLS coverage, in order to adequately blank high-angle backlobes (spillover) from the reflector. It is recommended that future ARSR omni antennas should be synthesized for greater high-angle coverage.

An azimuth pattern at +5 degrees elevation is shown in Figure 4-4. Variation from true omni-directionality is typically ±1 dB. Cross polarization is suppressed better than 22 dB.

Gain was measured as +7 dB, and input VSWR was measured as 1.25:1. A complete set of test data may be seen in the technical data report entitled ATCRBS Omni Directional Antenna (ARSR-2 Modification), 28 February 1974.

The omni array is housed in a sealed fiberglass radome which protects the array from moisture and ice, and provides a rigid structure to withstand high winds. Because the radome wall is separated from the array by several inches, a layer of ice will not severely de-tune the elements, thus preserving good patterns. The radome is made of filament-would fiberglass tubing, and will withstand 130-knots without failure.

Dipole Omni for ATCRBS Reflector

General

The omnidirectional antenna originally designed for the new rotator is a twelve-element collinear array of microstrip dipole elements, spaced at 0.59 wavelengths. A stripline corporate feed network provides the necessary phase and amplitude exictations to yield a sector elevation pattern similar to that of the reflector. A photograph of this array is shown in Figure 4-5. This antenna was subsequently replaced by a re-designed omni having improved high angle coverage and better azimuth omni-directionality. Therefore, the dipole omni has never been used in actual field tests.

Measured Characteristics

A comparison of elevation patterns for the omni and directional antennas is shown in Figure 4-6. The two patterns match closely across the main portion of the beam. The omni has slightly less gain at the horizon and slightly more gain at +30 degrees. A major drawback is that the omni level falls off quite rapidly at angles above +30 degrees, allowing possible

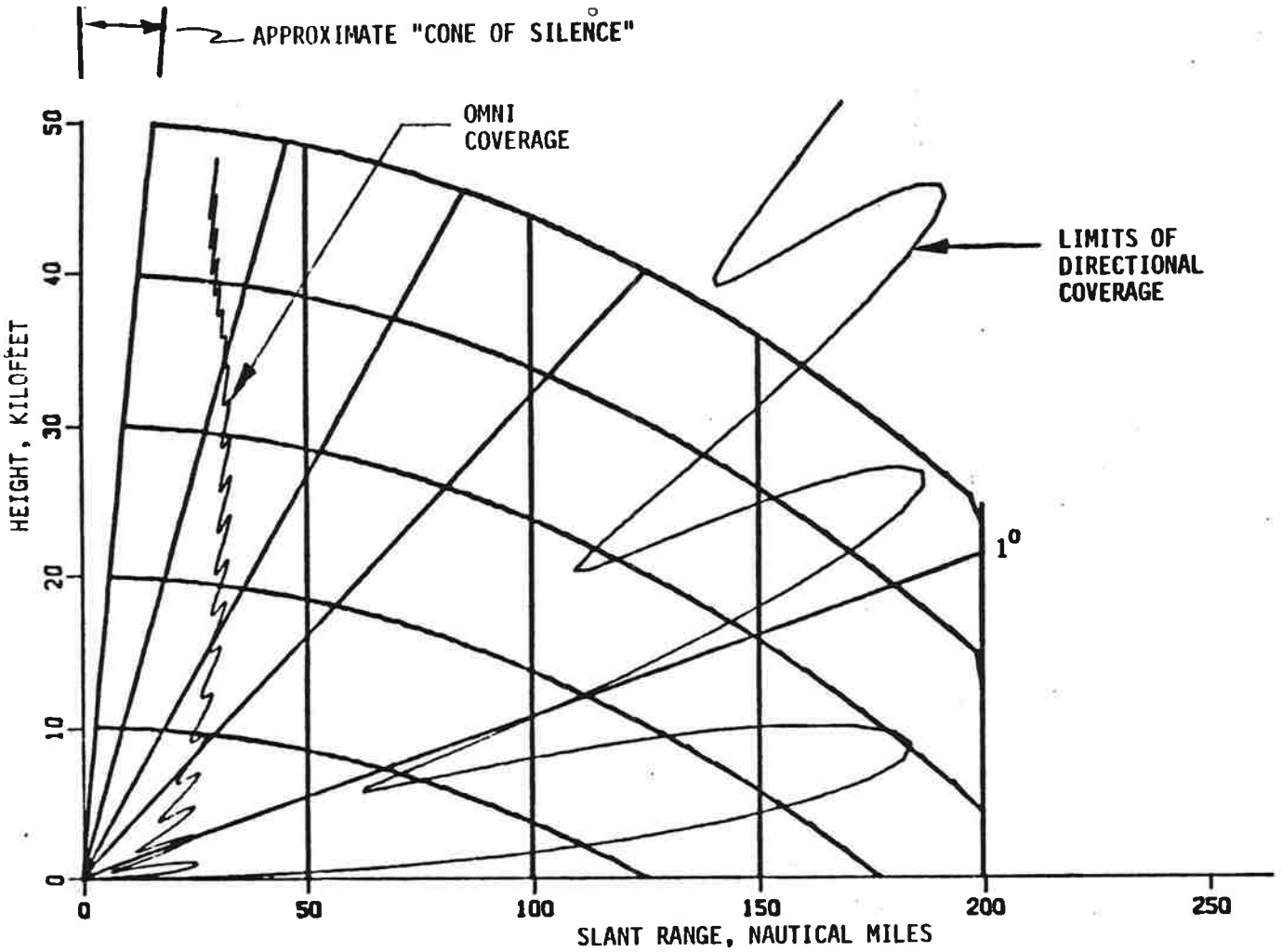

Figure 4-3. ARSR-2 Directional Elevation and Omni Elevation Patterns

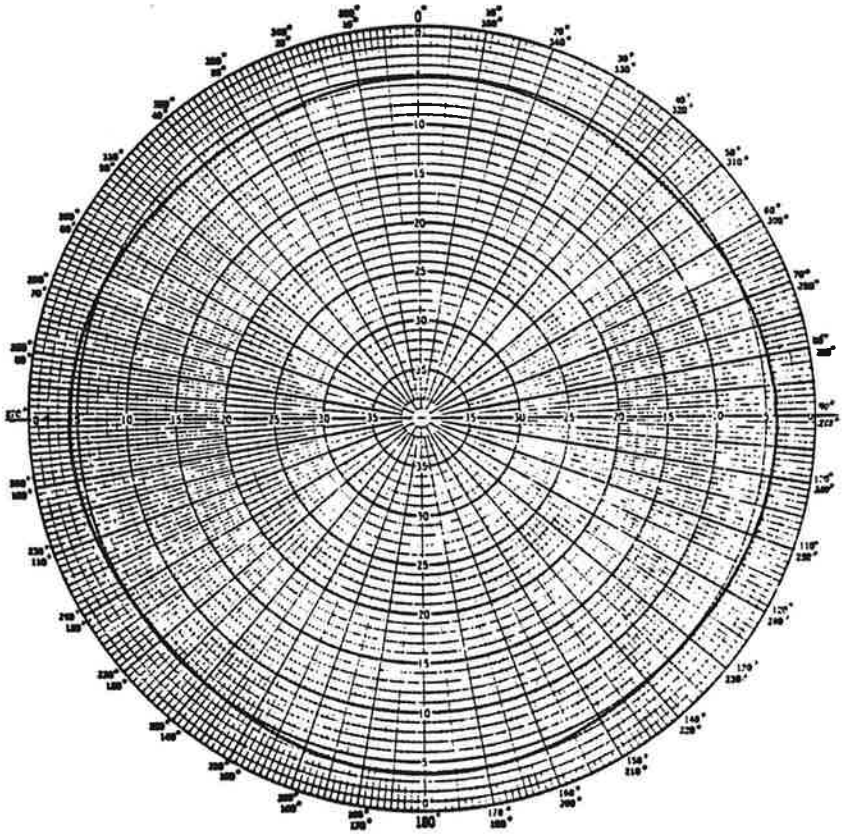

Figure 4-4. Azimuth Pattern at +5 Degrees Elevation

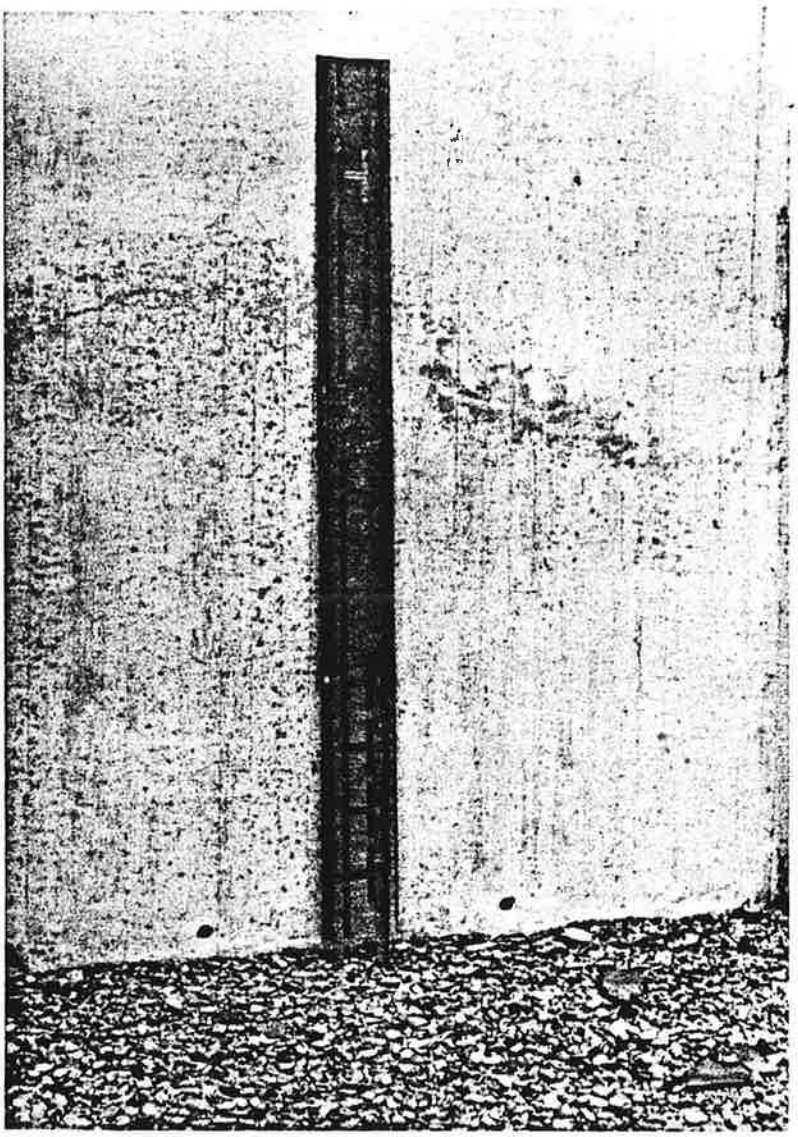

Figure 4-5. Collinear Dipole Array

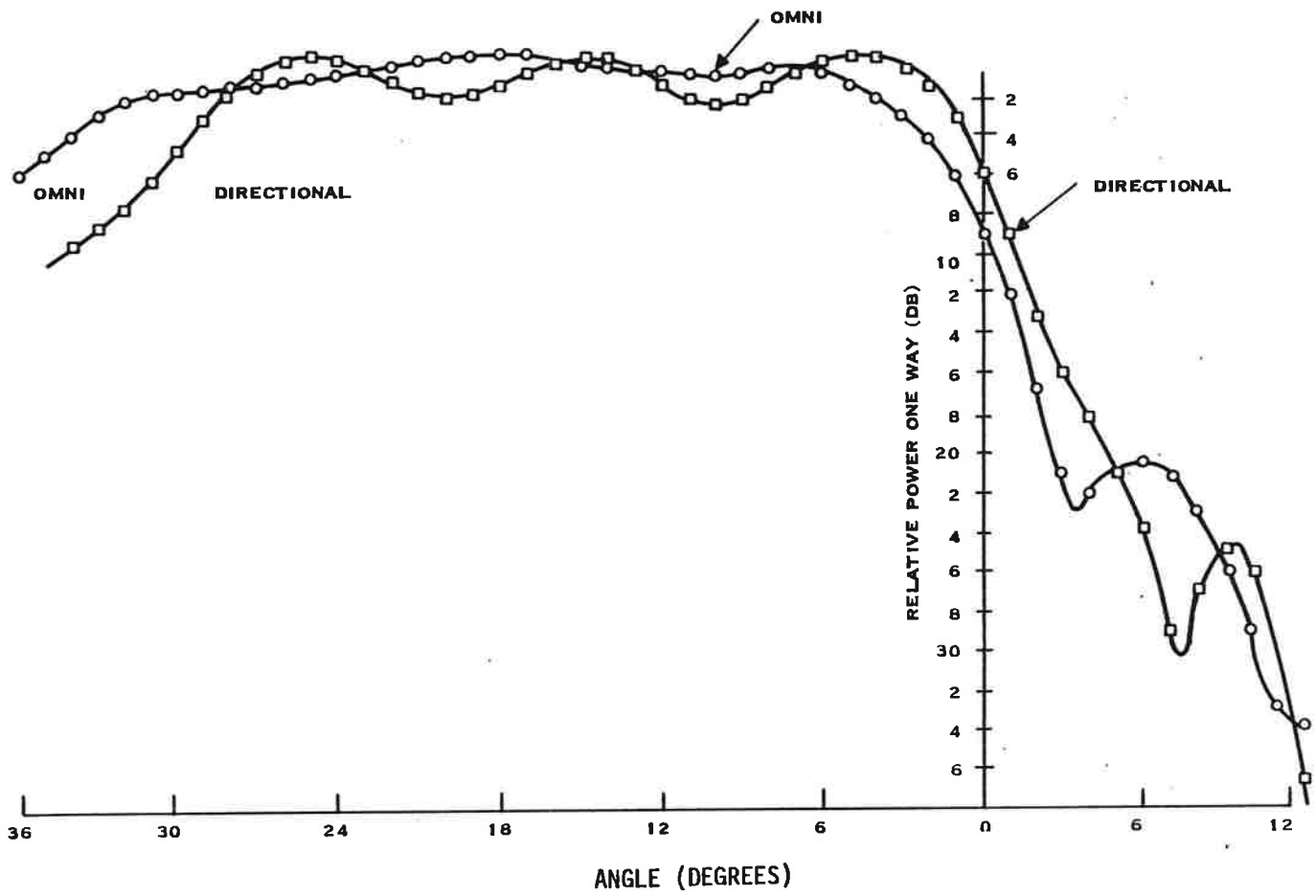

Figure 4-6. Comparison of Directional and Omni Patterns for ATCRBS Reflector

punch-through of high-angle sidelobes.

Figure 4-7 shows an azimuth pattern measured at +5 degrees elevation. It has an oval shape with a ripple of ±3.5 dB. The azimuth ripple could be tolerated for this antenna since it was intended for installation on top of the rotary ATCRBS reflector. The "peaks" of the azimuth pattern were aligned directly in front of and behind the reflector, to best cover all sidelobes and backlobes. Figure 4-7 also includes a measurement of the cross polarized component, which is rather high. A suppression grid of horizontal wires was subsequently placed inside the radome to suppress the cross polarized energy. The grid has a transmission loss of 10 dB to horizontally polarized energy, and was permanently installed inside the radome.

Peak gain for this antenna was measured to be +8.8 dB. This was higher than theoretical due to the oval shape of the azimuth pattern. VSWR was measured to be 2:1.

A complete set of patterns may be seen in a report entitled ATCRBS Improvement Program: Test Data for Omni-Directional Antenna (Separate Rotator Installation), May 20, 1974.

In mechanical construction and external appearance, the dipole omni is quite similar to ARSR omni described previously. The omni mounts centered on top of the ATCRBS reflector, as shown in Figure 4-8.

Improved Omni for ATCRBS Reflector

General

Following fabrication and test of the ATCRBS reflector and dipole omni, it was realized that the dipole omni did not have adequate elevation coverage to blank high-angle minor-lobe radiation from the reflector. Therefore a new omni was developed which had much-increased high-angle elevation coverage. In addition to improved coverage, this omni also uses the folded-slot element described for the ARSR omni to realize much improved azimuth omnidirectionality.

The improved omni has uniform gain elevation coverage to +45 degrees, with additional coverage at gradually reduced gain up to +75 degrees elevation. A ten-element, non-uniformly spaced array was used to produce this pattern. Non-uniform array spacing was used because synthesis of a broad pattern with good cutoff requires radiation of most of the energy from only a few elements in the center of the array: therefore the center four elements in the array were closely spaced (0.47 λ), and the remaining six elements were spaced at twice this distance (0.94 λ) to aid in realizing the required amplitude distribution.

The array is fed with stripline power dividers and semi-rigid coaxial cables, much like the omni for the ARSR modification described previously. A tubular fiberglass radome provides protection from the weather.

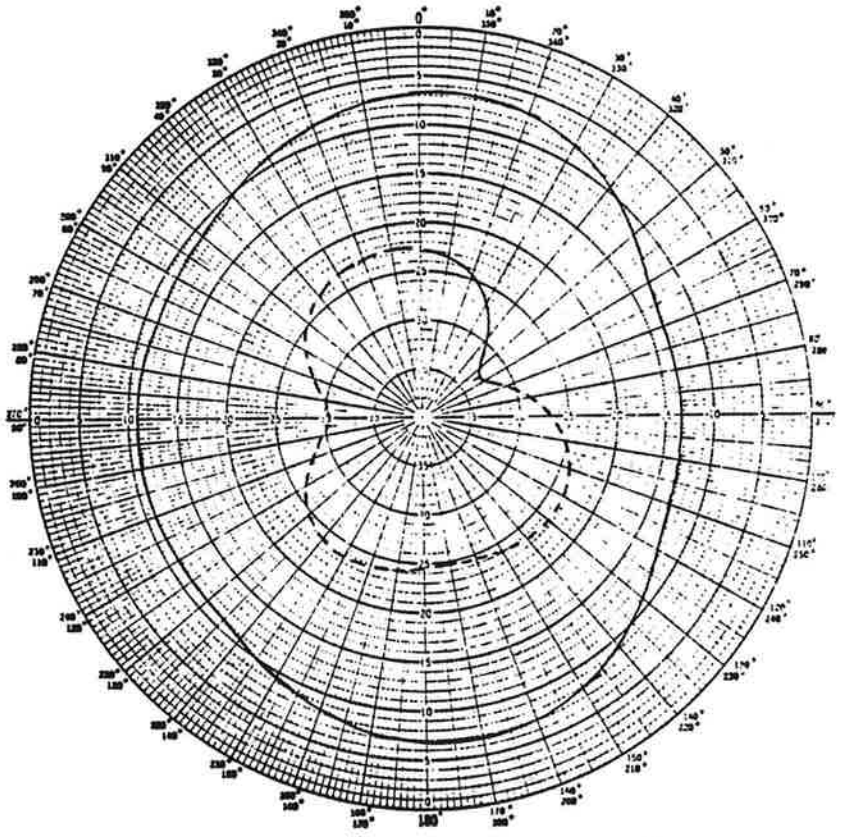

Figure 4-7. Azimuth Pattern at +5 Degrees Elevation

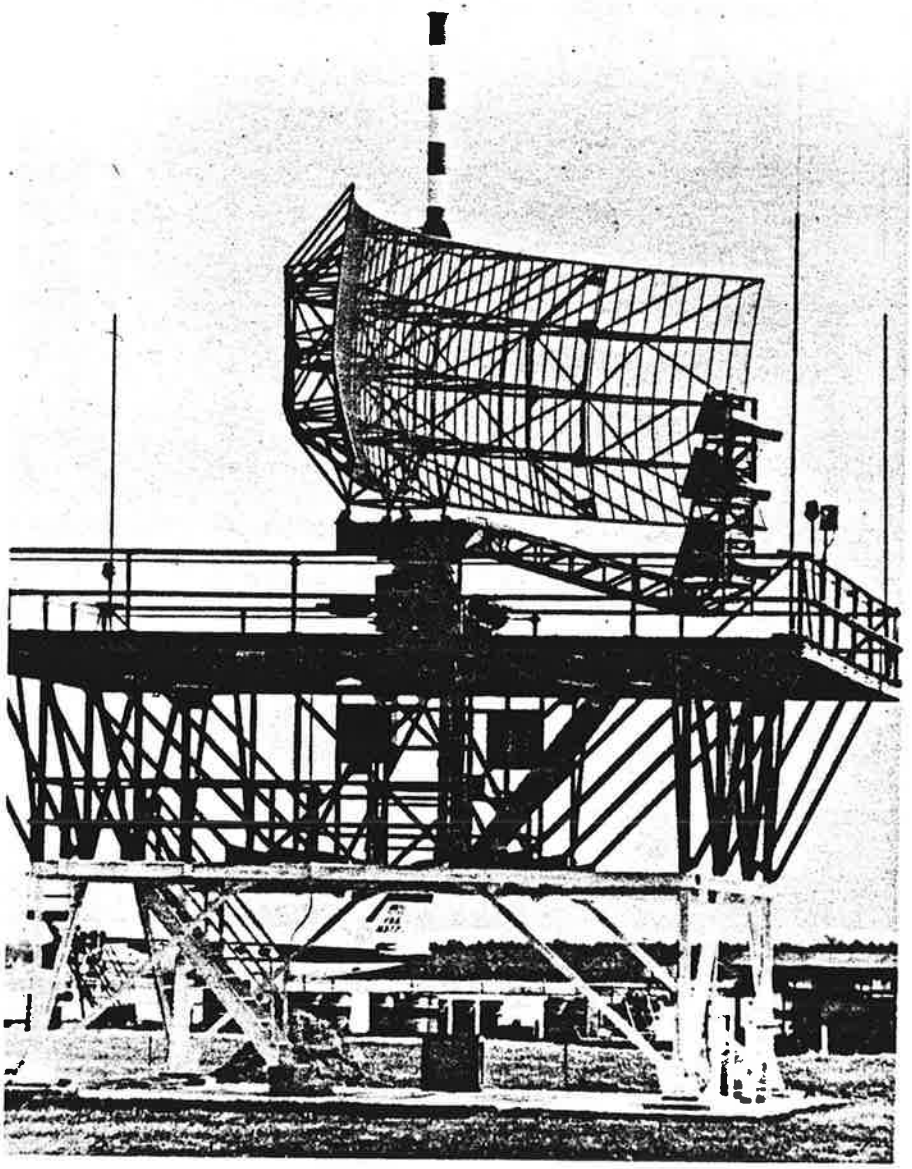

Figure 4-8. ATCRBS Reflector Showing Omni Installation

Radiation Patterns

Figure 4-9 compares elevation coverage of the dipole omni, the improved omni, and the reflector. The great improvment in high-angle coverage is obvious. An azimuth pattern, measured at +5 degrees, is shown in Figure 4-10. Azimuth coverage is omnidirectional within ±1.5 dB up to +60 degrees elevation.

Measured gain for this omni is +4.0 dB relative to a linear isotropic source. This antenna has lower gain than the previously described omnis because of its larger coverage volume.

Relative Omni Gain

It is generally agreed that for best SLS performance, the omni (P2) effective radiated power (ERP) should be approximately 15 dB below the directional (P1 and P3) ERP. Thus it would seem desirable for the omni gain to be approximately 15 dB lower than the directional gain. Typically, however, the omni gain is approximately 20 dB lower than the directional gain and it is necessary to attenuate the directional antenna to achieve the desired SLS ratio.

The 20 dB gain difference arises from the difference in coverage volume for the two antennas. Gain for any antenna can be calculated approximately from the azimuth and elevation beamshapes as follows:

$$\text{Gain} = 10 \log \frac{41253}{\theta_3 \phi_3}$$

where θ_3 and ϕ_3 are azimuth and elevation half-power beamwidths. For two antennas with the same elevation patterns but different azimuth coverage (such as the ATCRBS omni and directional antennas), the gain difference between the two will be simply the inverse ratio of the beamwidths:

$$\frac{\text{Gain of Omni}}{\text{Gain of Directional}} = 10 \log \frac{2.35^\circ}{360^\circ}$$

$$= -21.9 \text{ dB}$$

Therefore, without supplementary attenuators or P1/P2 power variations, the SLS ratio for a 2.35 degree system will be about 21 dB instead of the desired 15 dB.

For the ATCRBS reflector field test, the SLS ratio was changed to 15 dB by adding a 6 dB pad to the directional antenna.

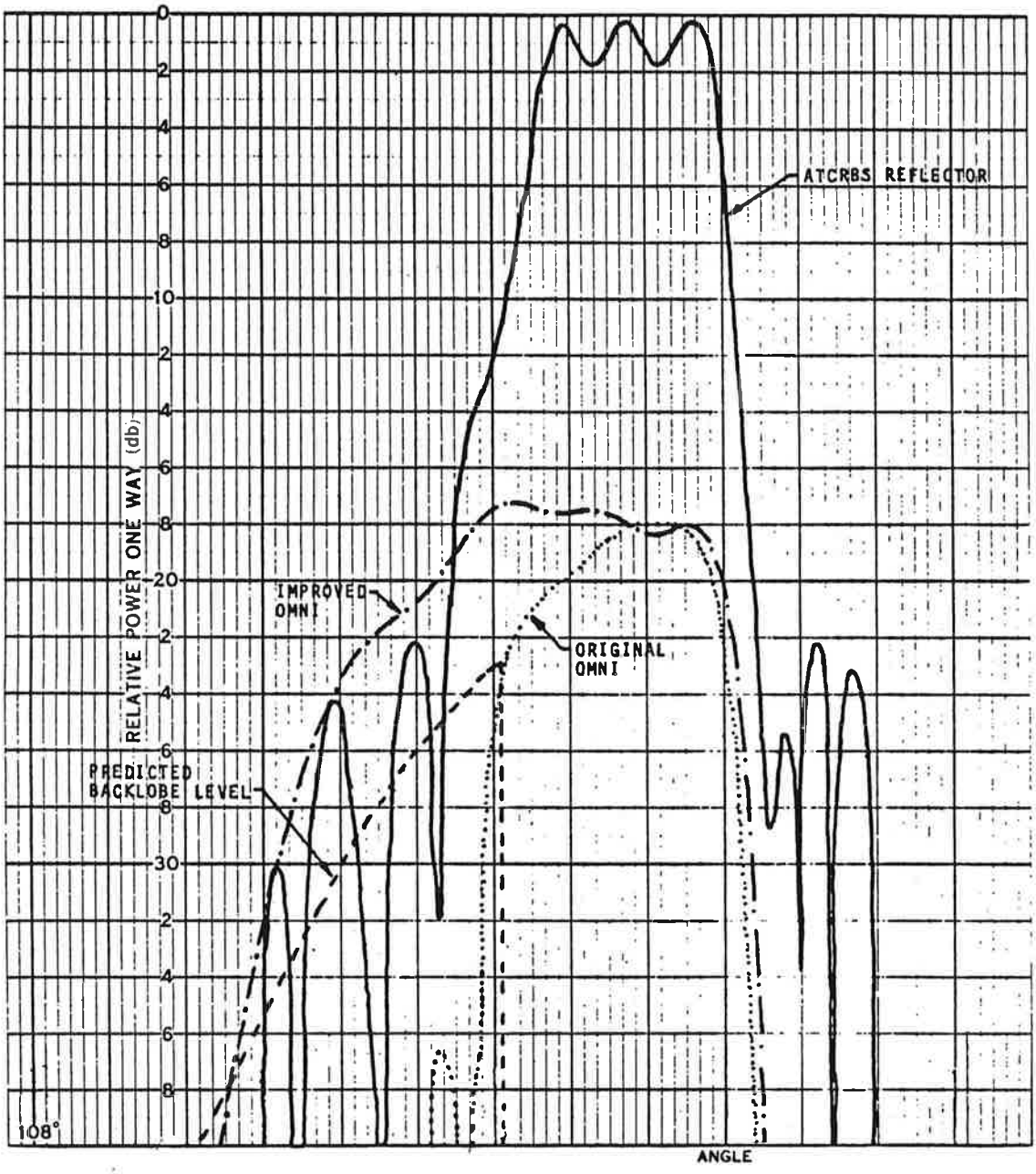

Figure 4-9. Omni and Directional Elevation Patterns

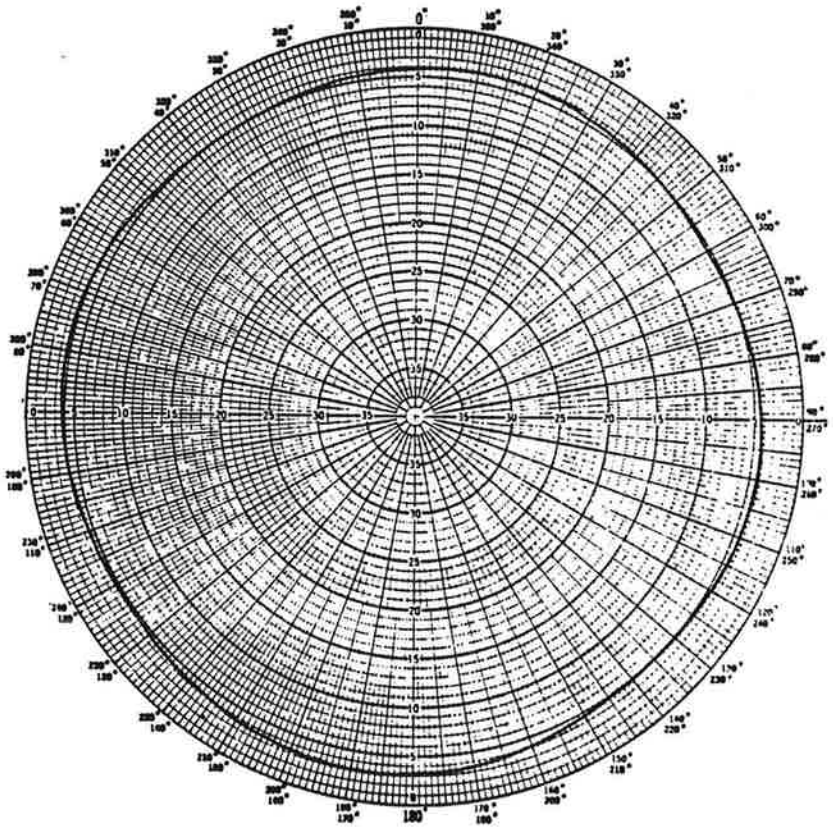

Figure 4-10. Omni Azimuth Pattern at +5 Degrees Elevation

SECTION V

ARSR-2 INTEGRAL BEACON FEED

General

As a part of the ATCRBS Improvement program, Texas Instruments designed and built an integral beacon feed for the ARSR-2 Radar. This feed is compatible with a passive radar horn, and yields a 2.3-degree azimuth beamwidth as does the present beacon array. The feed uses a very thin slot element located between the primary and passive radar horns, and dipole elements located on either side of the primary horn as shown in Figure 5-1. The feed also has an azimuth difference pattern for monopulse direction-finding.

The 2.35-degree azimuth beamwidth was achieved by tailoring the azimuth pattern of this array to illuminate only the central portion of the reflector. The two dipoles are spaced rather widely in the horizontal dimension (about 1.0λ), and the slot element fills the center of the array. The resulting azimuth feed pattern has a narrow beamwidth which illuminates only the desired portion of the reflector.

While the feed generally works as designed, it has several shortcomings which make it unsuitable for field use in its present form. First, the beacon elevation beam is tilted upward with respect to the radar about 1.25-degrees more than desired, which gives less gain at the horizon. Second, the feed pattern is too broad, causing spillover and backlobes which give false targets and ringaround. Third, an unusual phase behavior in the phase of the feed pattern causes the azimuth beamshape near the horizon to have a small dip in gain directly on boresight. Because of this, very distant weak targets appear as splits on a PPI display.

Possible Approaches

At the outset of the design it was decided that the beacon feed would be added onto the radar feed horn without any radar modifications, and that the two feeds would be, electrically, completely independent. An alternative approach would be to diplex the beacon signal into the radar feed horn so that the primary horn is shared by both systems. This requires redesign of the feed horn, and would render field modification of the ARSR antenna much more difficult; this approach was therefore not pursued.

Electrically Independent Beacon and Radar Feeds

To achieve aligned beams for beacon and radar, an add-on feed must have its phase center at the focus of the reflector, so the beacon elements must be symmetrically located around the radar horn. This leads to a basic problem inherent in any add-on feed; the fact that because the radar horn occupies a central area around the focus which is approximately

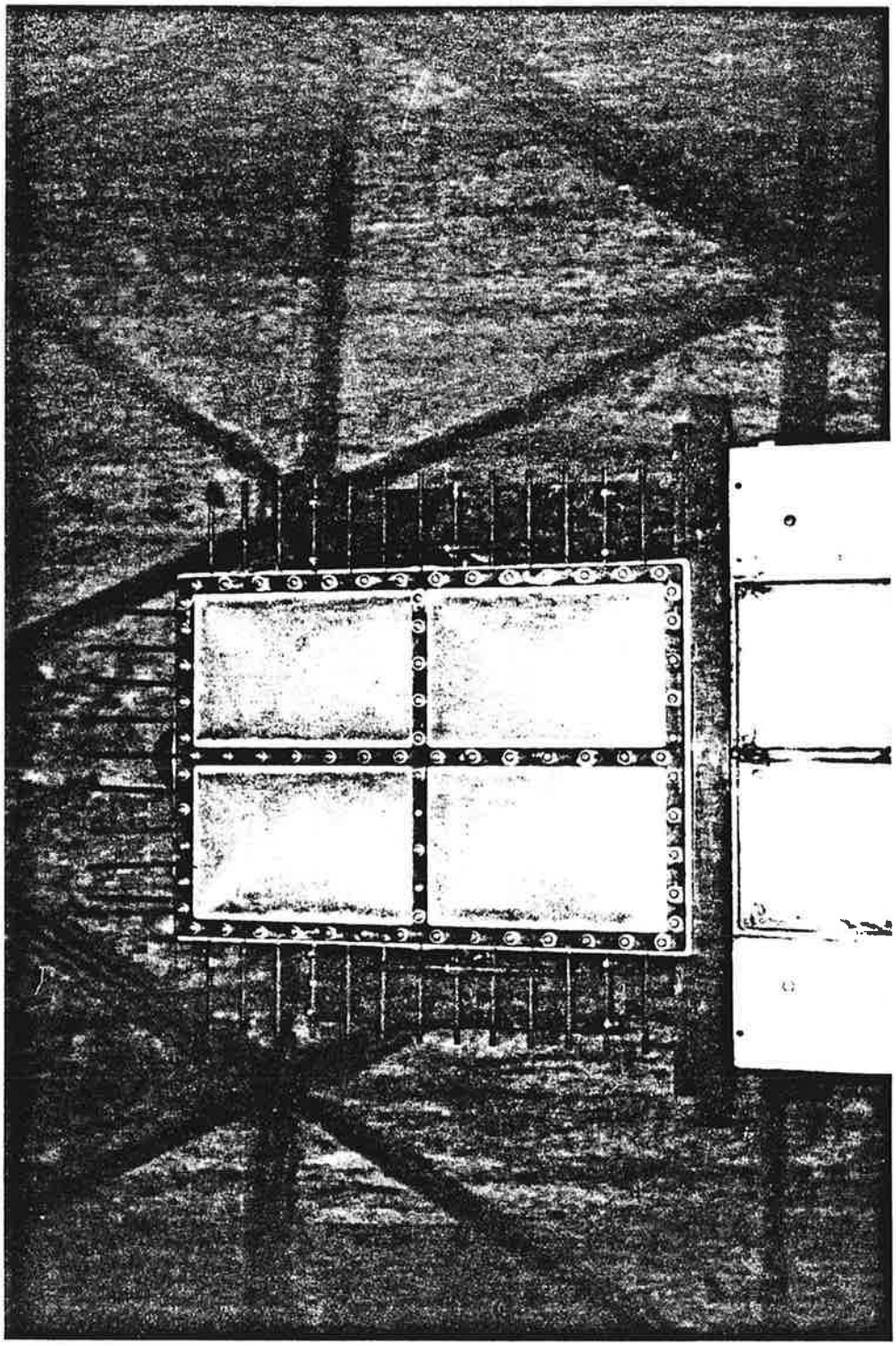

Figure 5-1. Texas Instruments ARSR-2 Beacon Feed Modification

0.8λ wide and 1.3λ tall, any beacon feed array added around the radar feed is thus constrained to have an unexcited area or "black hole" of this size in its center. Depending on how the beacon elements are arranged, either azimuth, elevation, or diagonal-plane sidelobes of high amplitude will certainly occur as a result of this hole, giving degraded pattern performance and/or high spillover.

Figures 5-2 through 5-5 show several possible element arrangements around the radar horns, and their resulting feed radiation patterns. In Figure 5-2, the feeds are close-spaced in azimuth, but widely spaced in elevation, resulting in good azimuth illumination, but high elevation sidelobes. The other configurations have better elevation patterns, but high azimuth or diagonal-plane sidelobes. The configuration of Figure 5-5 gives best overall feed patterns, and is the approach used for the Texas Instruments feed modification. Its design is complicated by the fact that a feed element is required between the active and passive radar horns.

Comments on the NADIF Modification

One integrated feed design, the NADIF (NAFEC Dipole Feed) modification, uses dipole elements above and below the radar horn in a configuration like Figure 5-2. Azimuth illumination for the NADIF feed is well behaved because the dipoles are closely spaced (6-inches or 0.6 wavelength). Figure 5-6 shows an azimuth feed pattern for NADIF. Note that the entire reflector is illuminated yielding approximately 1.5-degree secondary half-power beamwidth with good sidelobes.

Vertically, the dipoles are spaced 22-inches (2.0 wavelengths). A calculated vertical feed pattern for NADIF is shown in Figure 5-7; the patterns are calculated for a 90-degree phase offset, and various relative top dipoles is increased, the feed phase center moves upward, causing the secondary beam to scan down. Note also that increasing the top dipole level also causes an increasingly deep null on the upper section of the reflector. This causes a broader elevation beamwidth with increased energy in the cosecant portion of the beam. Figure 5-8 is a comparison of measured NADIF secondary patterns for top dipole amplitudes of -5 dB and -40 dB, demonstrating the beam scanning and broadening described above.

Figures 5-6 and 5-7 show that the NADIF feed has almost no azimuth spillover; however, elevation spillover is quite high, and particularly at the top of the reflector, is quite independent on top dipole amplitude. The feed sidelobes which spill over and under the reflector result in high backlobes from the reflector. In field installations these backlobes have led to occurrence of target ring-around for some targets.

TI Beacon Feed

The placement of the dipole pair below the primary radar horn precludes the use of a passive horn with a NADIF-type modification, so the Texas Instruments feed uses instead a feed like the one shown in Figure 5-5. A narrow-height slot element is used between the primary and passive

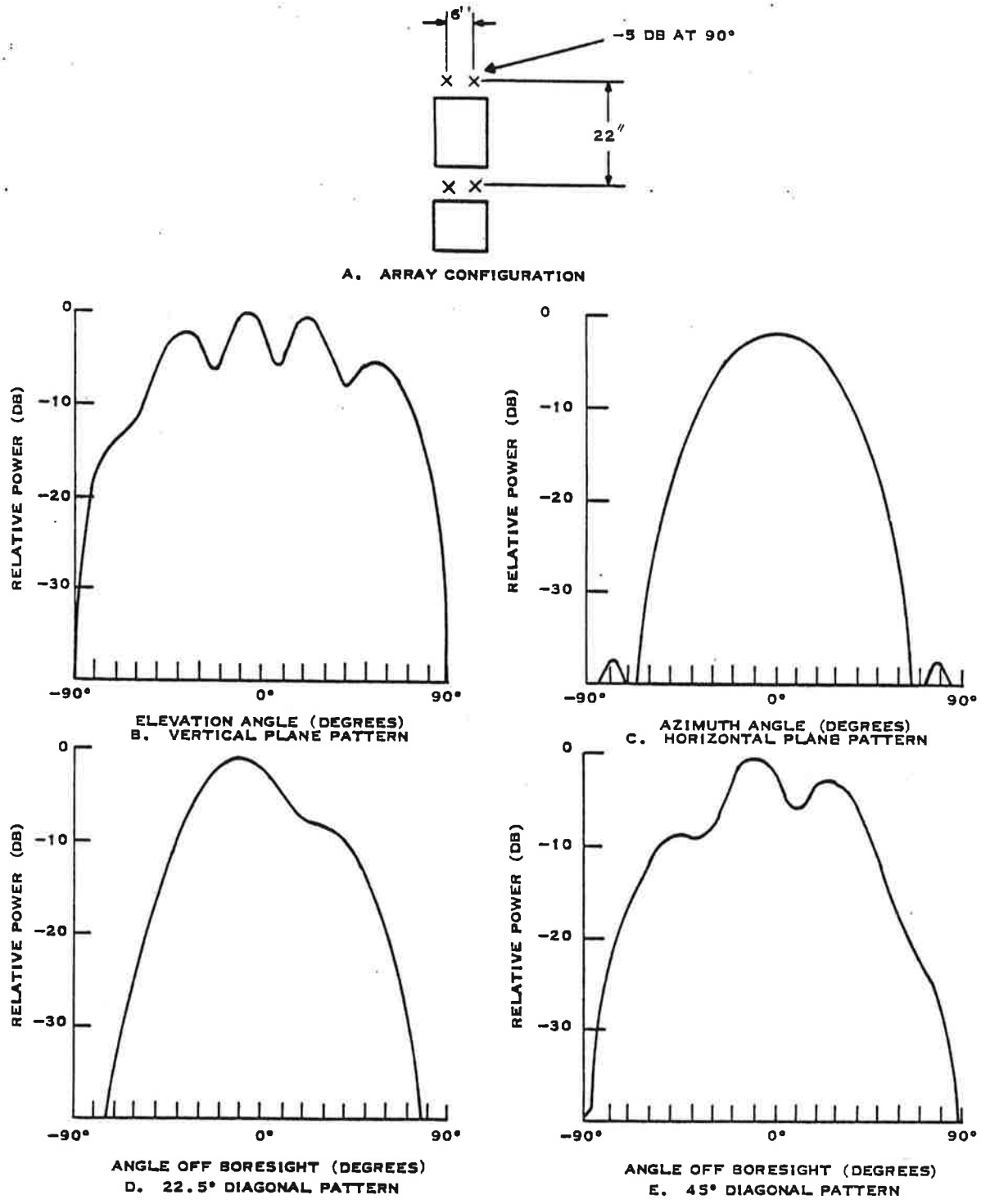

Figure 5-2. Four-Element Rectangular Array

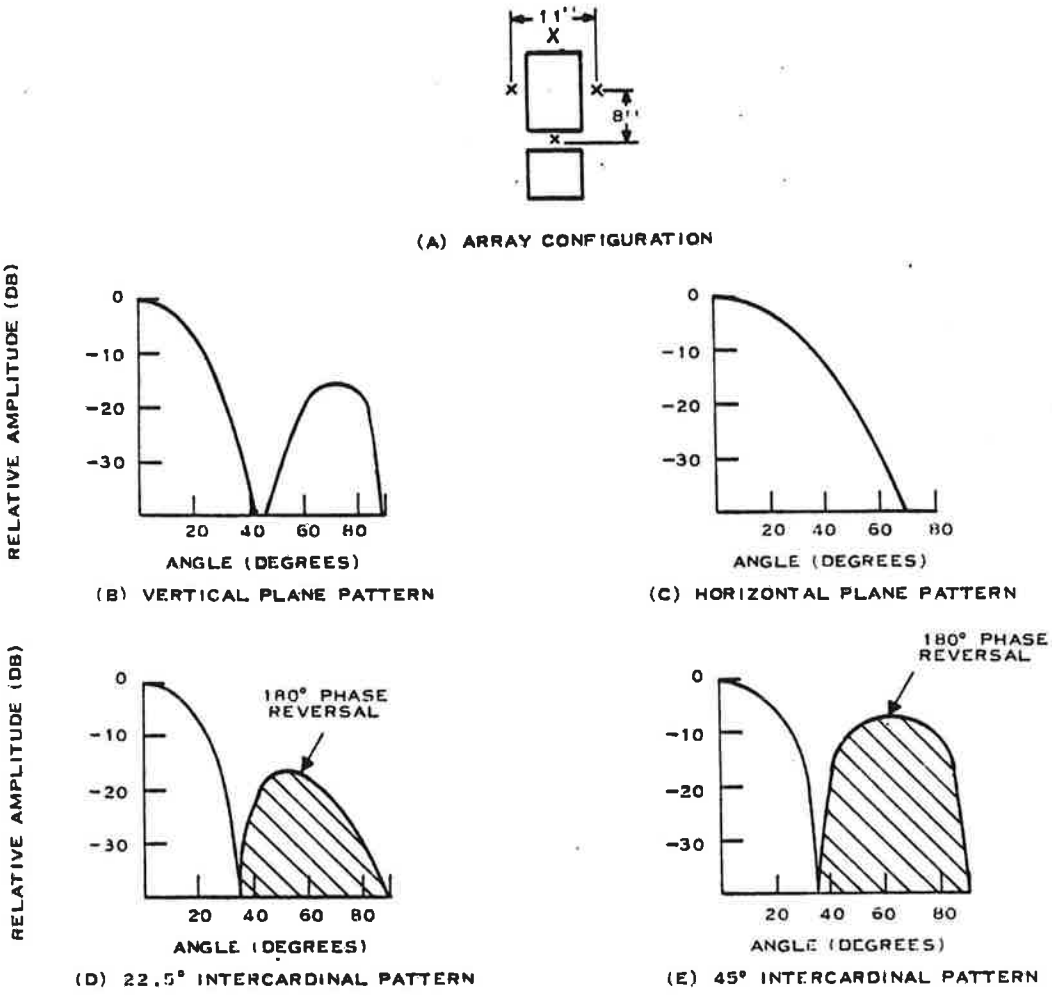

Figure 5-3. Four-Element Uniform Ring Array

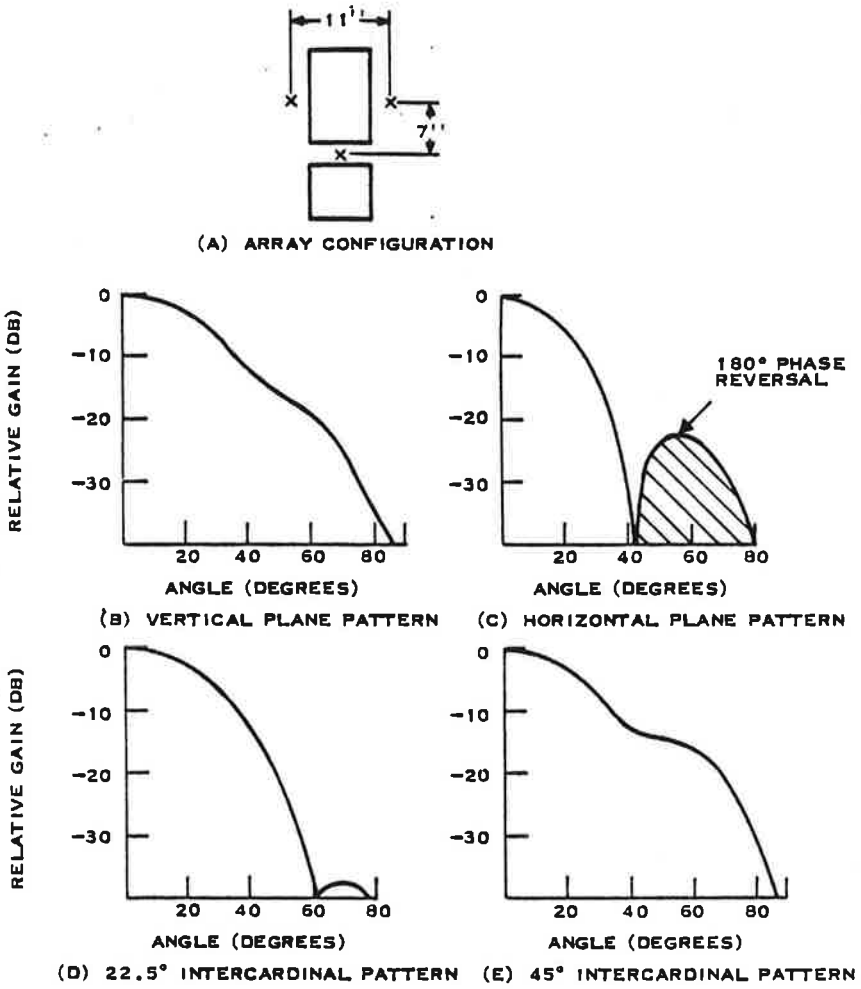

Figure 5-4. Three-Element Uniform Array Feed

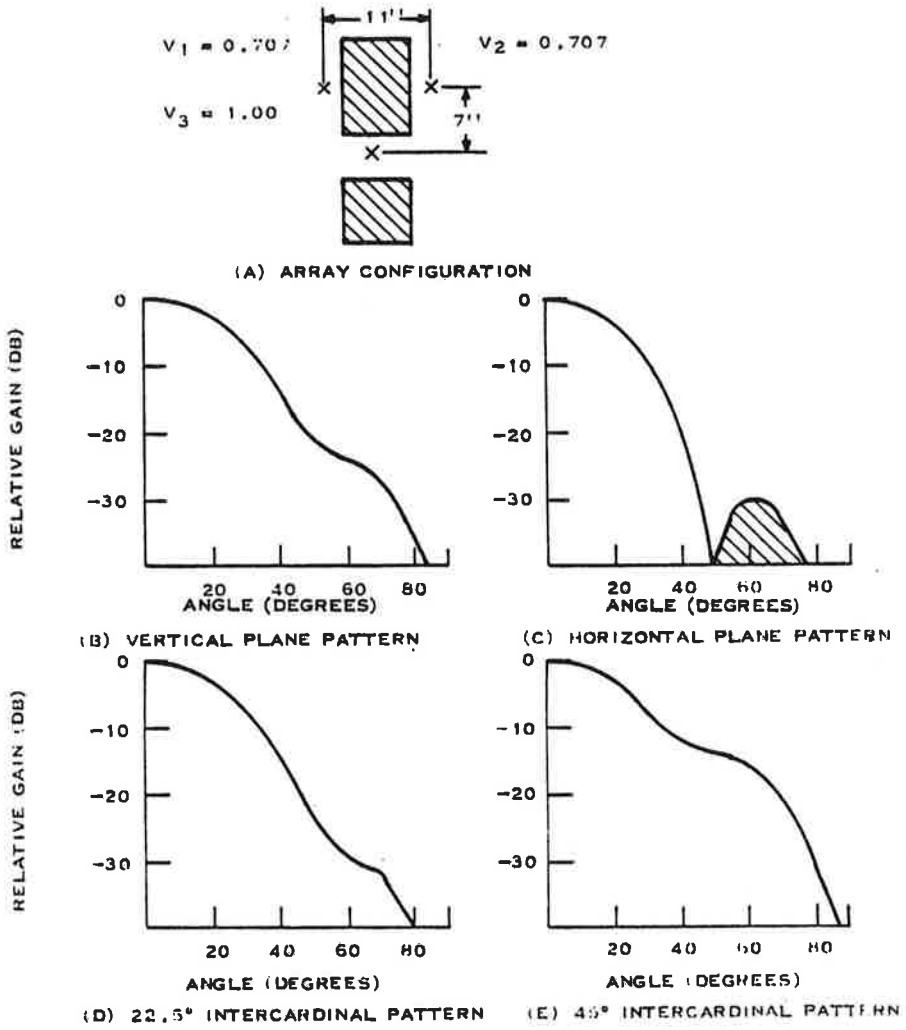

Figure 5-5. Three-Element Tapered Array Feed

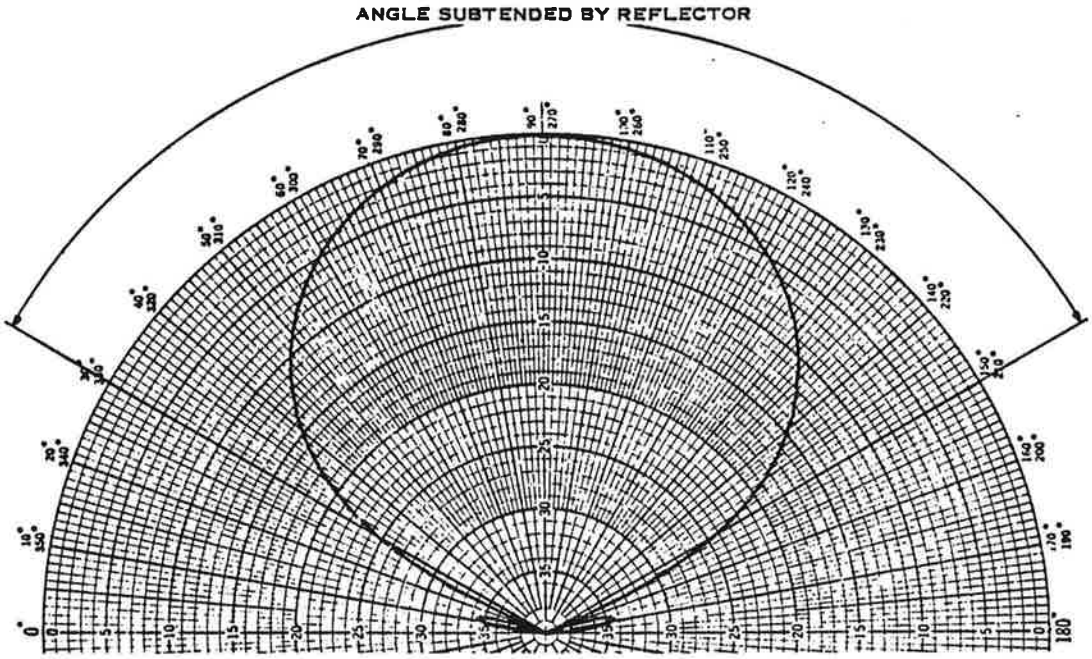

Figure 5-6. NADIF Azimuth Feed Pattern

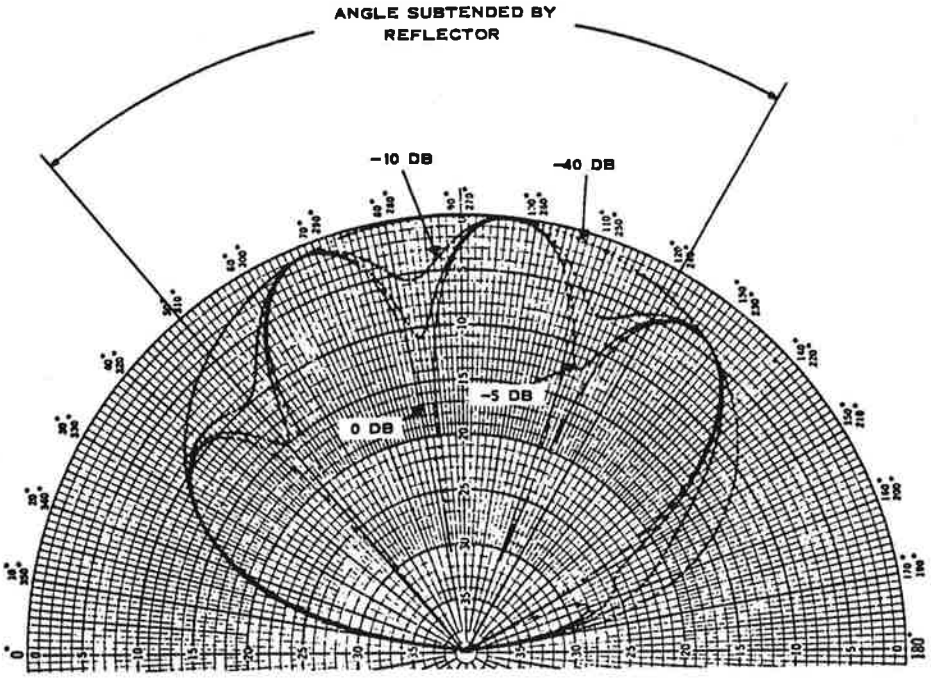

Figure 5-7. NADIF Elevation Feed Pattern for
Various Top Dipole-Pair Amplitudes

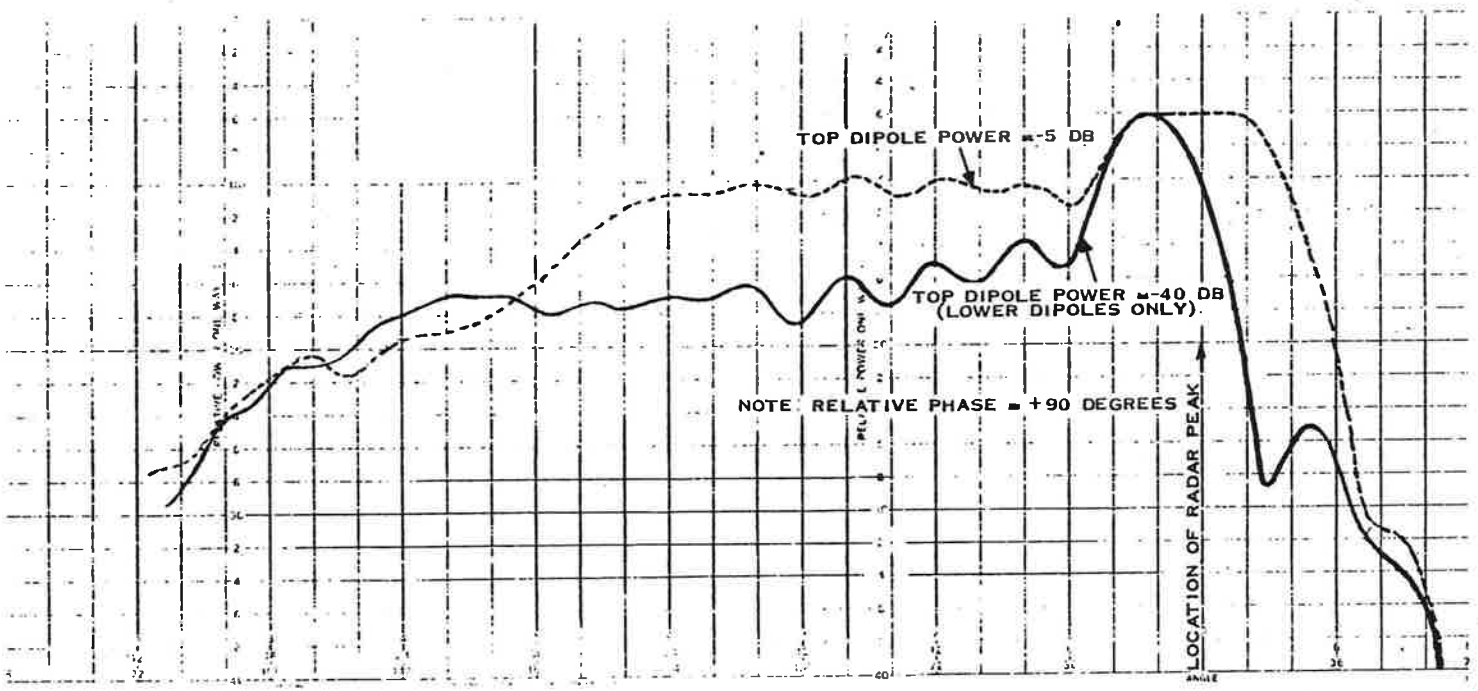

Figure 5-8. Measured NADIF Elevation Patterns for Top Dipole Power Levels of -5 dB and -40 dB

feed horns to minimize the phase-center separation. The two elements beside the radar horn are simple half-wave dipoles.

The slot element is a multimode design with optimized beamwidths for both its sum and difference modes. In the sum mode, the pattern is made as broad as practical so that it duplicates the broad azimuth pattern of the dipoles; this minimizes the out-of-phase sidelobe energy implemented to achieve low edge illumination and low sidelobes.

The vertical aperture of the slot is quite small, about 0.08λ, and it therefore presented a difficult impedance matching problem. The slot could not be matched over the entire beacon frequency band, so it was matched instead in two separate 10 MHz bands centered at 1030 and 1090 MHz.

The array is interconnected using the stripline feed network shown in Figure 5-9. This feed employs resonant-ring hybrids to distribute the input power among the two dipoles and the slot and to form the sum and difference beams. Coupled-line bandpass filters at the input prevent radar energy from being coupled into the beacon system. These filters ensure that coupled energy is suppressed by at least 60 dB in the 1280-to 1350-MHz band.

Measured Performance

Measured principal plane patterns are shown in Figures 5-10 through 5-13. Azimuth data for other elevations is summarized in Figures 5-14 and 5-15. Measured gain is as follows:

	No Passive Horn	With Passive Horn
1030 MHz	29.5	29.6
1090 MHz	30.2	28.7

Measured input VSWR is shown in Figure 5-16. The beacon elevation beam peak is in all cases tilted above the radar peak. Relative tilt is as follows:

	No Passive Horn	With Passive Horn
1030 MHz	1.9°	1.9°
1090 MHz	1.6°	1.9°

This indicates that the phase center of the beacon feed is located about 7 inches below the phase center of the radar feed.

Radar Performance

Radar patterns were measured before and after installation of the beacon feed. There was no detectable effect in the linear (horizontal) polarized patterns. In the circularly polarized mode, a slight broadening

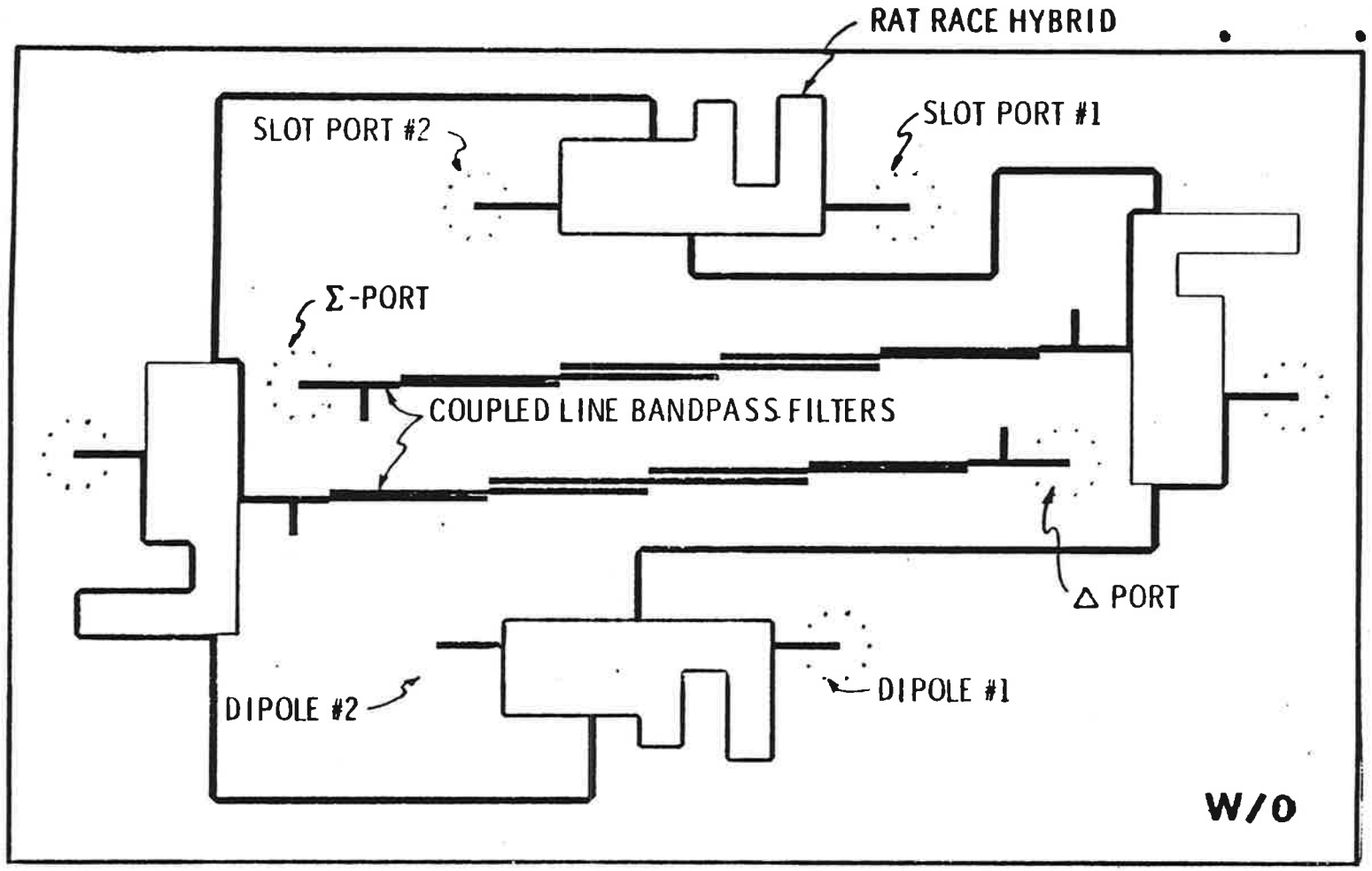

Figure 5-9. Stripline Feed Network

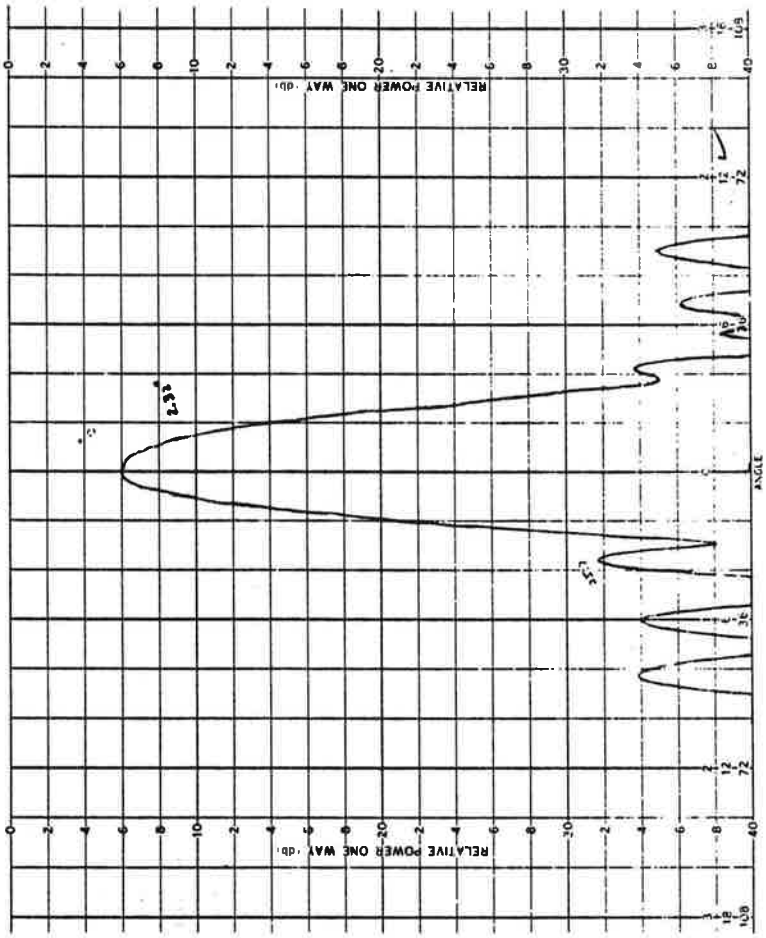

Figure 5-10. Azimuth Pattern, 1030 MHz

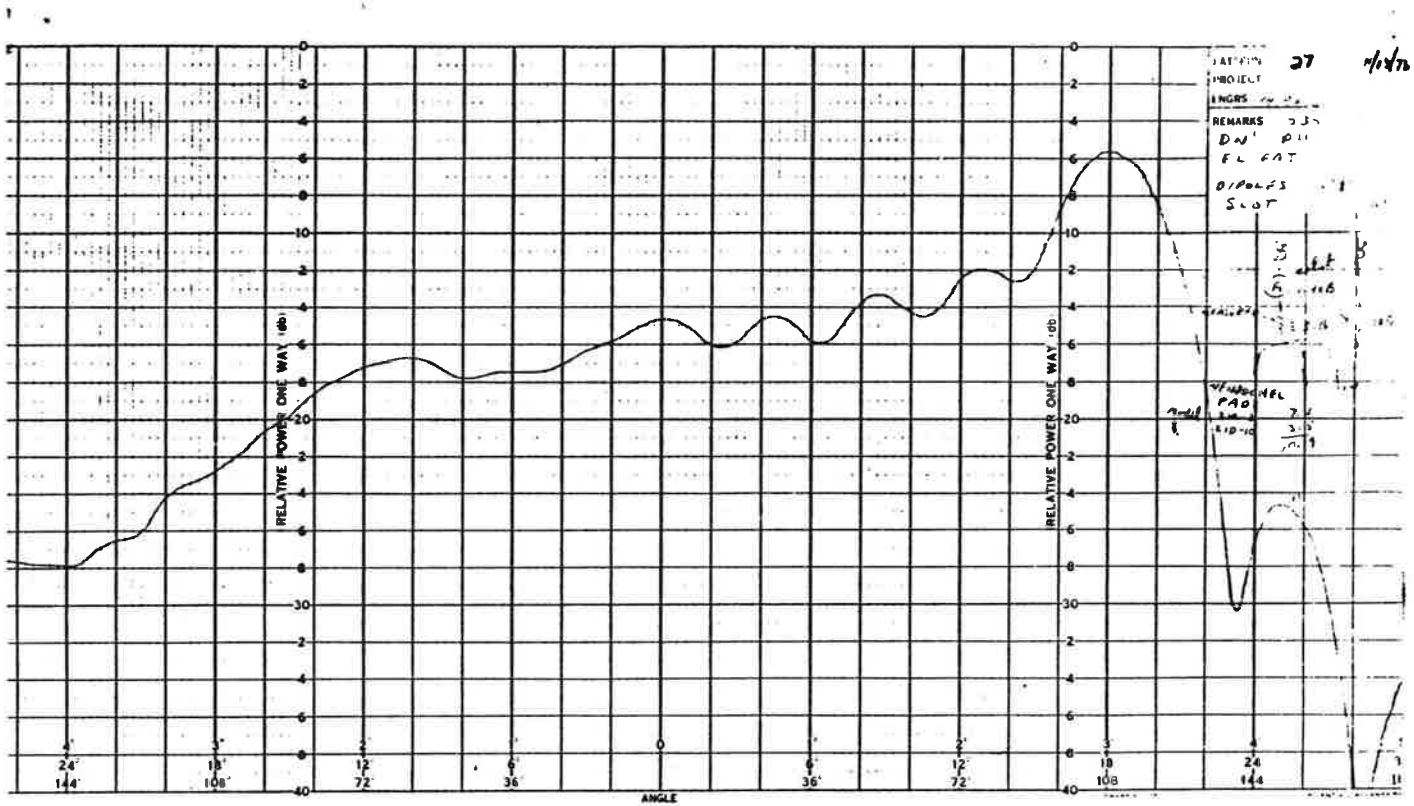

Figure 5-11. Elevation Pattern, 1030 MHz

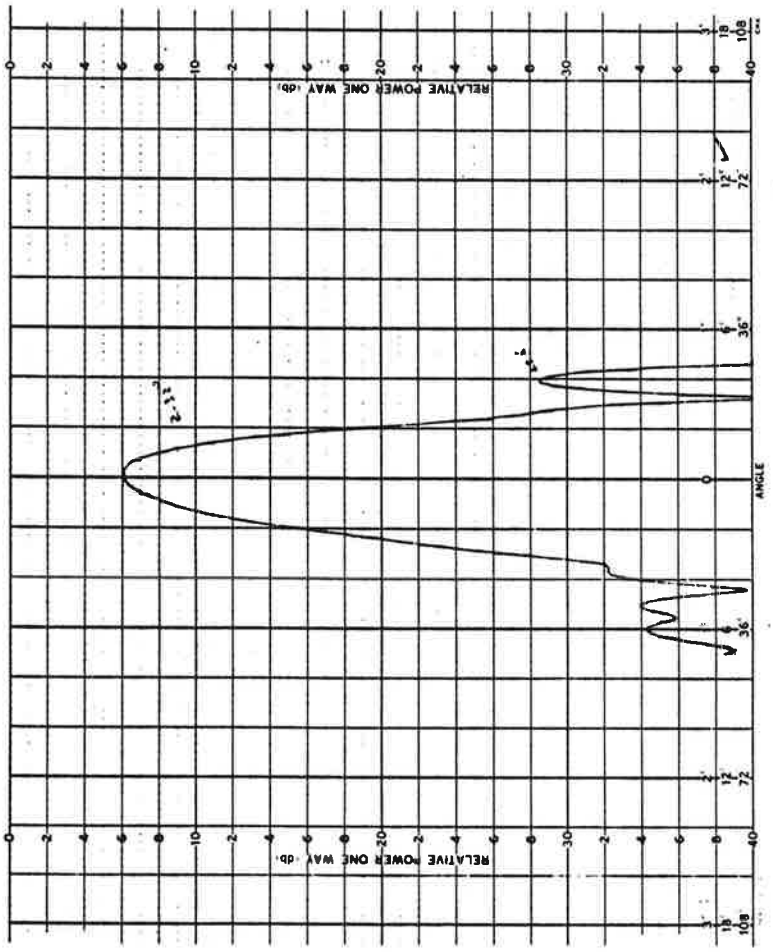

Figure 5-12. Azimuth Pattern, 1090 MHz

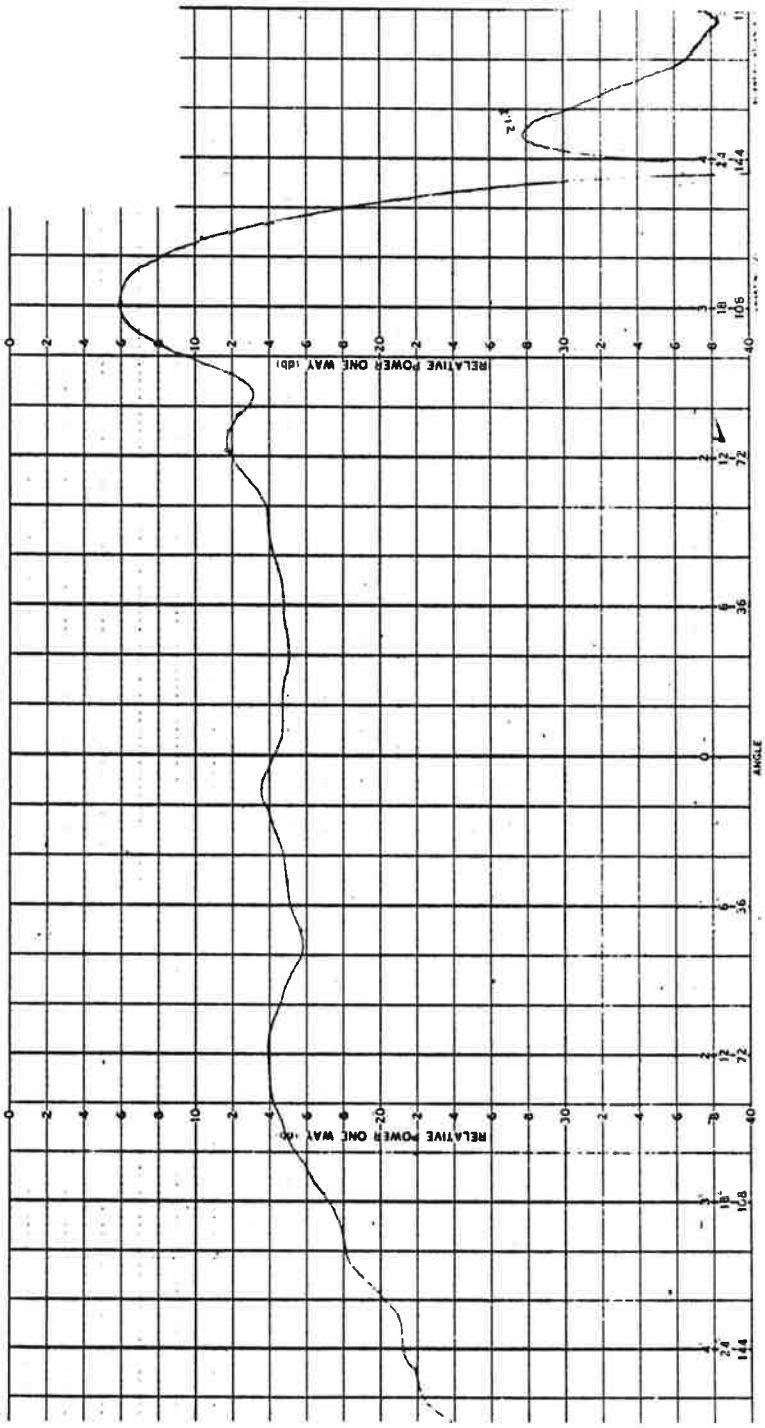

Figure 5-13. Elevation Pattern, 1090 MHz

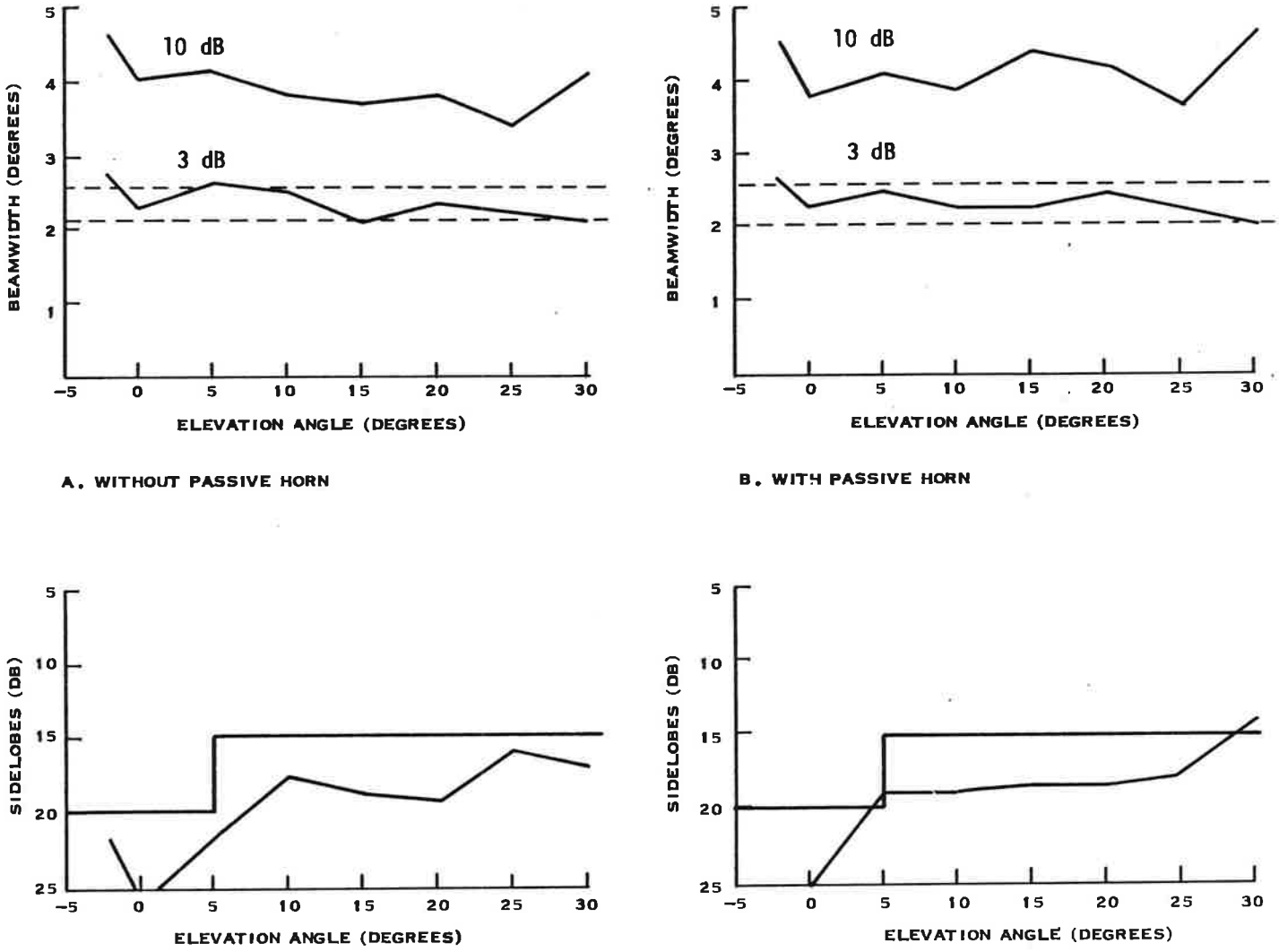

Figure 5-14. Azimuth Performance at Higher Elevation Angles, 1030 MHz

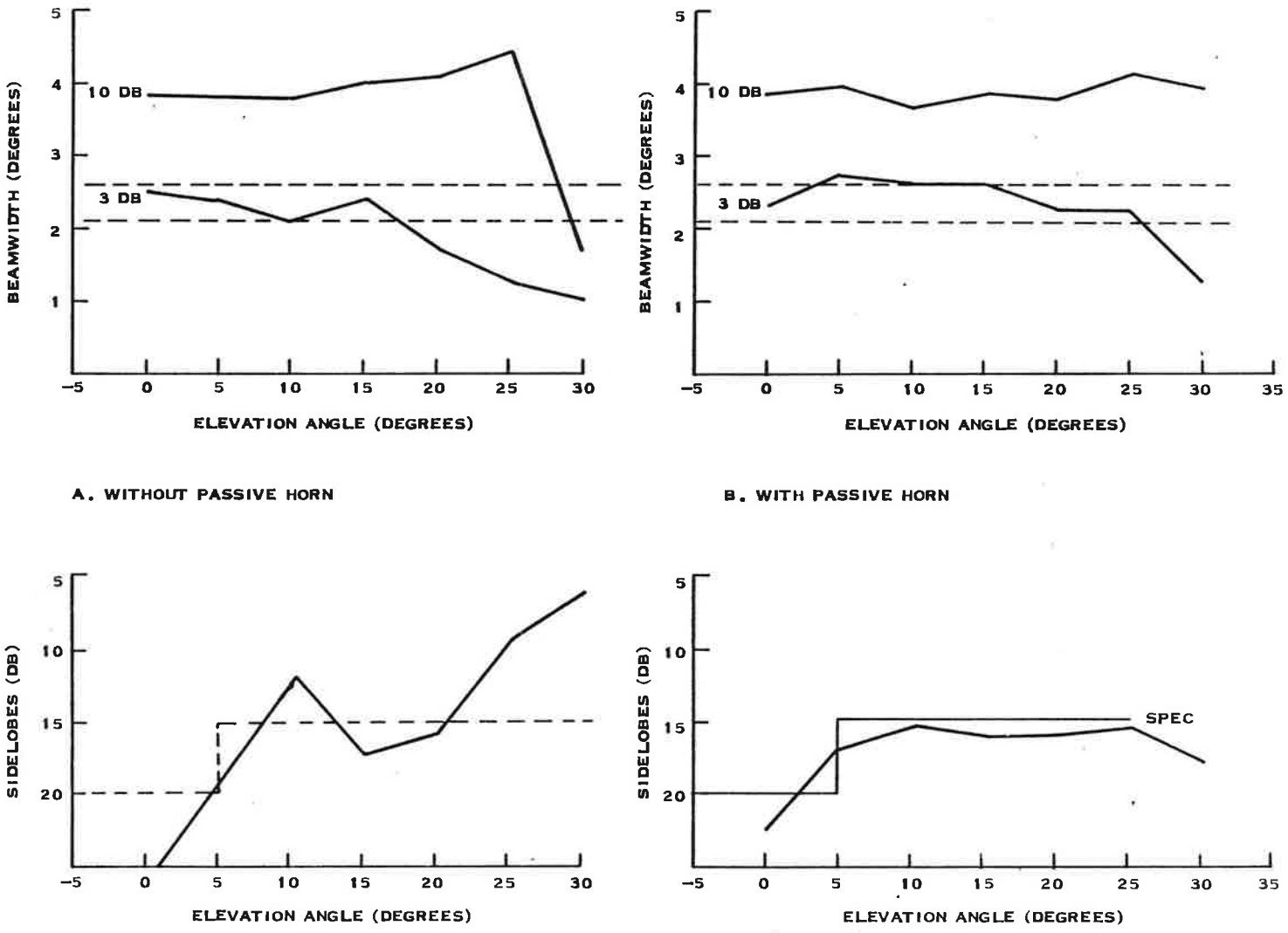

Figure 5-15. Azimuth Performance at Higher Elevation Angles, 1090 MHz

of the vertical component of the azimuth beam was noted around the -15 dB point of the beam. This broadening increased the axial ratio on one side of the beam and decreased it on the other. Calculated "ICR" for the measured patterns is

	Azimuth	Elevation
Before Modification	11.8 dB	15.9 dB
After Modification	12.2 dB	18.5 dB

It was calculated that the modification kit does not materially degrade the radar.

Problems Areas

Relative Beam Tilt

The elevation beam of the beacon was tilted approximately 1.9-degrees above the radar. This is higher than desired (the desired tilt is approximately 0.7 degrees) because the effective center of the feed array is located too low. It was intended that the dipoles should locate the effective feed point between the dipoles and slot, but the beam tilt measurements showed that the effective feed point is 7 inches below the radar feed point, which is only 1/2-inch above the location of the slot. It appeared that the dipoles contributed almost nothing to tilting the elevation pattern downward.

A measured secondary pattern for the dipole pair without the slot shows why this is true. The pattern shape is shown in Figure 5-16. Because the dipole pair is widely spaced, much out-of-phase sidelobe energy illuminates the reflector, giving a near null at azimuth boresight. With the secondary radiation of the dipole pair in a null, it contributes very little (at azimuth boresight) to the composite elevation pattern of the slot and dipole pair together.

It is therefore concluded that the dipole pair is quite ineffective in changing the beam tilt. A possible improved solution for the beam tilt problem is to add another feed element above the radar horn or to excite the radar horn itself with beacon energy.

Split Beam Near Horizon

On the underside of the elevation beam, the azimuth patterns gradually assumed a split-beam shape as shown in Figure 5-17. The cause of this split beam can be seen by referring to Figures 5-18 and 5-19. The secondary elevation pattern of the slot is tilted above the secondary pattern of the dipoles, because the slot is installed below the dipoles. Near the horizon, the slot radiation is rapidly decreasing because of the horizon cutoff of the reflector. This allows the dipole radiation, with its dual-peak shape (Figure 5-16) to predominate.

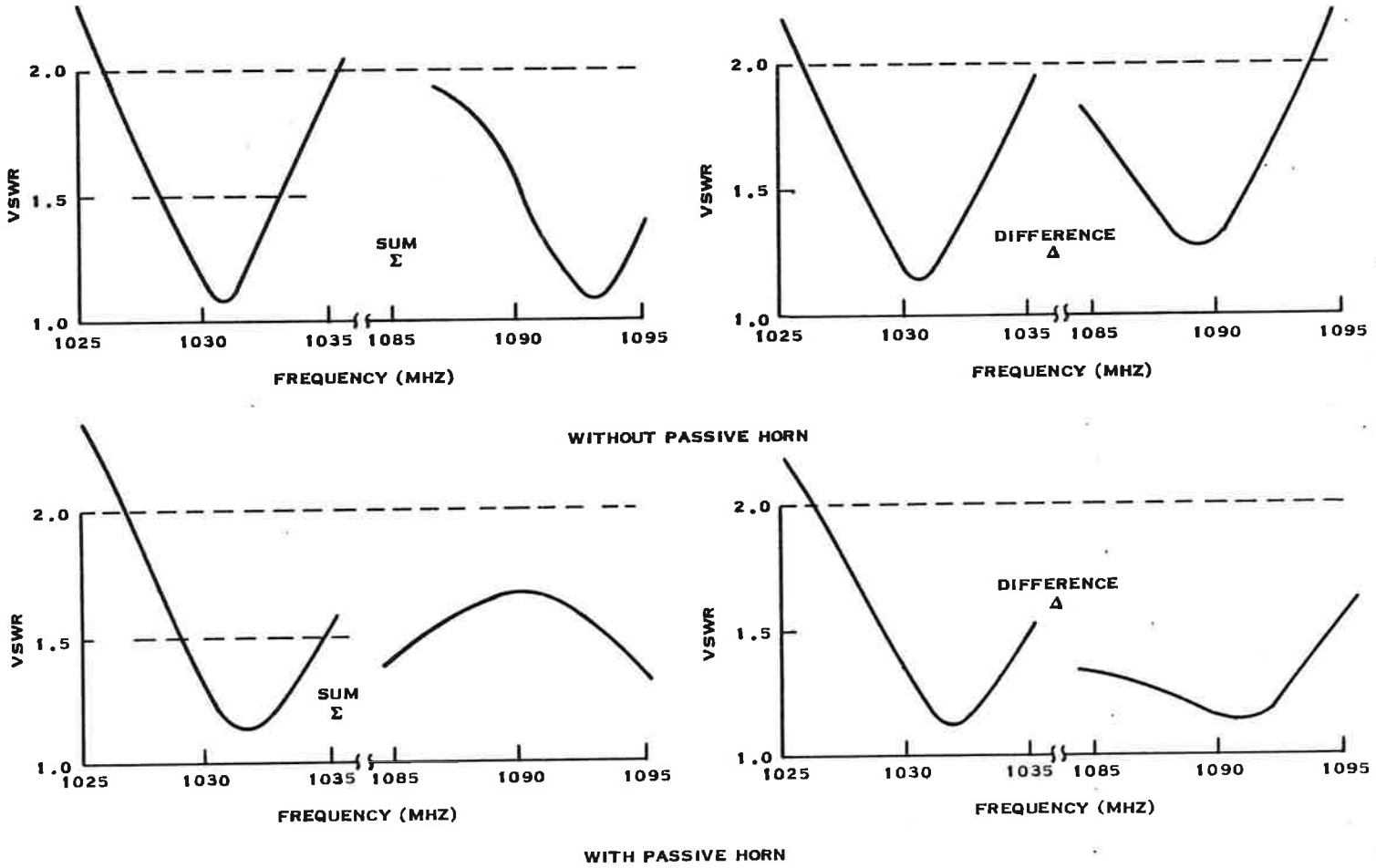

Figure 5-16. Measured Input VSWR

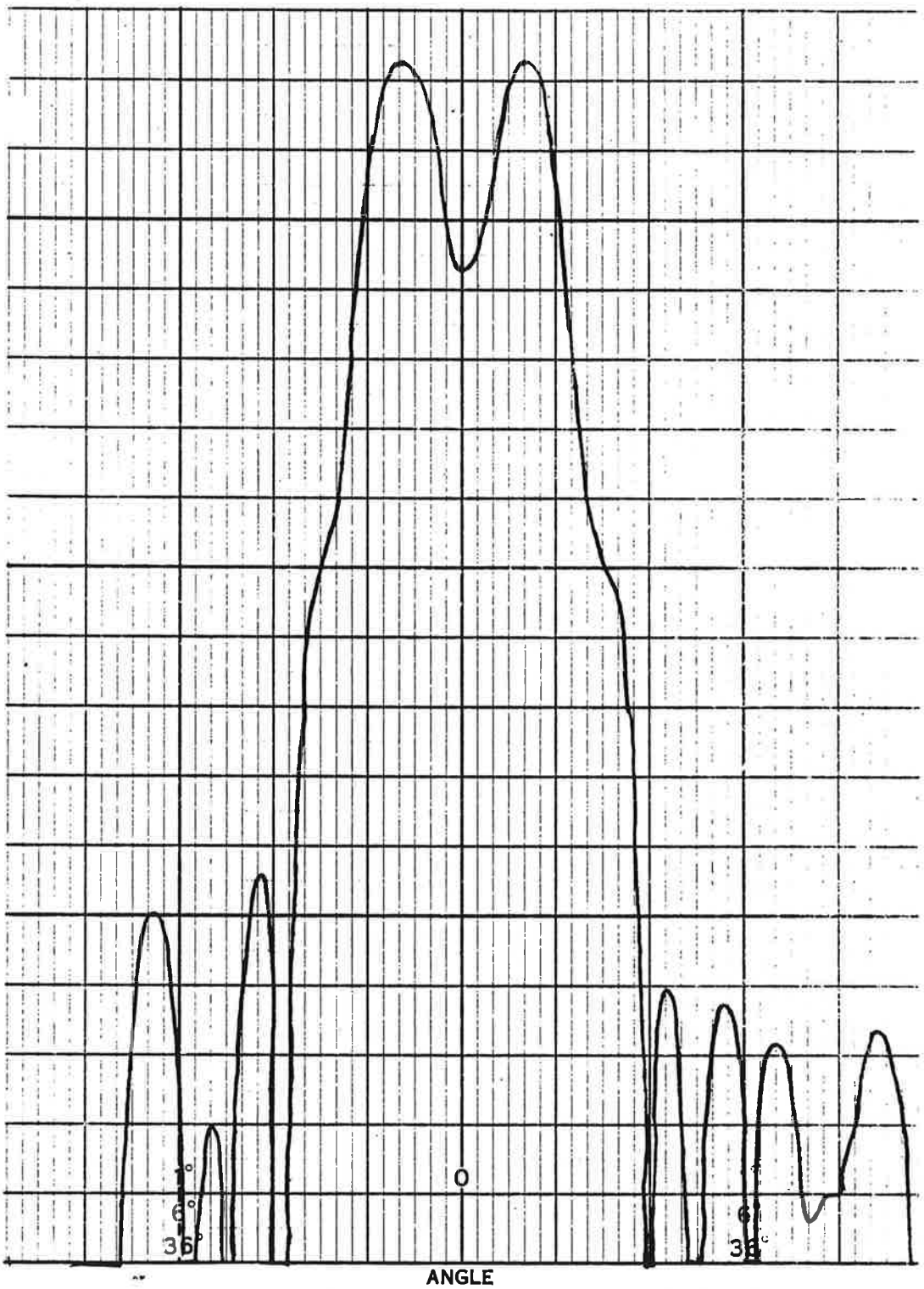

Figure 5-17. Azimuth Secondary Pattern for Dipoles Only

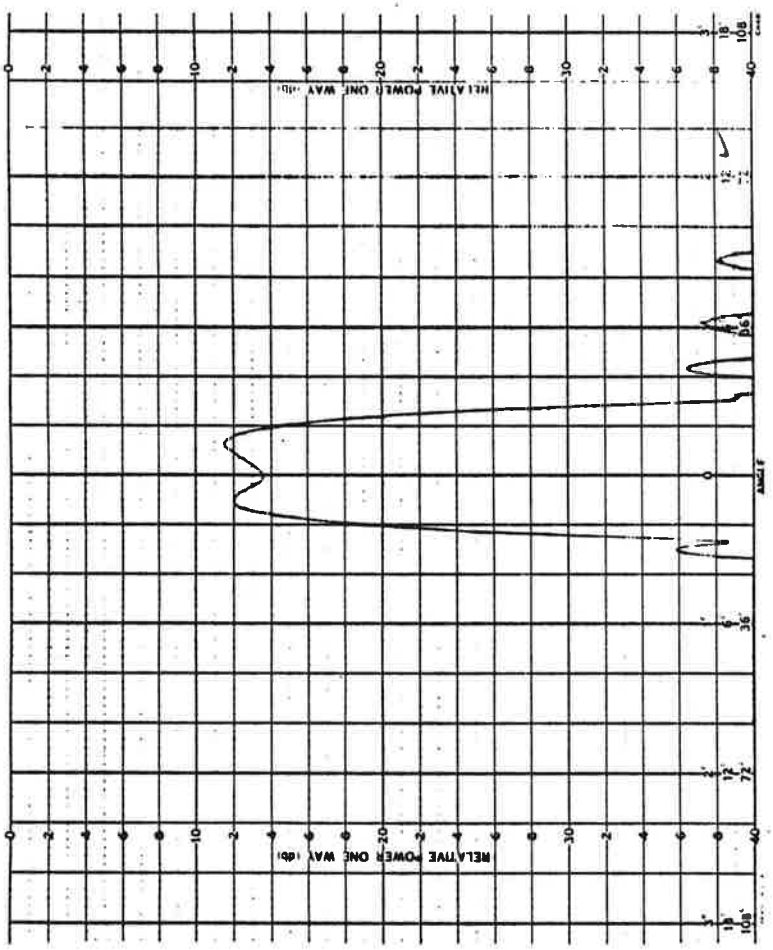

Figure 5-18. Azimuth Pattern at 3 Degrees Below Beam Peak

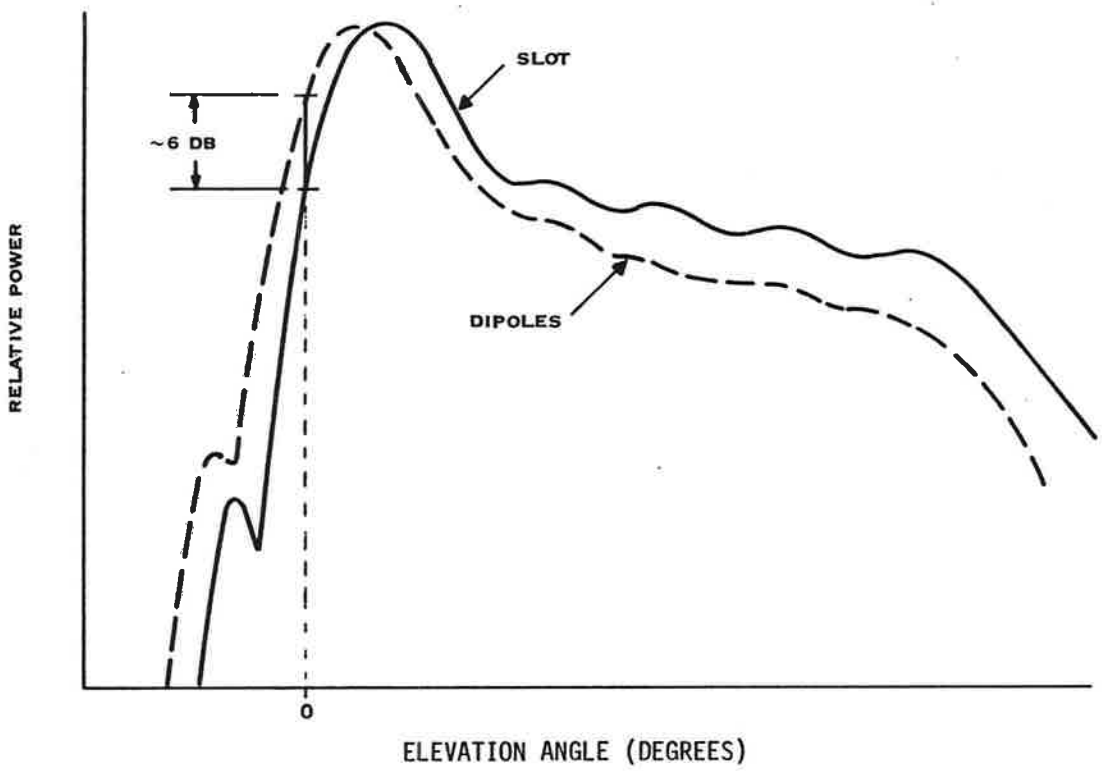

Figure 5-19. Elevation Coverage for Slot-Only and Dipoles Only

This problem would be alleviated by another NADIF-type element above the horn, or by exciting the radar horn at the beacon frequency.

Spillover and Backlobes

Backlobe level was not measured during pattern tests on the beacon feed, but during field tests, considerable backlobe punch-through and ring-around was noted on the PPI display. These backlobes are the result of a feed pattern which is too broad, allowing excessive energy to be spilled over the edges of the reflector.

Spillover at the top and bottom of the reflector is due primarily to the slot element. The very small vertical aperture of this element gives a broad elevation pattern which over-illuminates the top and bottom of the reflector.*

Spillover around the ends of the reflector is due to high azimuth sidelobes for the feed (Figure 5-5). These sidelobes are inherent in the feed geometry, and can only be reduced by eliminating the unexcited black hole in the center of the feed array.

By properly adjusting the transmitter power, STC characteristics, and omni power at the NAFEC test site, back-lobe punch-through with the ARSR modification was largely eliminated from the PPI display.

---

*The very broad slot pattern caused other problems too. The lack of edge taper causes elevation sidelobe below the horizon which is higher than desired, and energy scattered from the feed boom caused excessive ripple in the cosecant portion of elevation pattern until a layer of microwave absorber was added to selected parts of the feed structure.

SECTION VI

COVERAGE AND SLS PERFORMANCE

General

Based on measured performance of the ATCRBS Improvement antennas, computer modeling was used to predict volumetric coverage for the antenna in the presence of ground reflections and SLS effects. This modeling has shown that the improved antenna provides much better coverage than the hog-trough; the improvements are primarily due to reduced null depth in the directional pattern and to reduced ripple in the omnidirectional pattern. The model has also been useful in predicting the optimum SLS ratio (ratio of omni ERP to directional ERP) for the ATCRBS system.

Modeling

To predict ATCRBS system coverage, it was necessary to make several assumptions about system range, ground reflections, and SLS operation. These assumptions are discussed in the following paragraphs.

System Range

The maximum range of the ATCRBS system can be limited by either of two factors:

1. Insufficient transmit power and receive sensitivity in the uplink to trigger a reply from the airborne transponder, or

2. Inadequate transmit power and receive sensitivity in the down link to detect a reply from the aircraft transponder.

The maximum range for the uplink can be expressed as:

$$R_{up} = \left(\sqrt{\frac{P_I}{S_T}}\right)\left(\sqrt{\frac{G_i G_T \lambda^2}{(4\pi)^2}}\right)$$

where

P_I = Interrogator Transmitter Power
S_T = Transponder Minimum Triggering Level
G_i = Interrogator Antenna Gain
G_T = Airborne Transponder Antenna Gain
λ = Wavelength

For the down-link, maximum range is given by

$$R_{down} = \left(\sqrt{\frac{P_T}{S_I}}\right)\left(\sqrt{\frac{G_i G_t \lambda^2}{(4\pi)^2}}\right)$$

where

P_T = Airborne Transponder Reply Level

S_I = Interrogator/Receiver Minimum Detectable Signal

The maximum range of the ATCRBS system is limited to the smaller of up-link range or the down link range.

The two range equations are very similar, differing only in the ratio of transmit power to receiver sensitivity. (The airborne and ground-based antenna gains, as well as λ, vary slightly because of the 1030 to 1090-MHz frequency difference, but these effects are quite small and will be neglected in this discussion.) According to the ATCRBS National Standard the minimum values for transmit power and receive sensitivity are as follows:

P_T = +51 dBM

P_I = +57 dBM (Typical, not minimum)

S_T = -69 dBM

S_I = -85 dBM

Using these values the up-link ratio P_I/S_T is +126 dB, while the down link ratio P_T/S_I is +136 dB. This implies that the down-link range is greater than the up-link range by a factor of approximately three, and leads to the following postulate:

> The ATCRBS system range is limited by the up-link (interrogation) path. If a target is close enough to be interrogated, it is easily close enough for its reply to be detected.

The interrogator receiver employs a sensitivity-time-control (STC) circuit which reduces receiver sensitivity S_I for near in targets; in predicting maximum range, however, it is assumed that the target is far enough away so that the interrogator/receiver has recovered to maximum sensitivity.

One additional assumption is required: the transponder antenna (stub) is assumed to have a constant gain of 0 dB (isotropic). The maximum system range can then be predicted by the up-link range equation, using the measured gain and elevation pattern for the interrogator antenna.

Ground Reflections

Reflected energy from the earth has a singificant effect on the radiation pattern of the ATCRBS reflector. For targets at some elevation angles, the direct and reflected interrogations combine in-phase, giving a large increase in signal strength, while at other angles the signals combine out-of-phase, giving nulls in ATCRBS coverage. The "hogtrough" array, having a broad elevation pattern, allows much energy to illuminate the horizon, and reflections seriously degrade its coverage. The ATCRBS reflector, with rapid decay of energy below the horizon, is significantly affected by reflections for targets within about two degrees of the horizon. Higher targets are only slightly affected.

In the computer simulation, earth reflections are modeled as shown in Figure 6-1. A flat dielectric earth is assumed, and the reflection coefficient Γ is simply that for reflection of a vertically polarized uniform TEM wave obliquely incident on a lossy semiinfinite dielectric:

$$\Gamma = \frac{\bar{n}^2 \sin\psi - \sqrt{\bar{n}^2 - \cos^2\psi}}{\bar{n}^2 \sin\psi \quad \sqrt{n^2 - \cos^2\psi}}$$

where $\bar{n}^2$ is a vector describing the characteristics of the earth:

$\bar{n}^2 = \varepsilon_{r2} - j\, 60\sigma_2 \lambda$

λ = Wavelength in meters

σ_2 = Conductivity of earth in mho-meters per square meter

ε_{r2} = Relative dielectric constant of earth

The incidence and reflection angles ψ are assumed equal in accordance with Snell's law.

In the following calculations, the values

$\varepsilon_{r2} = 3.0$

$\sigma_2 = 7.15 \times 10^{-3}$

are used, these values are typical of a damp, sandy earth, which is a very reflective surface.

The flat dielectric earth is believed to be a "worst-case"; rough terrain or vegetation will give lower reflections. Nonetheless, measurements over the smooth open terrain common at airports has shown that this worst-case model is quite typical in many instances, so it is reasonable to investigate beacon performance for this situation.

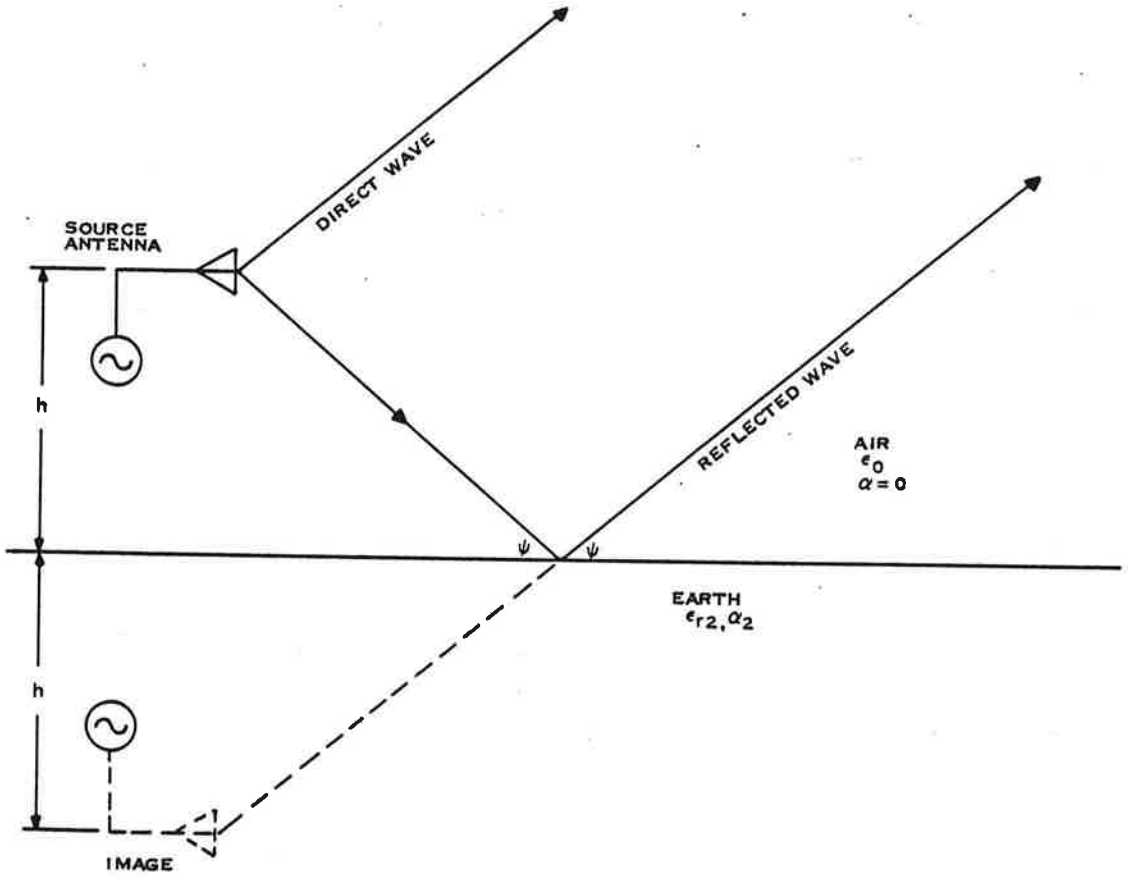

Figure 6-1. Ground Reflections

Antenna Patterns

The antenna elevation patterns used in the simulation are measured amplitude patterns for the ATCRBS reflector, ARSR feed modification, and the respective omni antennas. Pattern phase behavior was not measured (this is a difficult measurement on an antenna of this size) so all radiation was assumed to emanate from a phase center located at the physical center of the antenna, and all points on the antenna pattern are assumed to be in-phase. While these assumptions are not strictly correct, they are adequately accurate for the small region within ±3 degrees of the horizon where reflection effects are most significant, and indicate typical behavior at higher elevation angles.

The azimuth pattern was assumed to be a parabolic fit, in dB's and degrees, through the half-power beamwidth. Thus, if θ_3 is the 3 dB beamwidth, the beamwidth at any other dB level, P, is given by

$$\theta_p = \theta_3\sqrt{\frac{P}{3}}.$$

SLS Effects

Operation of the sidelobe suppression (SLS) system is diagrammed in Figure 6-2. Based on the relative amplitude of the directional and omni pulses, an airborne transponder either replies to a valid interrogation when

$$P_1 \geq P_2 + T$$

or suppresses its reply where

$$P_1 < P_2 + T$$

where T is the SLS threshold, typically between 0 and 9 dB.

In an ideal system the P_1/P_2 ratio (called the SLS Ratio) is approximately 15 dB, so that, for thresholds between 0 and 9 dB, transponders will reply within the main beam and suppress for all sidelobe interrogations.

Ground reflections and elevation pattern mismatch can cause the SLS ratio to deviate from its ideal value. If the ratio is too great, replies may occur in the sidelobe region, resulting in sidelobe punch-through. A too small SLS ratio can cause blanking of valid targets within the directional beam, resulting in main-beam kill. The computer simulation investigates the effects of variations in SLS ratio due to ground reflections and other causes.

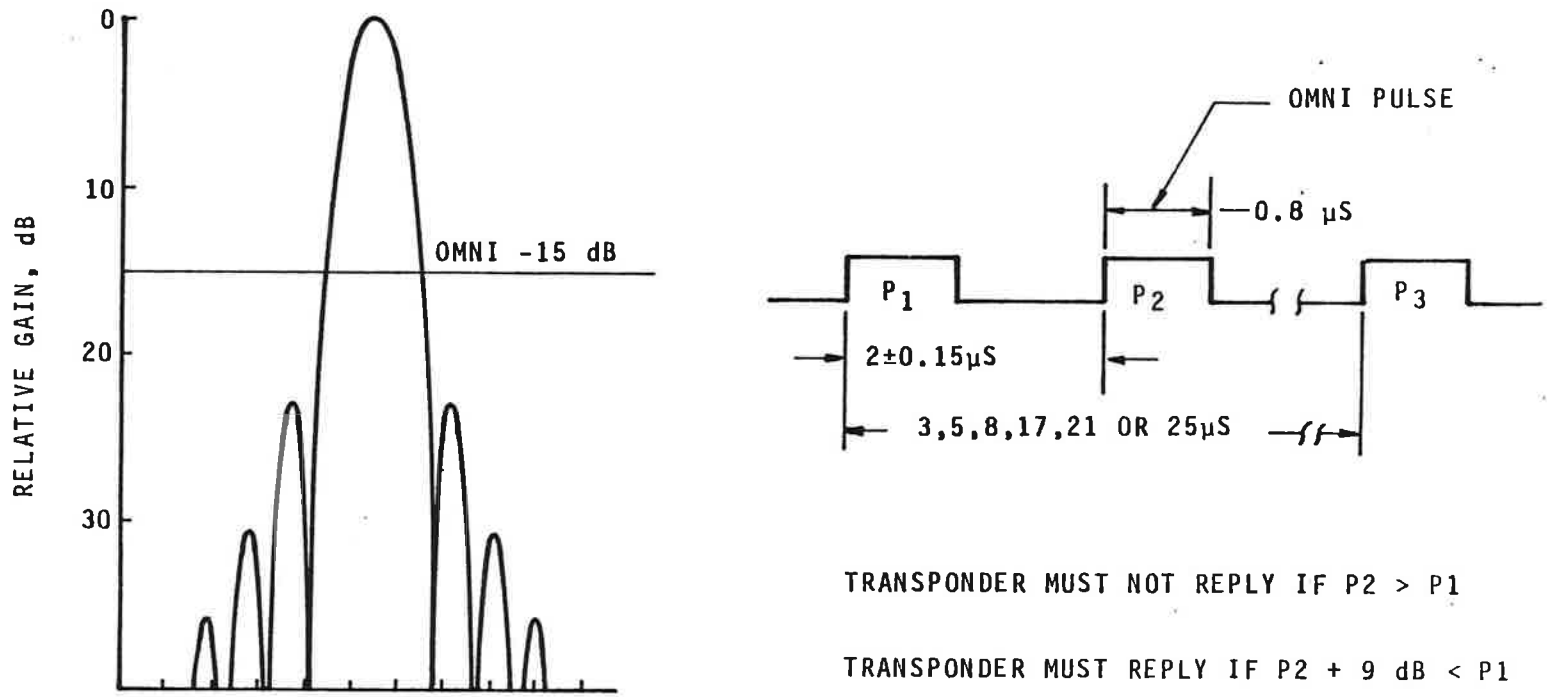

Figure 6-2. SLS Operation

System Coverage

Based on the model described in the previous section, ATCRBS system coverage has been calculated for three antennas:

ATCRBS Improvement Reflector
ARSR-2 Beacon Feed Modification
Hogtrough.

The input power, antenna gain, and other parameters used in the coverage calculations are listed in Table 6-1. Coverage limits are established at the range where the ratio of signal to minimum triggering level is 3.0 dB. Some coverage will exist beyond the calculated coverage volume but it is likely to be a broken or narrow target consisting of only a few hits.

ATCRBS Reflector

Coverage for the ATCRBS reflector is shown in Figure 6-3. The input power level is set for terminal area coverage, with 60 NMI maximum range. Increasing the power to

$$P_{in} = 110 \left(\frac{200}{60}\right)^2 = 1225 \text{ watts}$$

will increase the maximum range to 200 NMI, for en-route coverage.

The diagram shows the complete coverage is provided for targets at all altitudes, out to the terminal area limit of 60 NMI. Coverage falls off above 30 degrees elevation, giving a cone of silence approximately as indicated in the figure.

Airborne signal-strength measurements have generally confirmed the accuracy of the predicted coverage. Figure 6-4 shows a comparison of measured and calculated signal strength. Signal is above the minimum triggering level of the transponder at all ranges.

Omni coverage is also shown in the Figure. It shows that the SLS system operates only out to a maximum range of about 25 miles, since P_2 may not be detected beyond this range. Sidelobe punch-through is unlikely outside the omni coverage area because the omni has more gain than the sidelobes, so if the omni is out of range, the sidelobes are also out of range.

Main-beam kill is not likely to occur outside the omni coverage limits.

ARSR-2 Integral Feed

Coverage for the ARSR-2 Integral Feed is shown in Figure 6-5. The ARSR is used for en-route air traffic control, and requires a range of 200 NMI.

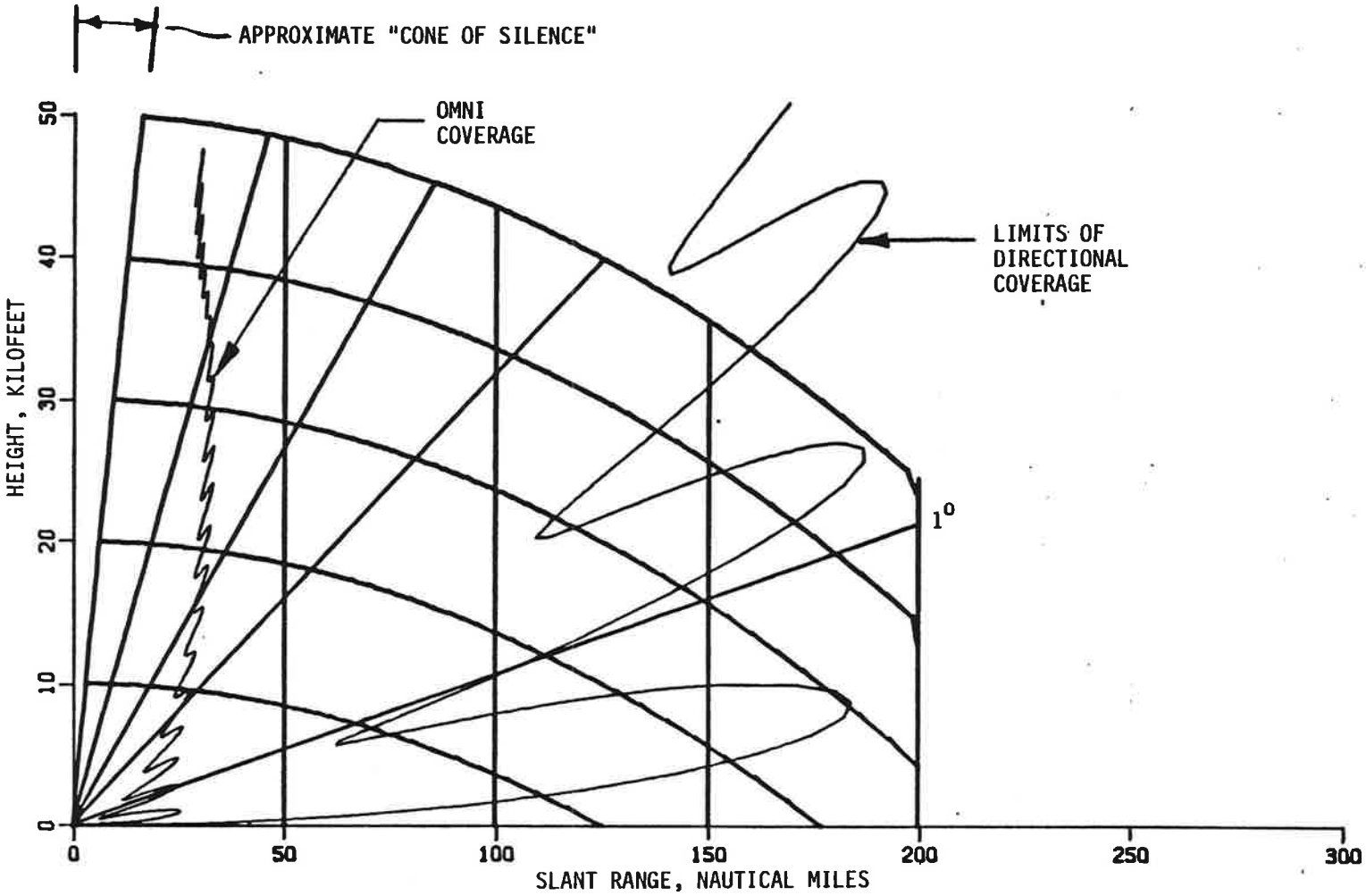

Figure 6-3. Coverage Diagram for ATCRBS Reflector

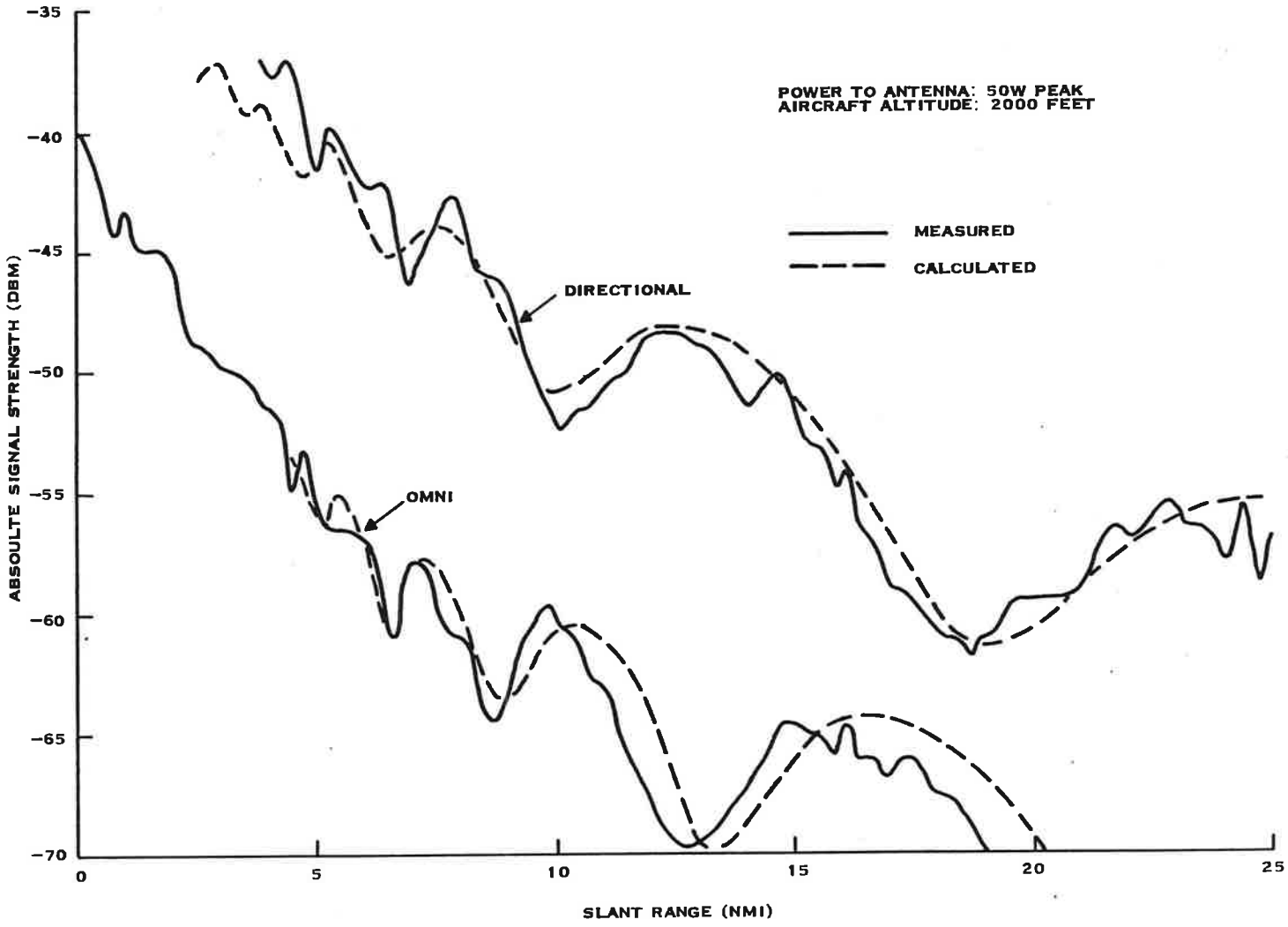

Figure 6-4. Comparison of Measured and Calculated Signal Strength for ATCRBS Reflector on 17-Foot Tower

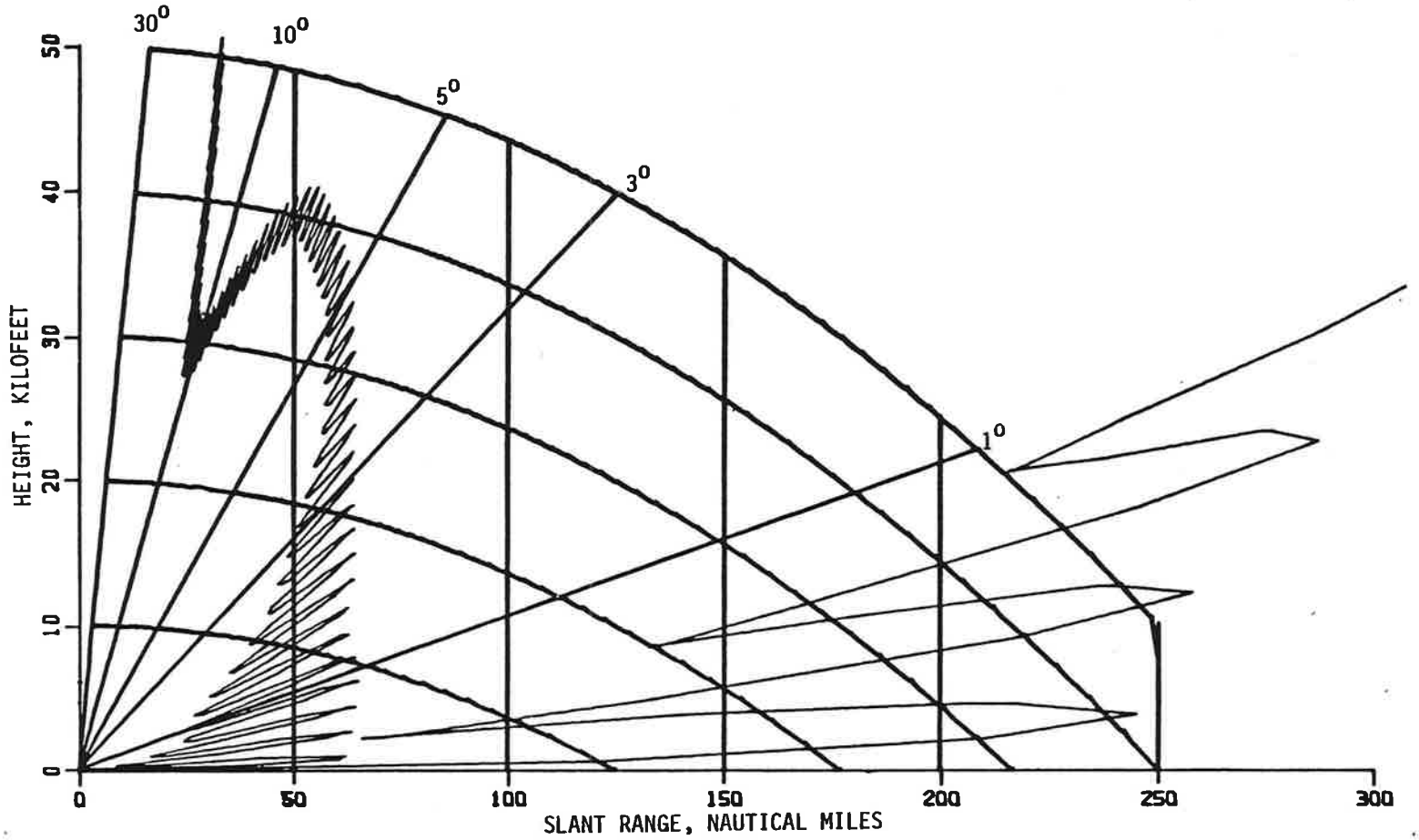

Figure 6-5. Coverage for ARSR-2 Beacon Feed, Antenna Tilt Optimized for Primary Radar

Table 6-1. Parameters for Coverage Calculations

	Antenna		
	ATCRBS Reflector	ARSR-2 MOD	Hogtrough
Gain	+25.7 dB	+29.5 dB	+21 dB
Input Power	110 Watts	325 Watts	275 Watts
Receiver MTL	-70 dBM	-70 dBM	-70 dBM
3 dB Beamwidth	2.3°	2.3°	2.3°
Rotation Rate	12.6 RPM	5.0 RPM	12.6 RPM
PRF	315 Hz	160 Hz	315 Hz
Omni Type	Improved Omni with High-Angle Coverage	ASR-2 MOD Omni	SLS Dipole
Relative Omni Level	-15 dB	-18 dB	-18 dB
Directional Antenna Height above ground*	31 feet	90 feet	36 feet
Omni Height*	38 feet	106 feet	38 feet

*Height to Phase Center

As discussed in the previous section, the elevation beam of the ARSR modification was tilted higher than desired: Figure 6-5 is calculated with the -11.9 dB point of the elevation beam at the horizon. This corresponds to the -4 dB point of the radar on the horizon, which is believed to be the optimum tilt for the radar at most sites. As a result of the beacon beam tilt, coverage near the horizon is not as good as desired, with some holes in the 200 NMI coverage volume. These holes can be reduced by mechanically tilting the antenna downward about 1.25 degrees, or by increasing the input power to the antenna.

Compared with the ATCRBS reflector coverage, the ARSR-modification nulls are more closely spaced in elevation. This happens because the ARSR radar is typically on a 75-foot tower, while the ATCRBS reflector is assumed to be on a 17-foot tower.

Figure 6-6 shows the effect of mechanically tilting the ARSR reflector 1.25-degrees downward. Although some nulls still exist, their angular extent is significantly reduced, so that coverage is much improved. If the input power were increased 325 watts to 1300 watts, the minimum range in the nulls would increase to 130 NMI.

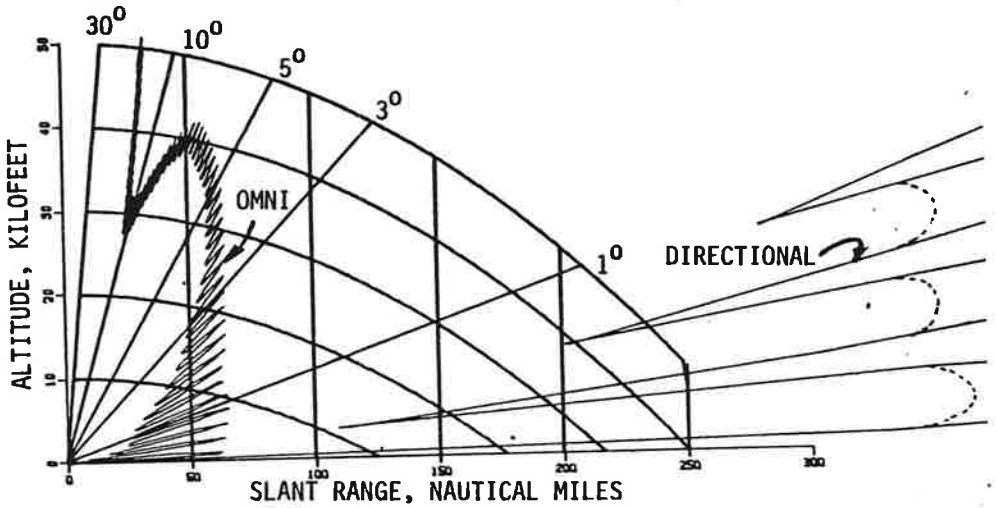

Figure 6-6. ARSR Beacon Feed Coverage, Antenna Tilt Optimized for Beacon System

Hogtrough Coverage

Figure 6-7 shows a coverage diagram for the hogtrough. Excessive illumination of the earth causes numerous nulls in the coverage. Even when the input power is increased to the ATCBI-4 maximum of 2200 watts, coverage in the first null is not extended to the terminal area limit of 60 NMI. With 2200 watts input, coverage at the peaks extends to 1000 MNI, resulting in needless interrogation of aircraft far outside the region of interest.

Because the SLS omni antenna is mounted above its associated directional antenna, nulls in the omni coverage occur at slightly lower angles than corresponding directional antenna nulls. This effect is shown in Figure 6-8, which shows omni and directional coverage plotted with the omni coverage expanded by 15 dB to emphasize the differences in lobing.

This is a phenomenon called differential lobing, and it degrades the operation of the SLS system. At nulls in the omni coverage, the ERP of pulse P_2 may be inadequate to cover all sidelobes of the directional antenna, allowing sidelobe punchthrough. At nulls in the directional pattern, the ERP of pulse P_1 may be inadequate to punch through the omni level even at the peak of the directional beam, resulting in main-beam kill. Main-beam kill is particularly likely for a transponder with a 9 dB threshold, because P_1 must exceed P_2 by at least 9 dB before a reply will occur.

Deviations from the desired -15 dB omni level are shown in Figure 6-9 for the ATCRBS reflector. The omni level never exceeds -9 dB, so there is no danger of main beam kill with this antenna; however the level does drop below 23 dB at several elevation angles, giving the potential for sidelobe punchthrough in those sectors. Sidelobes and backlobes for the reflector are typically -23 dB near the horizon.

Differential lobing also causes variations in the azimuth width of an ATCRBS target. Figure 6-10 shows that the target is interrogated over only a small part of the azimuth beamwidth when the omni level is high, and over a wider azimuth sector when the omni level is low. This causes variations in the target width as seen on a PPI display, and variations in the number of interrogations (or hits) for processing in an ARTS-III or other automated system.

Punch-Through with Differential Lobing

Figures 6-11 through 6-13 show the effect of differential lobing and directional/omni mismatch on sidelobe punchthrough. These figures show the sidelobe level that will punch through the omni coverage. Since all three antennas have typically 20 dB to 23 dB sidelobes, the chance for punch through is fairly small. Because of its more predominant lobing, the hog-trough is more likely to see punch-through than the other two.

Transponder threshold affects the possibility for punch-through; a 0 dB threshold transponder is less likely to be blanked by SLS than a 9 dB threshold transponder. The data in the figures is plotted for a 5 dB

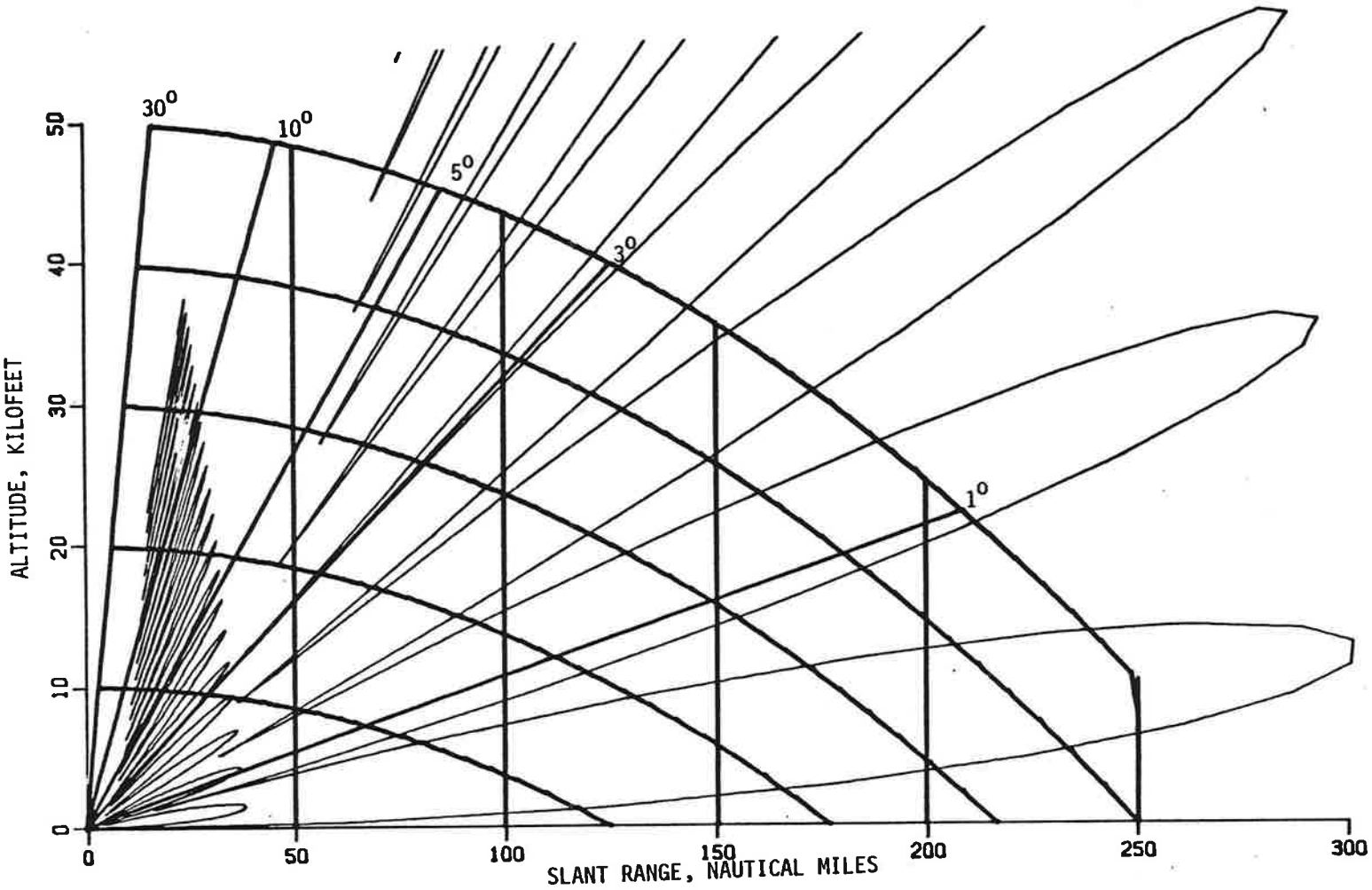

Figure 6-7. Hogtrough Coverage

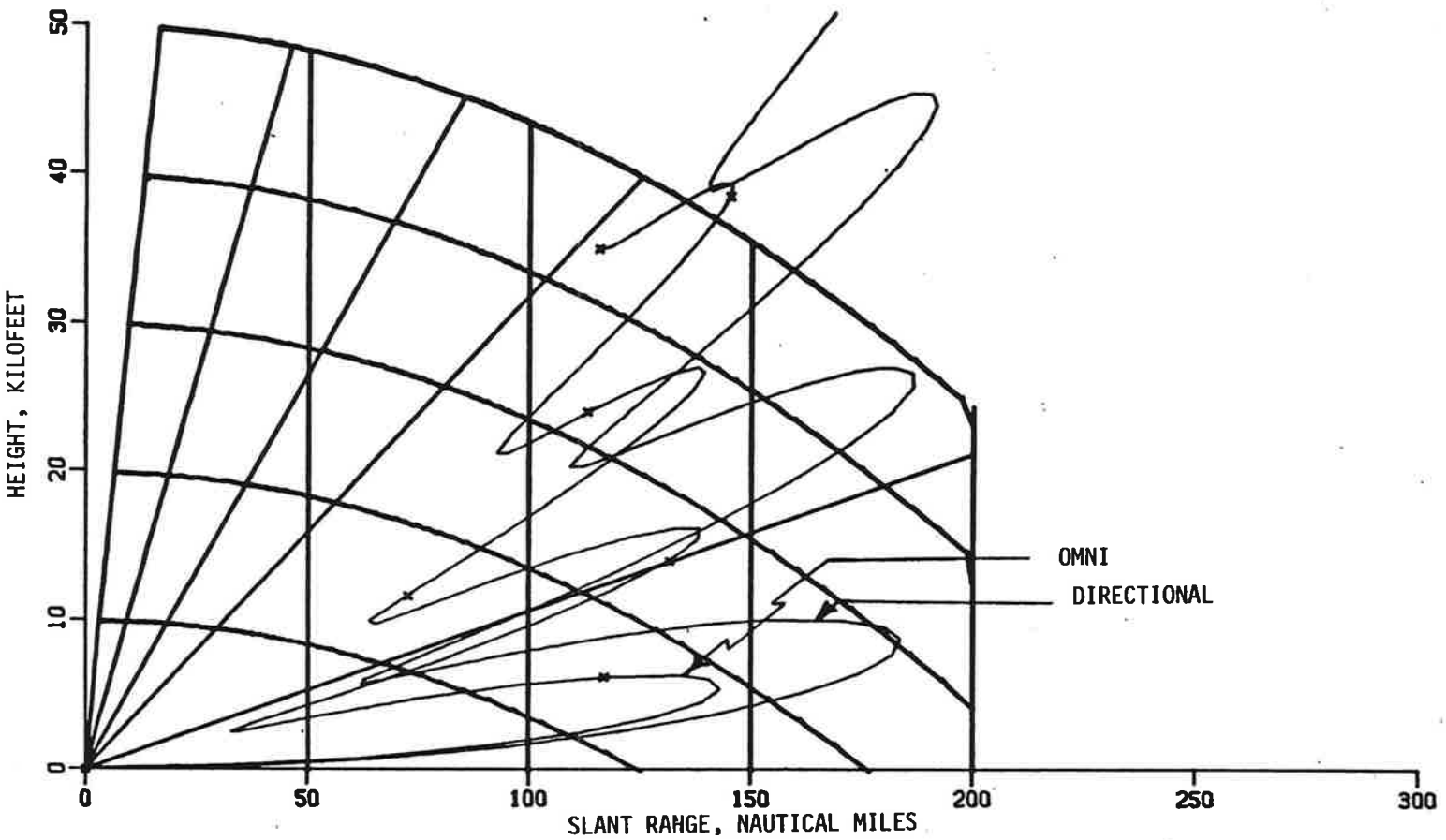

Figure 6-8. Differential Lobing

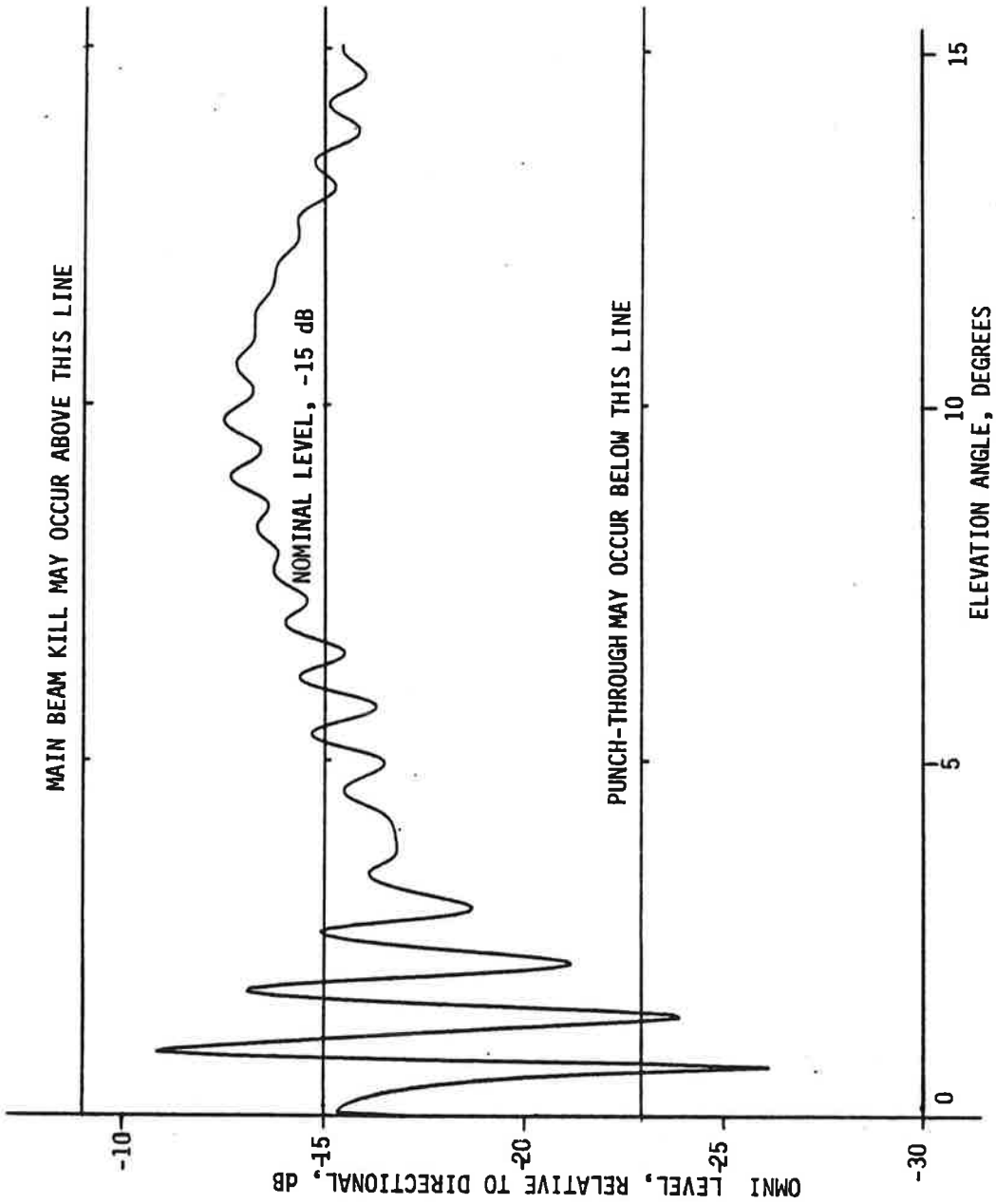

Figure 6-9. Actual Omni Level with Ground Reflections

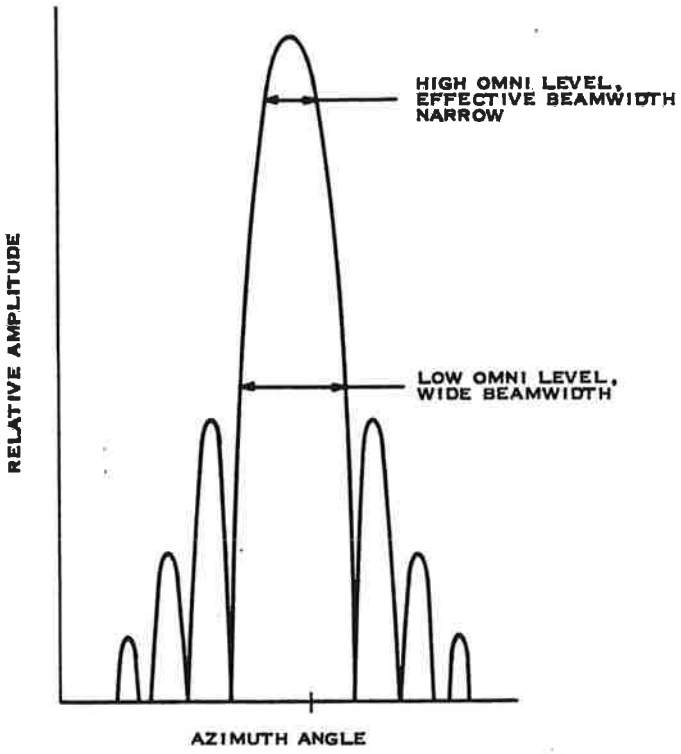

Figure 6-10. Effect of Omni Level on Interrogation Beamwidth

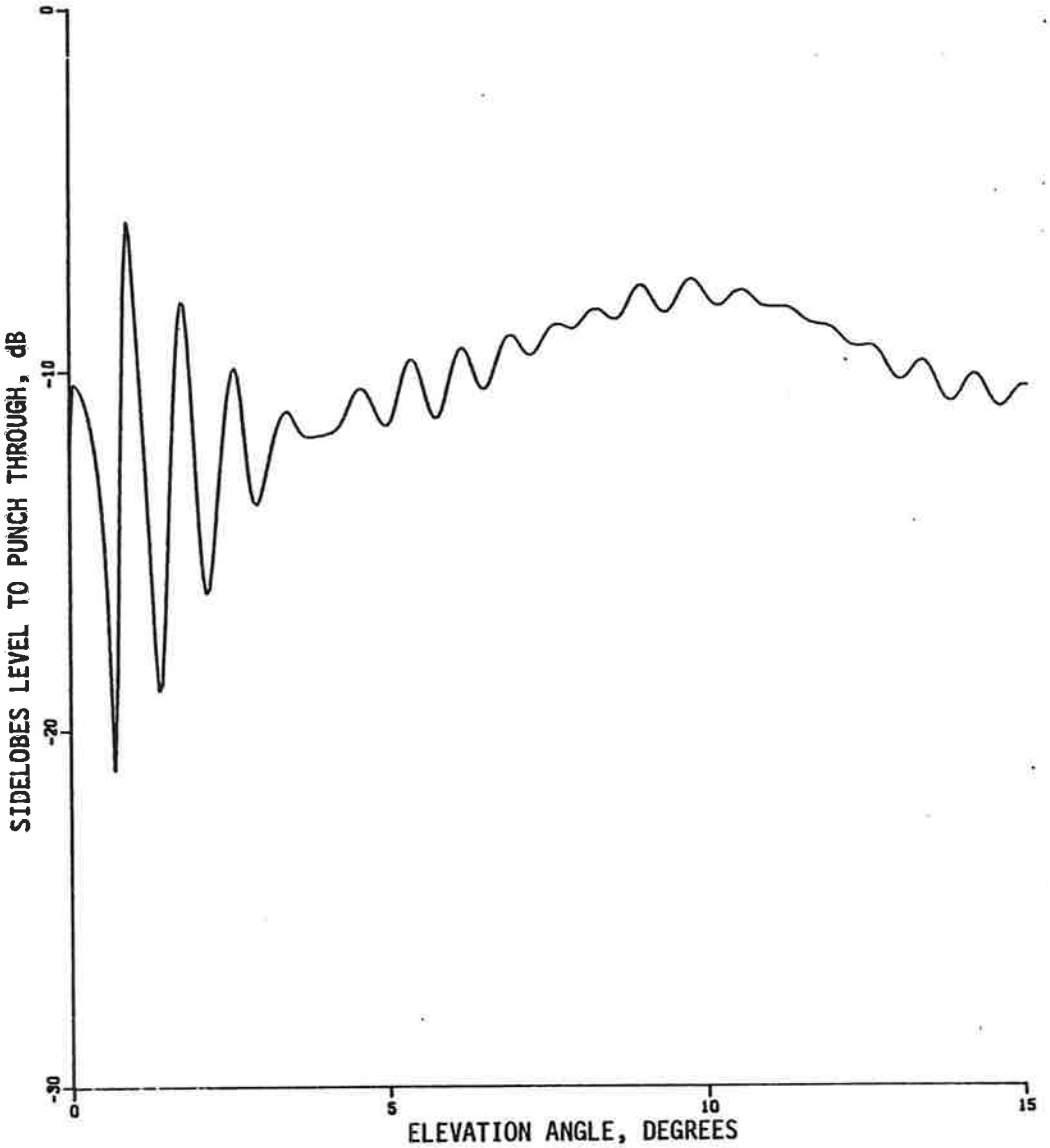

Figure 6-11. Sidelobe Level Which Would Punch Through SLS Coverage, ATCRBS Reflector and Omni

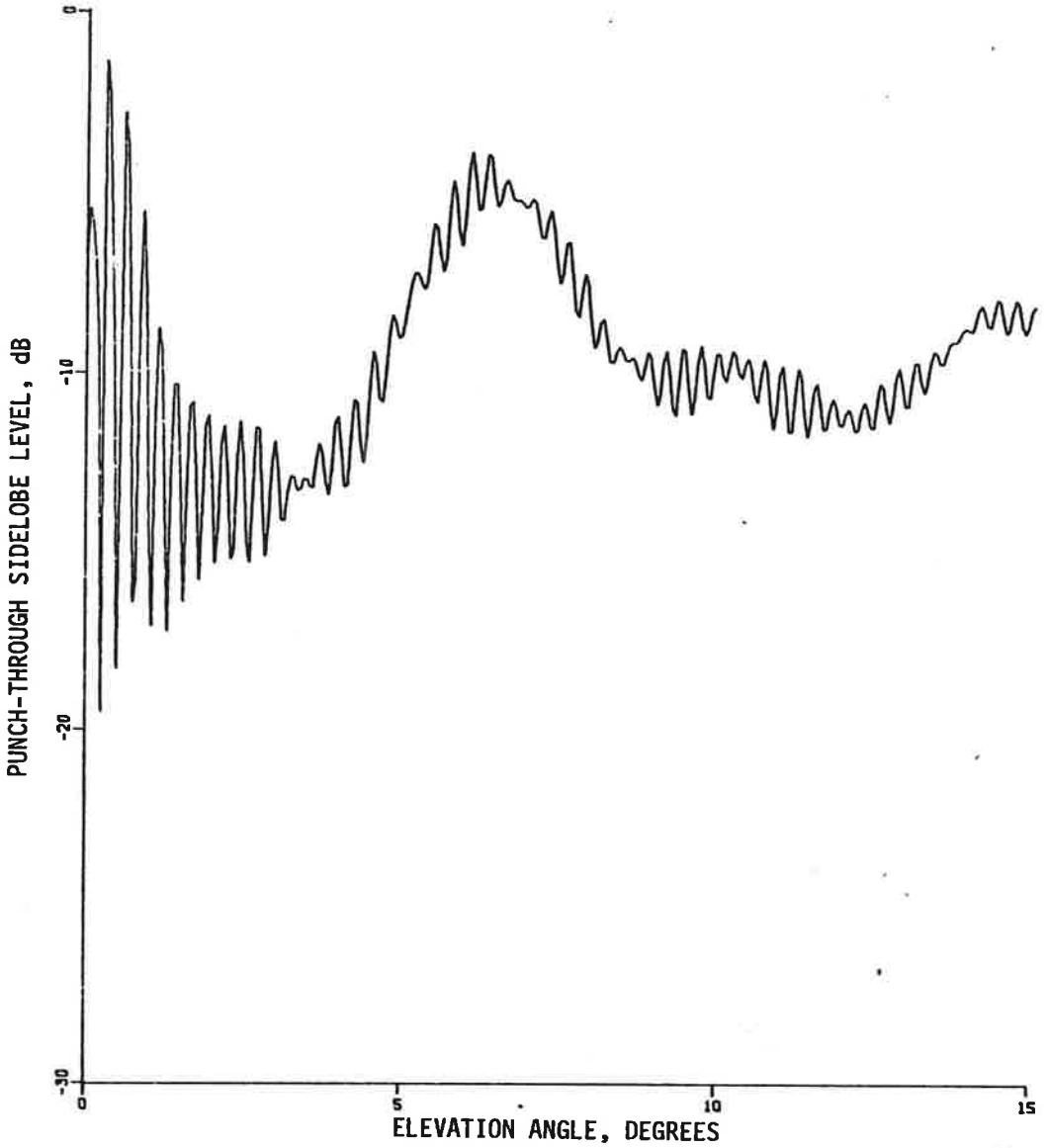

Figure 6-12. Punch Through Sidelobe Level for ARSR Feed Modification

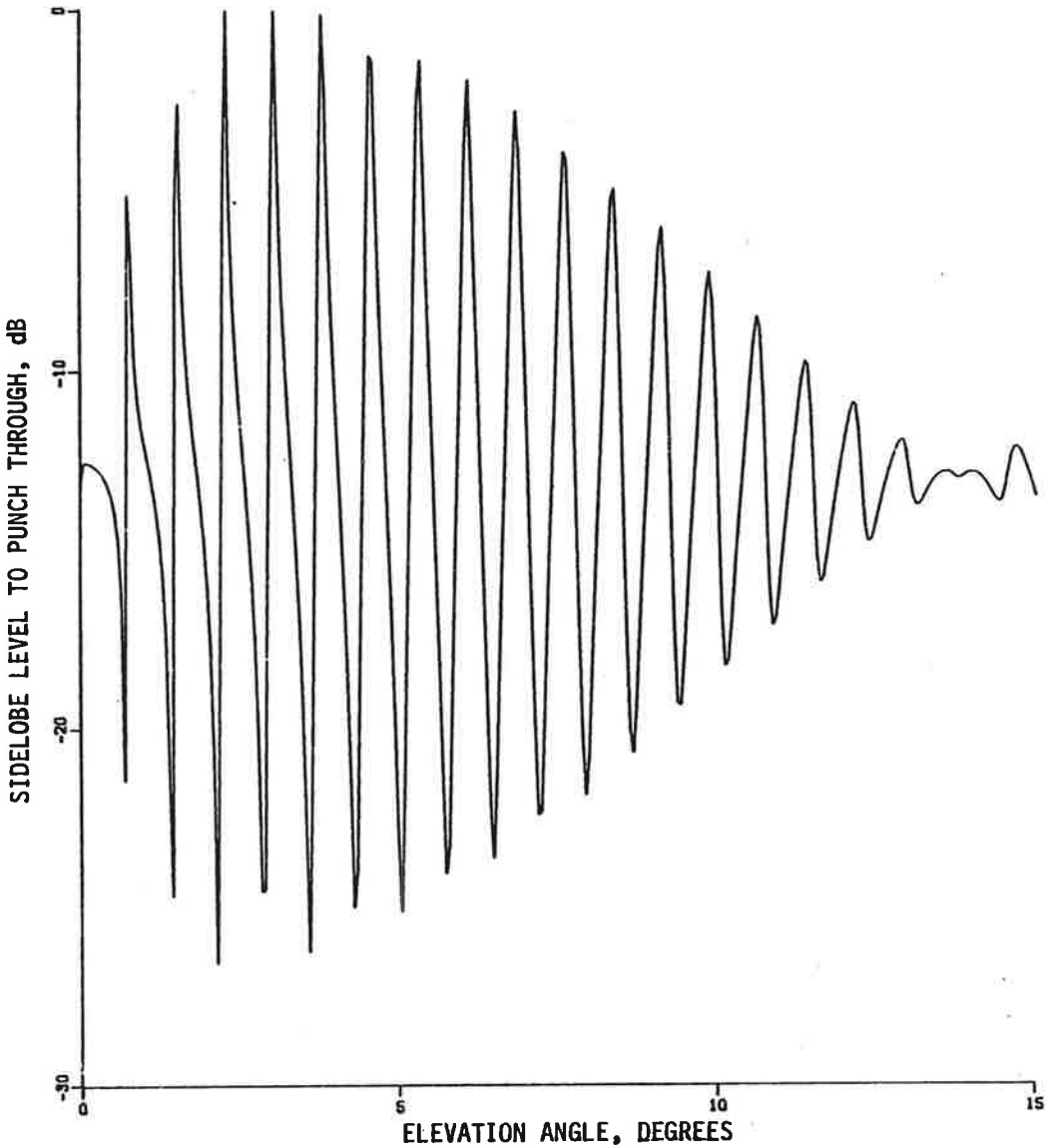

Figure 6-13. Punch Through Sidelobe Level for Hogtrough

threshold; for other thresholds the plot is identical except that it is shifted vertically by the appropriate number of dB's.

The "hump" at 6-degrees elevation in the plot for the ARSR modification is due to a mismatch in the free-space patterns for this antenna, wherein the omni has a broader half-power beamwidth than the directional antenna. Figure 6-14 shows the effect: at about 6-degrees elevation the omni relative gain is significantly greater than the directional. Operationally this should cause no problems except that some main-beam kill or target narrowing may be experienced for transponders with 9 dB thresholds.

Run-Length

Figures 6-15 through 6-17 are plots of variations in run length (number of interrogations) due to SLS effects. Again, the plots are for a transponder with a 5 dB threshold. Variations for the new ATCRBS reflector are not great enough to be significant. For the ARSR feed, greater lobing (due to the higher tower) gives more variation in run length. Target width will be reduced at 6-degrees elevation because of the directional/omni mismatch discussed previously. The hogtrough shows significant variations in runlength.

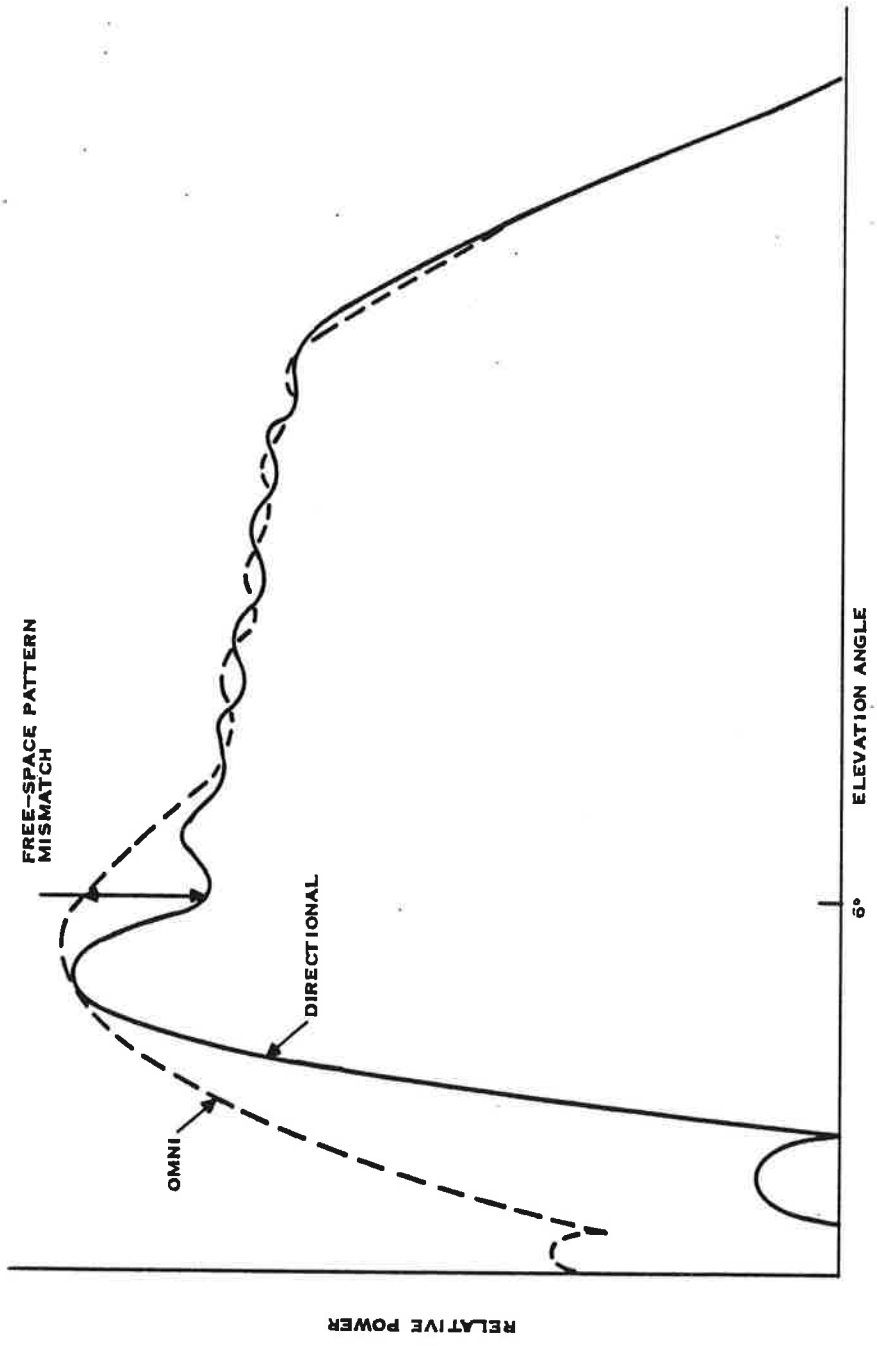

Figure 6-14. Directional/Omni Mismatch for ARSR-2 Modification

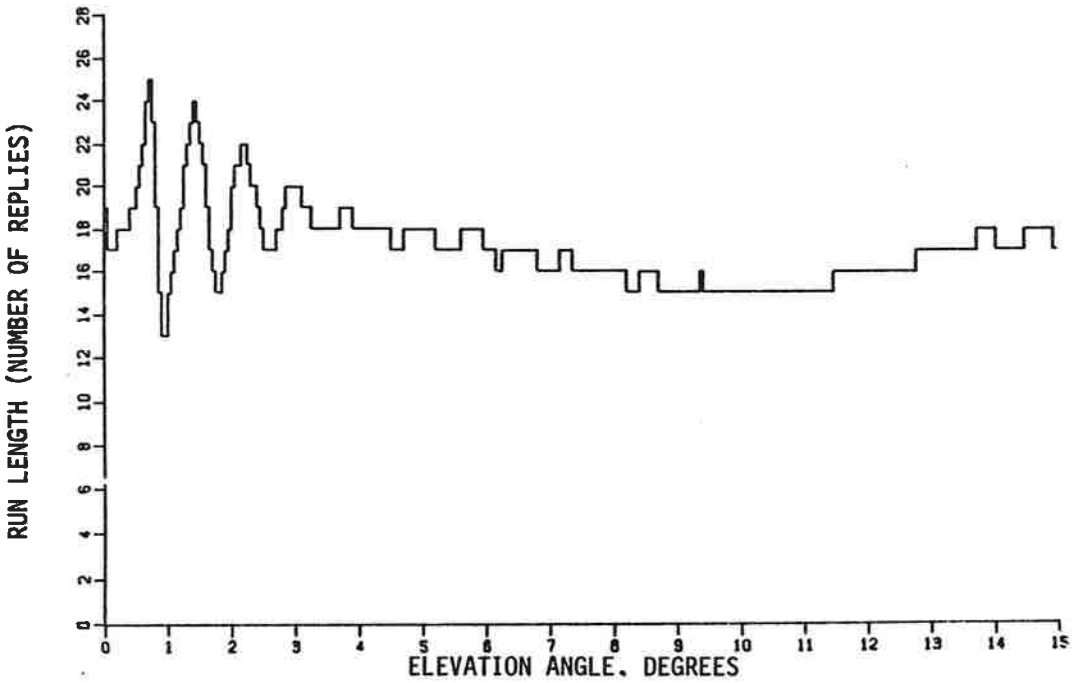

Figure 6-15. Variation in Number of Replies for ATCRBS Reflector

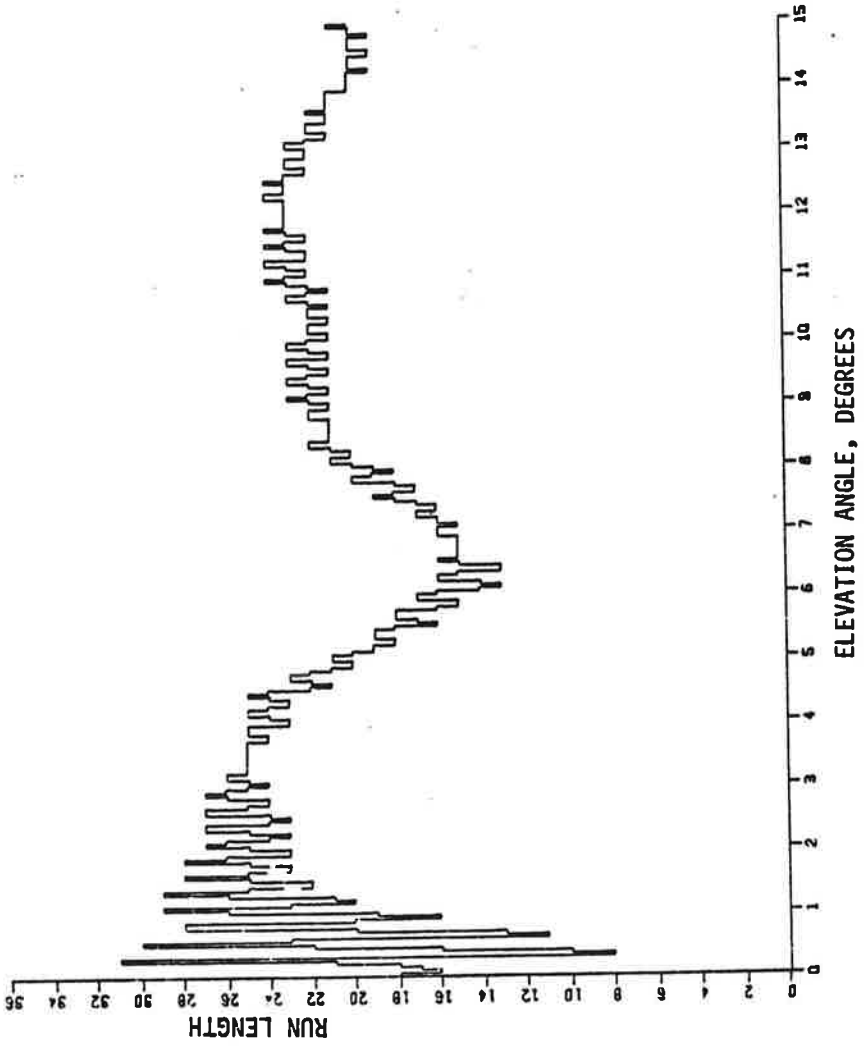

Figure 6-16. Run Length for ARSR Integral Feed

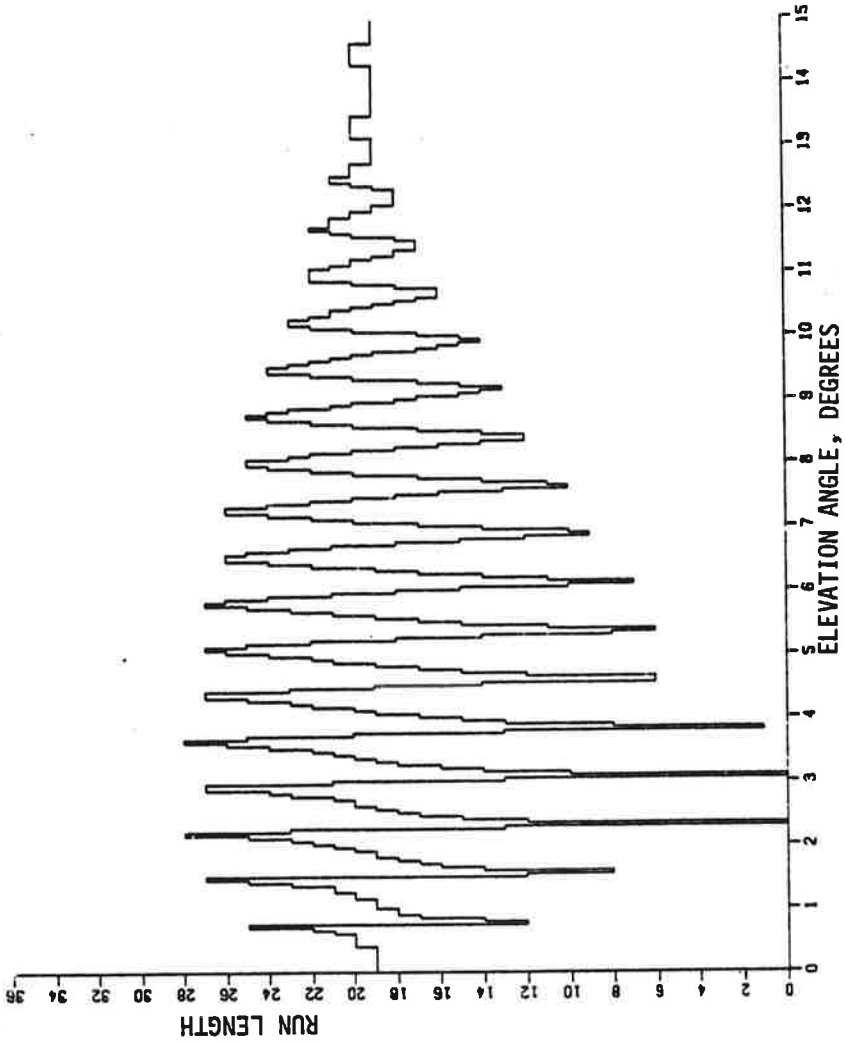

Figure 6-17. Run Length for Hogtrough

REPORT OF INVENTIONS
APPENDIX

Two significant developments were noted during the program covered in the main text.

DESIGN FOR AN OMNIDIRECTIONAL ANTENNA: A novel design open omnidirectional antenna was developed to overcome the pattern interference caused by the mechanical support and/or signal feed structure omnidirectional antenna.

The disclosure is of a design approach using elements consisting of folded slots which radiate an omnidirectional azimuth pattern. The feed for these slots is in the form of a microstrip or stripline transmission line board, thus keeping the diameter of the antenna a fraction of a wavelength. The stripline feed contains power divider circuitry to provide the desired amplitude end phase at each element.

PHASE ADJUSTING SPEED REDUCER: A variable ratio multistage planetary speed reducer using constant mesh gearing was invented to provide for the accurate orientation of two independent, rotating radar antennas. The problem was one of providing position orientation within specified limits while both antennas rotated. The antennas are both driven by induction motors, through a speed reducer, which drives a pedestal containing a right angle spiral gearset. The solution to the problem was the development of a narrow ratio constant mesh variable ratio speed reducer to correct the rotation phase of the pedestal.